A new upper Paleogene to Neogene stratigraphy for Sarawak and Labuan in northwestern Borneo: Paleogeography of the eastern Sundaland margin

Juliane Hennig-Breitfeld [a,*], H. Tim Breitfeld [a], Robert Hall [a], Marcelle BouDagher-Fadel [b] and Matthew Thirlwall [c]

[a] *SE Asia Research Group, Department of Earth Sciences, Royal Holloway University of London, Egham, TW20 0EX, UK*
[b] *Department of Earth Sciences, University College London, London, WC1H 0BT, UK*
[c] *Department of Earth Sciences, Royal Holloway University of London, Egham, TW20 0EX, UK*

** Corresponding author (e-mail: juliane.hennig-breitfeld@rhul.ac.uk)*

Abstract

The Miri Zone in Sarawak contains thick Paleogene to Neogene sedimentary successions that extend offshore into the Sarawak Basin (Balingian and Central Luconia Provinces) and Sabah Basin. Exploration offshore has shown the Sarawak Basin in the South China Sea contains major hydrocarbon reservoirs. The sediments on land are age equivalents of the offshore successions and can be used to provide insights into their sedimentological and stratigraphic relations. However, because the rocks are found in mountainous regions covered by dense rainforest much of the stratigraphy in the Miri Zone is poorly known, as are timings and causes of major unconformities in the region that are essential for understanding the tectonic history, basin development, and sedimentary pathways. In this study we integrate fieldwork, U-Pb zircon dating, biostratigraphy, and light and heavy mineral analyses to present a revised stratigraphy for the region as well as paleogeographic maps, including major paleo-river systems for the main sedimentary basins. Rocks studied include parts of the Cretaceous to Eocene deep marine Rajang Group, fluvial to marginal marine sediments of the Oligocene to Early Miocene Tatau, Buan, Nyalau and Setap Shale Formations, and the Miocene sediments which are assigned to the Balingian, Begrih and Liang Formations in the Mukah-Balingian province, and the Belait Formation on Labuan.

There is still much debate about the timings or even existence of some important unconformities offshore, such as the Middle Miocene Unconformity (MMU) and Deep

Regional Unconformity (DRU). We propose to avoid the ambiguous time-based terminology that has been used for different events by different authors. Instead, our results from the on-land stratigraphy show two main unconformities in northern Sarawak; one at c. 37 Ma (Rajang Unconformity), marking the change from deep marine to fluvial - marginal marine sedimentation, and another one at c. 17 Ma (Nyalau Unconformity) which is related to widespread uplift in Borneo and changing river systems.

Keywords: Borneo; Miri Zone; Balingian-Luconia; Rajang Unconformity; paleogeography; provenance; U-Pb zircon geochronology

1. Introduction

Sarawak in western and northwestern Borneo is a poorly studied region of hills and mountain ridges covered by dense rainforest vegetation. Haile (1974) subdivided the area of Sarawak and West Kalimantan into four different zones, which are from south to north the Borneo basement, and the Kuching Zone, Sibu Zone, and Miri Zone (Fig. 1). The Miri Zone is the youngest zone, and includes thick sedimentary sequences of Paleogene to Neogene age (Liechti et al., 1960; Wolfenden, 1960). It is separated from the Sibu Zone to the south by the Bukit Mersing Line (Haile, 1974; Hutchison, 1996).

The majority of geological observations in the Miri Zone still follow Liechti et al. (1960), Wolfenden (1960), and Heng (1992) who assigned similar lithologies in the Tatau region to different formations based on limited field observations and palaeontological evidence. The sediments continue into the offshore basins, however, they were assigned to different cycles based on seismic data (Hageman, 1987; Madon, 1999) with limited attempts to correlate them to the on-land stratigraphy, resulting in uncertain timings and positions of main unconformities. On land, major tectonic lineaments associated with the Miri Zone, such as the Bukit Mersing Line and the West Baram Line (Fig. 1), are also poorly understood.

This study focused on Paleogene and Neogene sedimentary successions in Sarawak and Labuan which are assigned to the Miri Zone (Fig. 2). They were studied in the field and analysed for light and heavy minerals accompanied by U-Pb dating of detrital zircons to assess provenance. Zircons from magmatic rocks were also dated and the biostratigraphy of limestones exposed in the Tatau region was investigated. The results are used to produce a revised Cenozoic stratigraphy for Sarawak and Labuan in northwest Borneo (Fig. 3), including more precise estimates for main unconformities, such as the Rajang and Nyalau Unconformities, and can help to understand the main tectonic events in the region, as well as stratigraphic relations offshore. This can be used to distinguish between important unconformities and sequence boundaries which may be mislabelled as unconformities in seismic data.

2. Geological background

2.1 Tectonic setting

The Kuching and Sibu Zones of Sarawak (Fig. 1) both include upper Cretaceous to Paleogene sediments. Sediments of the Kuching Supergroup in the Kuching Zone were deposited in fluvial to shallow marine environments (Khan et al., 2017; Breitfeld et al., 2018; Breitfeld and Hall, 2018), whereas the Rajang Group of the Sibu Zone, including the Lupar and Belaga Formations, are mainly turbidites deposited in a deep marine setting (e.g. Haile, 1974; Tan, 1979; Bakar et al., 2007; Galin et al., 2017). The zones are separated by the Lupar Line (Fig. 1), which has been interpreted as a suture (e.g. Tan, 1979; Hutchison, 1996, 2005) associated with subduction and collision at the Sarawak margin. Hutchison (1996) suggested subduction until c. 60 Ma and proposed a subsequent collision of Borneo with the Balingian - Luconia continent, resulting in the Sarawak orogeny at c. 45 Ma, but later revised to 37 Ma (Hutchison, 2005). Haile (1973), however, had already questioned the interpretation of the Lupar Line as a suture and Hall and Sevastjanova (2012) and Hall (2013a) questioned the Sarawak orogeny. Recent studies (Galin et al., 2017; Breitfeld and Hall, 2018) have demonstrated a similar provenance for sediments in the Kuching and Sibu Zones based on light and heavy mineral assemblages, and similar zircon U-Pb age populations, indicating the Rajang Group sediments are the reworked lateral distal equivalents of the Kuching Zone sediments. The sediments were derived mainly from Cretaceous rocks of the Schwaner Mountains (Davies et al., 2014) that formed by subduction of the Paleo-Pacific at the eastern margin of West Borneo (Breitfeld et al., 2017a; Hennig et al., 2017a). U-Pb zircon geochronology of the Schwaner intrusive rocks by Davies et al. (2014) and Hennig et al.

(2017a) concluded that subduction-related magmatism ceased around 85 Ma, but not due to collision with the Dangerous Grounds block, but to termination of Paleo-Pacific subduction. The Lupar Line was argued to represent a much younger strike-slip fault, possibly in the position of the Paleogene shelf break (Hall, 2012; Breitfeld et al., 2017a; Galin et al., 2017). Later uplift of the Rajang Group sediments is explained by a plate reconfiguration around 45 Ma and re-initiation of subduction around SE Asia. The onset of subduction of the proto-South China Sea beneath NW Borneo at the Sabah-Cagayan Arc (Hall, 2013a; Hall and Breitfeld, 2017) might have been the major contributing factor to the uplift in Borneo.

The tectonic change at c. 45 Ma is marked by the Rajang Unconformity which reflects the change from deep marine sedimentation of the Rajang Group to fluvial - shallow marine environments of Oligocene to Miocene stratigraphy in the Miri Zone, indicating uplift of Borneo (Hall and Breitfeld, 2017).

2.2 Stratigraphy

In this section we review previous stratigraphy of northwestern Borneo in Sarawak and Labuan, as well as provide a short summary of our revised stratigraphy for each unit, which is supported by new field and age data presented in the sections 4 to 9 and discussed in section 10. The textual juxtaposition of old and new stratigraphy is supported by Fig. 3 which shows our revised stratigraphy alongside a summarised previous stratigraphy column based on Madon (1994), Hutchison (2005) and Balaguru and Lukie (2012).

2.2.1 Rajang Group (Lupar and Belaga Formations)

Previous stratigraphy

The Rajang Group consists of the Upper Cretaceous Lupar Formation and the Upper Cretaceous to Upper Eocene Belaga Formation (Fig. 3) which both include steeply dipping, folded and slumped sandstones, siltstones, shales, and slates, forming debrites and turbidites (Wolfenden, 1960; Liechti et al., 1960; Tan, 1979; Bakar et al., 2007; Galin et al., 2017) that were deposited in submarine fans (Tongkul, 1997; Galin et al., 2017). The Belaga

Formation is exposed mainly in the Sibu Zone (Fig. 1) in Central Sarawak (Haile, 1974) but extends also into the southern part of the Miri Zone. Its thickness was estimated at 15 km by Haile (1974) and 4.5 - 7.5 km by Hutchison (2005).

Liechti et al. (1960) subdivided the Belaga Formation into five members (Fig. 3), which are the Layar, Kapit, Pelagus, and Metah Members in the Sibu Zone, and the youngest Bawang Member in the Miri Zone, but they recognised that this subdivision was only “approximately possible” due to monotonous lithologies and limited palaeontological evidence, and the relative ages of the upper members were speculative. In contrast, Heng (1992) extended the Metah Member northwards across the Bukit Mersing Line as far as the Pelugau River valley in the Miri Zone (Fig. 2a).

A more recent study by Galin et al. (2017) subdivided the Belaga Formation in the Sibu Zone into three units based on their depositional ages and provenance signatures (Figs. 1 and 3). Unit 1 (latest Cretaceous to earliest Eocene) consists of the Lupar Formation, Layar Member and Lower Kapit Member, Unit 2 (Early to Middle Eocene) includes the Upper Kapit and Pelagus Members, and Unit 3 (Middle to early Late Eocene) corresponds to the Metah Member. The term Bawang Member was retained for turbiditic sequences north of the Bukit Mersing Line because of their unknown depositional age and stratigraphic position. The Bawang Member has some provenance similarities to Unit 1 and Unit 2 (Galin et al., 2017).

Revised stratigraphy

Based on new field observations, age dating, and provenance analysis we propose that the turbidite sediments between the Bukit Mersing Line and the Arip River are equivalents of the Rajang Group in the Sibu Zone. Deeper parts of the successions have a well-developed cleavage and are exposed as fault blocks. They are here correlated with Units 1 and 2 of the Sibu Zone, while the youngest part of the sequence, termed here Unit 4 (Bawang Member), lacks a cleavage and is interbedded with volcaniclastics and limestones. This indicates that Unit 4 (Bawang Member) is tectonically/ structurally distinguishable from the underlying units (Units 1 and 2).

2.2.2 Igneous rocks (Bukit Piring, Arip Volcanics)

Previous stratigraphy

Magmatic rocks in the southern Miri Zone include granitoid rocks forming Bukit Piring and volcanic rocks along the northeastern flank of the Arip anticline (Wolfenden, 1960; Liechti et al., 1960; Heng, 1992; Hutchison, 2005) (Fig. 2a). The granitic to granodioritic Bukit Piring forms an E-W trending stock southwest of Tatau that has intruded steeply dipping turbiditic rocks (Wolfenden, 1960). Further to the east, volcanic rocks of the Arip Volcanics with a thickness of c. 450 m are exposed along the Arip ridge (Hutchison, 2005). Rocks are rhyolites, including welded tuffs and lavas, and andesites at the base (Wolfenden, 1960; Kirk, 1968) which are intensely hydrothermally altered forming agate and chalcedony alongside quartz in veinlets (Hutchison, 2005). Both the Bukit Piring granitoids and the Arip Volcanics show high-K calc-alkaline chemistries and were interpreted to have formed from the same magma as post-subduction Eocene volcanic rocks farther south in Kalimantan (Piyabong, Muller, and Nyaan Volcanics) related to extensional processes (Pieters et al., 1987; Bladon et al., 1989; Hutchison, 1996, 2005).

Revised stratigraphy

In this study we dated two samples of the Bukit Piring stock and one sample of the Arip Volcanics which have intruded or are interbedded with sediments of Unit 4 (Bawang Member). They yielded late Middle Eocene U-Pb zircon ages, which define Unit 4 (Bawang Member) as the uppermost part of the Belaga Formation within the Miri Zone but which is stratigraphically below the Rajang Unconformity (Fig. 3).

2.2.3 Arip Limestones

Previous stratigraphy

The Arip Limestones are poorly studied. They are interbedded with steeply dipping turbidites above the Arip Volcanics outcropping along the Arip ridge (Fig. 2a). Limestones reported from the area between the Pelugau and Arip Rivers by Wolfenden (1960) yielded foraminifera considered to be Late Eocene, and were assigned to the Tatau Formation. However, most of the assemblages reported could be Middle Eocene as the East Indian letter stages are difficult to correlate with the modern geological time scale (Adams et al., 1986; BouDagher-Fadel and Banner, 1999; McGowran, 2005). Wong (2011) also analysed foraminifera of the Arip Limestones which were reported to be Middle to Late Eocene, and retained the unit within the Tatau Formation.

Revised stratigraphy

Biostratigraphy carried out for eleven samples of the Arip Limestones in this study confirmed late Middle Eocene ages. However, in our stratigraphy we now consider the limestones to be parts of Unit 4 (Bawang Member) of the Belaga Formation (Fig. 3), as they are conformably interbedded with the Arip Volcanics and Unit 4 (Bawang Member) and not to be part of the Tatau Formation.

2.2.4 Tatau Formation

Previous stratigraphy

Originally De Boer et al. (1952) included the Tatau Formation in the Rajang Group. Kirk (1957) reported an unconformity above the Belaga Formation at Bukit Mersing in the Anap River region (Fig. 2a). The overlying rocks were described as medium-grained arenaceous well-bedded feldspathic sandstones and sandy shales, and assigned to the Tatau Formation. To the west, Wolfenden (1960) reported similar rocks in the Pelugau and Arip Rivers, including (calcareous) sandstones, shales, marls, lenses of limestones and volcanic rocks (i.e. Arip Limestones and Arip Volcanics), however, no unconformable contact with the Belaga Formation was found and the succession resembled turbidites of the Belaga Formation. Nevertheless, Liechti et al. (1960) and Wolfenden (1960) assigned these rocks north of the Bukit Mersing Line to the Tatau Formation and locally to the Bawang Member at the 'Tatau Horst' and east of the Bawang River.

North and south of the 'Tatau Horst' are exposures of the Rangsi Conglomerate (Mat-Zin, 2000; Hutchison, 2005) (Fig. 2a), or Tunggal-Ransi Conglomerate (Peng et al., 2004). The stratigraphic position of the conglomerate was interpreted differently by various authors. Liechti et al. (1960) proposed a Pliocene age and correlated it with the Begrih Formation; Mat-Zin (2000) suggested a correlation with the Miocene Balingian Formation, and Wong (2011) considered it to represent the base of the Tatau Formation together with the Arip Limestones. The depositional environment of the Rangsi Conglomerate was interpreted by

Wong (2011) as lower coastal plain to shallow marine, including fan delta and river lag deposits. North of Tatau, alternations of sandstones, siltstones, and shales on top of the Rangsi Conglomerate were reported as Oligocene by Wolfenden (1960) and also assigned to the Tatau Formation.

Revised stratigraphy

In our new stratigraphy (Fig. 3), we split the former Tatau Formation into three different parts. The first represents the lowermost Eocene part of Wolfenden's (1960) Tatau Formation between the Bukit Mersing Line and the Arip River. This is now assigned to the Rajang Group based on the lithological and structural similarities and new dating of interbedded magmatic rocks and limestones. In contrast, the term Tatau Formation is used here only for the Oligocene rocks above the Rajang Unconformity which are the Rangsi Conglomerate (lower Tatau Formation) and the overlying sandstones, siltstones, and shales (upper Tatau Formation) (Fig. 3).

2.2.5 Buan Formation

Previous stratigraphy

The Buan Formation is a c. 600 m thick succession of carbonaceous mica-rich shales which contain some thin siltstone and sandstone beds (Wolfenden, 1960) interpreted as deposited in a littoral to inner neritic environment by Liechti et al. (1960). It is conformable on the Tatau Formation and considered Oligocene based on its stratigraphic position (Wolfenden, 1960).

Revised stratigraphy

The Buan Formation is not discussed further in this paper and in our stratigraphy we follow Wolfenden (1960) in placing the Buan Formation conformably above the upper Tatau Formation (Fig. 3).

2.2.6 Nyalau Formation

Previous stratigraphy

The Nyalau Formation comprises c. 5000 to 5500 m thick clastic sediments of Oligocene to Early Miocene age which are exposed in the area between Balingian and Suai (Wolfenden, 1960; Liechti et al., 1960; Hutchison, 2005) (Figs. 1 and 3). The depositional environment was interpreted to be tide-dominated to coastal floodplain with some fluvial influence (Hutchison, 2005; Hassan et al., 2013). The Nyalau Formation is either conformably above or interfingers with the Buan Formation, or unconformably on top of the Belaga Formation, and grades laterally into the Setap Shale Formation (Wolfenden, 1960; Hutchison, 2005) (Fig. 3). The top of the formation is marked by an erosional surface (Wolfenden, 1960).

Revised stratigraphy

The Nyalau Formation is not discussed further in this paper, and in our stratigraphy (Fig. 3) we follow Wolfenden (1960), Liechti et al. (1960) and Hutchison (2005).

2.2.7 Setap Shale Formation

Previous stratigraphy

The Setap Shale Formation consists of a monotonous succession (c. 700 - 4700 m thick) of shales interbedded with thin sandstones and a few limestone lenses (Liechti et al., 1960; Kho, 1968). The basal boundary of the Setap Shale Formation is presumably unconformable (Liechti et al., 1960). The formation is of Late Oligocene to Early Miocene age (Haile, 1962; Sandal, 1996) and interpreted as the holomarine equivalent of the Nyalau Formation (Liechti et al., 1960; Hutchison, 2005). Its actual depth of deposition is uncertain, but Liechti et al. (1960) concluded inner neritic conditions for the majority of the Setap Shale deposits in the Miri Zone. Previously, some authors have also used the term Setap Shale to refer to the fine-grained muddy equivalents of the Miocene sandy formations in the northern Miri Zone/ Brunei region (e.g. Sandal, 1996) which led to an ambiguous use of the term.

Revised stratigraphy

In our stratigraphy we only use the term Setap Shale Formation for the inner to middle neritic equivalents of the Nyalau Formation in Sarawak, while some of the younger shales, for example the ones on Labuan which were studied in this work, have been assigned to the Lower Belait Formation (Fig. 3).

2.2.8 Balingian Formation

Previous stratigraphy

In the coastal region between the towns of Mukah and Balingian (Fig. 1), the Balingian Formation is unconformably on top of the Nyalau Formation, and overlain by the Begrih and Liang Formations (Liechti et al., 1960; Mat-Zin, 2000).

The Balingian Formation was described by Liechti et al. (1960) as sandstone with intercalations of clay and shale with abundant lignite. The thickness of the formation was estimated to exceed 3500 m (Wolfenden, 1960). Wolfenden (1960) and Liechti et al. (1960) assumed a Late Miocene age based on foraminifera assemblages, and its depositional environment was interpreted to be estuarine, lagoonal to very shallow marine (Wolfenden, 1960; de Silva, 1986). More recently, facies interpretations from heterolithics and coal seams by Nugraheni et al. (2014) include intertidal flats, floodplain, river mouth, and upper delta plain environments, and the depositional age of the formation was interpreted either as Early Miocene by Sia et al. (2014) based on palynomorphs and the architecture of coal seams observed in the Mukah coalfield, or Early to Middle Miocene by Murtaza et al. (2018) based on palynology.

Revised stratigraphy

Here, we believe that an uppermost Early to Middle Miocene age seems most appropriate (Fig. 3), as an Early Miocene age would suggest it to be a lateral equivalent of the upper part of Nyalau Formation, which conflicts with the unconformable contact between the Nyalau Formation and the Balingian Formation.

2.2.9 Begrih Formation

Previous stratigraphy

The Begrih Formation (Figs. 2b and 3) is composed of sandstone, conglomerate, clay, and coaly layers (Liechti et al., 1960; de Silva, 1986). The basal part is formed by a thick basal conglomerate that was interpreted to mark the supposed unconformity with the Balingian Formation (Wolfenden, 1960; Sia et al., 2014). In some places, however, the contact has been described as conformable (Liechti et al., 1960). Wolfenden (1960) reported a brackish-water fauna, and the formation age was presumed to be Early Pliocene (Liechti et al., 1960) or Late Miocene by Murtaza et al. (2018) based on palynology.

Revised stratigraphy

Based on our field observations, which identify similar lithologies below and above the massive conglomerates, we challenge the interpretation of Wolfenden (1960) and Sia et al. (2014), who described the Begrih Formation as unconformable above the Balingian Formation. Here we consider the previously reported unconformity to represent a sequence boundary. We placed the Begrih Formation in the Middle Miocene (Fig. 3) based on recent dating of the underlying Balingian and overlying Liang Formations by Murtaza et al. (2018) and Ramkumar et al. (2018).

2.2.10 Liang Formation

Previous stratigraphy

The Liang Formation forms the uppermost unit in the Mukah-Balingian province, and is faulted against the Belaga Formation (Wolfenden, 1960; Hutchison, 2005). It was initially termed the Sikat Formation (Liechti et al., 1960; Peng et al., 2004) until Liechti et al. (1960) and Wolfenden (1960) renamed this unit to Liang Formation because it showed some similarities to the Upper Pliocene to possibly Pleistocene Liang Formation in northern Sarawak and in Brunei, where it has its type locality.

The Liang Formation near Mukah is c. 500 - 3000 m thick and composed of clay, sand, lignite, and conglomeratic sand lenses (Liechti et al., 1960; de Silva, 1986; Hutchison, 2005). The contact with the Begrih Formation was initially described as unconformable (Wolfenden, 1960), but de Silva (1986) did not find a distinction between the Liang and Begrih Formations and suggested combining both units using the informal formation name 'Begrih-Liang'. Nonetheless, they remained separate units in the revised geological map of Heng (1992). The formation also includes coal seams which are referred to as the Balingian coalfield by Hakimi et al. (2013) and Sia et al. (2014). The depositional environment was interpreted as brackish marginal to shallow marine (Wolfenden, 1060; Hakimi et al., 2013).

Murtaza et al. (2018) concluded a Late Pliocene to Pleistocene age for the Liang Formation based on palynology. More recently, a tephra deposit within the coalfield has been dated by Ramkumar et al. (2018) and revealed a latest Middle Miocene age (c. 12 Ma), thus indicating a slightly older age for the sequence than previously assumed, and a correlation with the Liang Formation in the northern Miri Zone/Brunei therefore seems inappropriate.

Revised stratigraphy

In this study we retain the separation between the Begrih and Liang Formations for geographic reference of the samples, but illustrate their similar character and provenance by using the same colour in Figs. 2b and 3. The age of the Liang Formation in the Mukah-Balingian province is latest Middle Miocene as defined by the interbedded tephra layer reported by Ramkumar et al. (2018).

2.2.11 Belait Formation

Previous stratigraphy

The Belait Formation (Figs. 2c and 3) is extensively exposed on Labuan (Wilson and Wong, 1964) and in Brunei (Sandal, 1996), and only locally exposed in Sarawak, where it is mapped in the interior around the town of Beluru (Fig. 1) and belongs to the Miocene formations in the northern Miri Zone of uncertain stratigraphy (Liechti et al., 1960; Heng, 1992) (Fig. 3).

The Belait Formation has an estimated thickness of 2500 m (Liechti et al., 1960) and is composed of mostly cross-bedded coarse-grained white sandstones, clays, and sandy shales (Kirk, 1957; Haile, 1962). Haile (1962) interpreted a paralic environment with sporadic marine influence for the formation. The formation contains no age diagnostic fauna in Sarawak (Kirk, 1957; Haile, 1962); Sandal (1996) reported Lower to Upper Miocene foraminifera from Brunei.

Revised stratigraphy

Based on the similar ages, lithologies, depositional environments, and provenance we propose that the fluvial to shallow marine successions on Labuan (Figs. 1 and 2) are equivalents of the Balingian, Begrih and Liang Formations in the Mukah-Balingian province, and are termed Lower, Middle, and Upper Belait Formations in our stratigraphy (Fig. 3).

3. Methodology

Field observations were made in the Mukah-Balingian and Tatau regions of Sarawak and on Labuan (Figs. 1 and 2), and included sampling, and measurements of bedding, cleavage, and faults, recorded using dip direction and dip angle.

Two samples of the Bukit Piring stock were analysed by whole-rock X-ray fluorescence (XRF) spectrometry at Royal Holloway University of London on a PANalytical Axios sequential X-ray fluorescence spectrometer equipped with a 4 kW Rh-anode X-ray tube (Supplementary File 1). Rocks were ground in a tungsten-carbide barrel to a fine homogeneous powder, which was used to prepare fusion disks and pressed pellets for major and trace element analyses, respectively. Reproducibility was tested by re-analysis of three samples of the same batch. The data was plotted using GCDkit 2.3 (Janoušek et al., 2006).

Covered thin sections were prepared for limestone samples of the Balingian Formation, Bau Limestone Formation, and Arip Limestones, and analysed for biostratigraphy, following the approach described in BouDagher-Fadel (2008) which primarily use the Planktonic Zonation scheme (PZ) of BouDagher-Fadel (2018b), which is tied to biostratigraphical time scale and the radioisotopes (as defined by Gradstein et al., 2012 and revised by Cohen et al., 2013). In this paper, the PZ scheme of BouDagher-Fadel (2018b) is also correlated with the larger benthic foraminiferal 'letter stages' of the Far East, as defined by BouDagher-Fadel and Banner (1999) and later revised by BouDagher-Fadel (2008, 2018a).

Twenty-three thin sections were analysed for light minerals. The slides were stained for K-feldspar and plagioclase following standard procedures. Point-counting analysis was performed on a Zeiss Axiolab with an automatic stepping stage and the software PetrogLite. The classification used is based on the Gazzi-Dickinson method (Dickinson, 1970; Gazzi et al., 1973). Five hundred counts were made for each sample over an evenly distributed grid to obtain 221 to 499 framework grains (Supplementary File 2). The samples are classified using the QFL diagram of Pettijohn et al. (1987), and the QFL and QmFLt provenance diagrams of Dickinson et al. (1983).

Heavy minerals from nine samples were identified using optical and secondary electron microscopy. Analysis was carried out on a Hitachi S3000N SEM equipped with a SDD-X-Max^{50} EDS/EDX detector using heavy mineral separates which were mounted in Araldite resin and polished for exposure. Only translucent grains were counted, with counts ranging between 264 and 650 in all samples (Supplementary File 3). Opaque minerals were mainly ilmenite, and subordinate pyrite and ilmenorutile. All TiO_2 minerals were counted as rutile. Samples MB-12 and TB200a contained chlorite at 15.4% and 23.1% respectively which was excluded from the heavy mineral assemblage as chlorite is often related to alteration processes.

Zircons were separated from sedimentary rocks using mortar and pestle, and washed using disposable nylon meshes to extract a grain size fraction of 63 to 250 µm. The grains were further washed with sodium hexametaphosphate to remove any muds from the samples before standard density separation techniques were used, including LST heavy density liquid and Frantz magnetic separation. Magmatic rocks were crushed in a tungsten-carbide disk mill, sieved using nylon meshes and zircons ≤250 µm were extracted using a Wilfley table, Frantz magnetic separation, and DIM heavy liquid density separation.

The separated zircons were mounted in Araldite resin, polished for exposure, and imaged by transmitted light and cathodoluminescence to detect cracks and inclusions, as well as internal morphologies, used for laser spot selection and data interpretation. Zircon U-Pb LA-ICP-MS analysis was performed at UCL/ Birkbeck College on a New Wave NWR 193 nm laser ablation system coupled to an Agilent 7700 quadrupole-based inductively-coupled plasma mass spectrometer. Analyses were made using a 25 µm beam size and reference to the Plešovice zircon (337.13 ± 0.37 Ma; Sláma et al., 2008) and NIST 612 silicate glass (Pearce et al., 1997) standards. Data reduction was carried out using the GLITTER software package (Griffin et al., 2008). The U-Th-Pb isotope ratios (± 1σ errors) were corrected for common Pb (Andersen, 2002). ^{206}Pb-^{238}U ages were reported for ages <1 Ga; ^{207}Pb-^{206}Pb ages for ages ≥ 1Ga (Supplementary File 4). The ages were considered as discordant if the ^{206}Pb-^{238}U/ ^{207}Pb-

^{235}U or the ^{207}Pb-^{206}Pb/ ^{206}Pb-^{238}U age difference, respectively were greater than 10%. Histograms and probability density plots were calculated using a script written by I. Sevastjanova based on Sircombe (2004) for the R language (R Core Team).

4. Field observations and petrography

4.1 Belaga Formation

Exposures of the Belaga Formation are described from south to north in this section. South of the Bukit Mersing Line are steeply dipping debrites and turbidites which were assigned to the Metah Member of the Belaga Formation (Liechti et al., 1960; Heng, 1992) or Unit 3 of the Rajang Group (Galin et al., 2017). The contact with the Neogene Liang Formation (Fig. 2b) is not exposed along the road between Mukah and Balingian, however, a c. 50 m wide depression separates the units and likely represents a wide fault zone.

Farther to the east, the road crosses the Bukit Mersing Line and exposes highly weathered grey phyllites. They are calcareous in places with calcite veins, probably related to hydrothermal alteration along the fault zone. Similar rocks, although non-calcareous, were found approximately ten kilometres farther to the northeast, which are likely related to a fault zone subparallel to the Bukit Mersing Line along the Pelugau River. Rocks between the Bukit Mersing Line to the south and the Pelugau River to the north are here assigned to the Belaga Formation (similar to Units 1 or 2) (Fig. 2a). Sediments of this unit were studied from an outcrop near the Balingian River (Fig. 2a), exposing steeply dipping slates (bedding: 170/70) (Fig. 4a), which are interbedded with planar-bedded siltstone lenses (Fig. 4b). The rocks are folded at mesoscopic scale and contain several elongated and folded quartz lenses.

The area to the north between the Pelugau and Arip Rivers (Fig. 2a) is highly vegetated and inaccessible. Limited outcrops of shaly mudstones interbedded with white-greyish volcaniclastics (Fig. 4c) are exposed at the roadside east of the Bawang River and assigned here to Unit 4 (Bawang Member). These sediments are adjacent to a nearby outcrop which exposes deeper parts of the Rajang Group formed by subvertically dipping alternations of thick beds of medium-grained sandstones and fine-grained dark slates interbedded with siltstone layers, resembling the exposures between the Bukit Mersing Line and Pelugau

River (Fig. 4d). The beds dip at high angles to the NNW (bedding: 355/81) and a younging trend towards the north was determined from scoured bases and normal grading in sandstone beds. The contact is interpreted as faulted. In contrast to Unit 4 (Bawang Member), no volcaniclastic layers were observed and the slates show a pervasive cleavage (Fig. 4e) (cleavage: 198/65), suggesting a deeper burial depth compared to the shaly mudstones of Unit 4 (Bawang Member).

Sediments immediately north and south of the Arip River (Fig. 2a) are also included in Unit 4 (Bawang Member). They consist of thick steeply dipping beds of medium- to coarse-grained sandstones (c. 2 m thick) and dark shales (c. 2-20 cm thick), which dip at a similar orientation as the sediments studied to the south (beddings south of Arip fault: 335/72; north of Arip fault: 341/55), and are also interbedded with white-greyish volcaniclastics (c. 2-5 cm thick) (Fig. 4f), as well as rhyolites of the Arip Volcanics along the Arip valley (Fig. 2a). Rocks of Unit 4 (Bawang Member) continue approximately 4.5 km farther to the northeast of Arip River, where steeply dipping grey siltstones to medium-grained sandstones with fine-grained weakly cleaved shale lenses were observed that are also interbedded with white clay-rich volcaniclastics (Fig. 4g) (TA-01).

To the northeast, the Belaga Formation is exposed north of the Kelawit Fault (Fig. 2a). This low-lying countryside was referred as the 'Tatau Horst' by Liechti et al. (1960) and Hutchison (2005). Here the term Tatau high is used to describe this fault-bounded block as it does not resemble a horst structure. Mat-Zin (2000) interpreted it as a positive flower structure related to transpressional strike-slip deformation. A large roadcut at the northern part of the Tatau high exposes c. 5 m of sandstone - shale alternations with shale-dominated turbidites at the bottom followed by more sand-dominated units at the top (Fig. 4h). The shales are weakly cleaved in places. Interbedded sandstones show current ripples highlighted by mud drapes on the foresets (Fig. 4i). Other exposures in the area consist of deeply weathered, steeply dipping shale-sandstone alterations that are mostly covered by dense vegetation. These rocks are here assigned to the middle parts of the Rajang Group turbidite sequences (Figs. 2a and 3).

4.2 Igneous rocks of Unit 4 (Bawang Member)

The Arip Volcanics immediately north of the Arip Fault were studied (TB55) (Fig. 2a). The rocks are intensely weathered, showing a fine-grained clay-rich matrix with angular quartz crystals that suggest a rhyolitic composition. In thin section, the rocks show a fine-grained sub-volcanic texture of granoblastic quartz and feldspar phenocrysts.

Granitoid rocks of Bukit Piring (Fig. 2a) were sampled from a stock pile on the southern side (BP-01) and from higher elevations at the northern flank (BP-02). Sample BP-01 is an un-oriented medium-grained fresh rock which consists of quartz, K-feldspar, and plagioclase, as well as subordinate amphibole, garnet, and an opaque phase. Some quartz phenocrysts have embayed grain boundaries and some inclusions, indicating a hypabyssal character (Fig. 5a). Feldspar often has a myrmekite texture, and amphiboles show symplectites at rims. Secondary calcite is also present, which indicates hydrothermal alteration.

Sample BP-02 is a moderately weathered granitic sample. It has a more felsic composition than BP-01, including undulose quartz and quartz subgrains, and sericite-altered K-feldspar and plagioclase.

4.3 Arip Limestones of Unit 4 (Bawang Member)

The Arip Limestones were sampled at three locations of the 'stone road' mine along the northern flank of the Arip ridge (Fig. 2a). Samples AL1 and AL2 are located very close to one another, c. 13 km southeast from the main road (Fig. 5b), while sample AL3 comes from another outcrop c. 8 km into the valley from the main road. Three to five hand specimens were collected from each location. The rocks are fine-grained dark slaty marls and limestones that contain abundant planktonic foraminifera.

4.4 Tatau Formation

The Tatau Formation is revised in this study to include the deposits around the Tatau high (Fig. 2a), as well as along the western flank (Wong, 2011). The Rangsi Conglomerate forms the base of the Tatau Formation which lies unconformably above the Belaga Formation (Fig. 3).

The conglomerates, locally exposed by the road south of the Tatau high (TA-04, TB54), consist of c. 1 - 3 m thick, low dipping beds of clast-supported conglomerates with a sand matrix (Fig. 6a). The rocks are interbedded with a c. 0.5 m thick matrix-supported conglomerate layer with a mud-dominated matrix (bedding: 255/40) (Fig. 6b). The clasts are pebble- to boulder-size subangular to subrounded quartz, slates, medium-grained sandstones, quartzites, and weathered rhyolites (Fig. 6c). Locally, the matrix-supported conglomerates are cut by a clastic dyke with reworked fragments of the overlying sandy conglomerate layer (Fig. 6d), indicating overpressured sedimentary layers or seismic activity.

To the north of the Tatau high, a c. 20 - 30 m thick sequence of sand-dominated conglomerate beds unconformably overlie moderately dipping alternations of slates and siltstones of the Belaga Formation, as described by Galin et al. (2017). The conglomerate beds (TB199b) are c. 1.5 m thick and interbedded with mud- to siltstones of c. 10 - 60 cm thickness, dipping at low to moderate angles to the NE (bedding: 028/30) and are overlain by thick sandstone beds (Fig. 6e). The conglomerate bases are often scoured. The clasts are predominantly of quartzites, cherts and gabbros. The sandstone beds include thin mudstone layers of max. 5 cm thickness, and show trough cross-beds, representing 3D mega-ripples (Fig. 6f). This might indicate a rapid change from fluvial to shallow marine/ nearshore facies related to rapid deepening of the basin, which is supported by Wong (2011) who described bioturbated sandstones from this outcrop.

Farther to the northeast, the dip of the bed decreases; these low north-dipping beds of sandstones (TB200a) and shales (bedding: 020/05) (Fig. 6g, h) are assigned to the upper Tatau Formation (Fig. 3). They also show planar and trough cross-bedding, indicating a fluvial depositional environment.

4.5 Balingian Formation

The northernmost outcrop along the road from Selangau to the coast between Mukah and Balingian (Fig. 2b) exposed a c. 0.5 m thick mudstone unit at the base, followed by c. 1 m thick subhorizontally-bedded quartz-rich siltstones and sandstones which include thin coal layers (c. 0.1 - 0.3 mm thickness), and some plant fragments and rootlets.

Two kilometres farther to the south, a 2 m thick unit of subhorizontal sand- and mud-dominated heterolithics is exposed at the roadside (Fig. 7a). The rocks consist of laminated fine-grained sandstones and siltstones, and thin irregular carbonaceous mudstone layers or lenses. Locally, the bedding is more crude and wavy or convolute. The beds contain abundant irregular granules- to pebble-size coal fragments, often in layers at the top of beds, as well as subangular to rounded clasts of sandstones, limestones, quartzites, dark-red chert, and basic igneous rocks in conglomerate layers (Fig. 7a). All clasts are between c. 3 - 10 cm in length. Coal debris is also present in thin bands parallel to the bedding. The bedding is cut by vertical rootlets. Nearby, the heterolithics are interbedded with thick alternating carbonaceous mudstone and coal seams (max. 35 cm thickness) (Fig. 7b), which contain some fossilised wood. Locally, the heterolithic beds are inclined (bedding: 020/22) (Fig. 7c).

Approximately 2.5 km north of the boundary to the Begrih Formation (Fig. 2b), a relatively sharp contact was observed between the carbonaceous mud-dominated heterolithics at the base and coarse-grained sandstones (0.5 - 3 m thick) on top (Fig. 7d) which show some trough cross-bedding. The beds dip to the south at low to moderate angles and fine- to medium-grained sandstones are exposed for c. 50 m along the road (Fig. 7e). The sandstones are subhorizontal, showing planar cross-bedding with thin coal layers or mud drapes on the foresets, and are interbedded with thin undulated subhorizontal mudstone layers (c. 1 cm thick) or lenticular mud lenses (Fig. 7f). Large coal fragments (max. 20 cm in length) are scattered within the sandstone unit, and locally brownish elongate mud clasts were observed in layers or clusters. Some bioturbation includes rounded burrows, possibly *Ophiomorpha* (Fig. 7f). The sequence is cut by vertical to subvertical syn-sedimentary faults which are partly filled with mudstones and show small vertical displacement (offset c. 5 cm)

(Fig. 7g). The sandstones form stacked lenticular bodies in places which are capped by mudstones (Fig. 7h).

4.6 Begrih Formation

The lower boundary of the Begrih Formation is marked by a thick unit (c. 10 m) of conglomerates, pebbly sandstones, and sandstones (Fig. 8a), which is interbedded with thin mudstone or mudstone - siltstone heterolithics layers (c. 5 - 20 cm thickness).

Dark homogeneous mudstones and convolute-bedded sandstone-mudstone heterolithics with thin coal layers are exposed at the base of the conglomeratic unit (Fig. 8b). They are overlain by medium-grained sandstones (c. 15 - 20 cm thick), which form erosive bases overlain by coarse-grained sandstone lag deposits (Fig. 8c). The sequence consists of massive sandstones, pebbly sandstones, and interbedded conglomerates, which form inclined layers of up to 50 cm thickness, and show coarsening and fining upward sequences, as well as planar cross-bedding (Fig. 8d). The clast-supported conglomerates are poorly sorted and contain subrounded to rounded pebbles of quartz, fine-grained sandstone, mudstone and slate (c. 3 - 5 cm in length) in a sand-dominated matrix. Locally, large reworked coal blocks of up to 60 cm in length were observed in the conglomerates. Ironstone from weathering is abundant throughout the conglomerates, as well as on the bedding planes of the sandstones and pebbly sandstones, forming hard bands along the beds.

Farther to the south, small outcrops of subhorizontally or moderately dipping heterolithics are exposed. They consist of fine-grained sandstones (max. 20 cm thick), some show coarsening upward sequences, *Skolithos* Ichnofacies, and thin mudstone layers (c. 1-3 cm thick) with carbonaceous mud and lignite bands that form a wavy bedding (Fig. 8e). The sandstones show a pervasive limonitic weathering in the pore spaces throughout the section. Locally, the beds form stacked packages with erosive bases (Fig. 8f), and show iron-oxide weathering along the bedding planes, as well as ironstone nodules.

The southernmost outcrop of the Begrih Formation is c. 3 m high (Fig. 8g) and shows a subhorizontal succession of massive conglomerates at the base (c. 1.5 m thick), which are interbedded with thin siltstone to sandstone layers, and have erosive bases with scours (Fig. 8h). The middle part of the section is dominated by heterolithics (c. 0.5 m thick) of siltstones and (carbonaceous) mudstones, which alternate with pebbly sandstones (Fig. 8i). A c. 10 cm thick conglomerate bed forms the base of the pebbly sandstones. The heterolithics show wavy lamination and current-ripple cross lamination. A c. 4 cm thick mud layer forms the top of this bed, which is followed by c. 15 cm of fine-grained sandstone that grade upwards into alternating beds of fine-grained sandstones with mud lenses, and small bands of heterolithics which show a wavy lamination. Towards the top of this c. 0.5 m thick bed, the sandstones become more dominant again. A thin mudstone band forms a sharp boundary to a similar sequence on top, indicating cyclic deposition. The unit contains abundant rounded or elongated burrows (*Ophiomorpha*), some with iron-oxide crusts (Fig. 8k). Herringbone cross-stratification was observed in a small sandstone layer (c. 3 cm thick) (Fig. 8l).

4.7 Liang Formation in the Mukah-Balingian province

The lower part of the Liang Formation in the Mukah-Balingian province is marked by heterolithic alternations of subhorizontal mudstone and siltstone layers of 2 to 20 cm thickness, which show flaser bedding and current ripple cross-lamination (Fig. 9a), as well as convolute bedding in places (Fig. 9b). Locally, the mudstones contain thin lignite bands. Planar cross-bedding with lignite foresets was observed in the siltstones as well as occasionally lenses of reworked coal fragments.

The heterolithics are abundant in the lower part of the formation and show variable dip of beds. Locally, medium-grained poorly-sorted sandstones are exposed in between which contain small clay pebbles (0.5 - 1.0 cm in length) forming rip-up clast conglomerates.

Sediments farther towards the south are planar-bedded medium- to coarse-grained sandstones, which are interbedded with thin mudstone layers and a small conglomerate band (c. 5 - 10 cm thick) (Fig. 9c). The latter are poorly sorted and contains subrounded to rounded sandstone pebbles and cobbles, as well as angular granule- and pebble-size quartz. Thin bands of reworked coal fragments are at the top of the sandstone beds. A c. 1.5 m thick layer of thinly bedded shaly mudstones forms the top of the sequence.

The southernmost deposits of the Liang Formation represent the top of the Mukah-Balingian formations and are moderately dipping alternations of conglomerates and pebbly sandstones with heterolithics of mudstone and siltstone layers (bedding: 177/46) (Fig. 9d). The conglomerate and pebbly sandstone beds are between c. 5 cm to 1 m thick, erosive-based, and show coarsening- and fining upward sequences, as well as pinching out structures. They are poorly sorted and have a mud-dominated matrix. The majority of clasts are angular quartz granules, subangular to rounded pebbles of sandstone and siltstone, and elongate mudstone and slate clasts (Fig. 9e). Subordinate small coal bands were locally observed.

The heterolithics form thick beds of subhorizontally laminated to wavy-bedded siltstone layers and mudstones (c. 0.5 - 1.5 m thick). Locally, some thicker siltstone layers (c. 5-10 cm thick) also show convolute bedding, or trough cross-bedding with truncation of top sets, interpreted as hummocky cross-stratification (Fig. 9f). The heterolithics contain some coal clusters or are interbedded with thin lignite or coal bands. They also contain abundant burrows of *Ophiomorpha* and *Skolithos* (Fig. 9g, h), and show several syn-sedimentary structures (Fig. 9i, k), such as flute casts (flow direction towards WNW), flame structures, and dewatering structures. The rocks are fractured and cut by several small faults. Subordinate moderately dipping thrust faults are cut by steeply dipping fractures.

4.8 Belait Formation on Labuan

The Belait Formation is the youngest unit on the island of Labuan (Figs. 2c and 3) and is correlated in this study with the late Early to Middle Miocene sediments in the Mukah-Balingian province.

4.8.1 *Lower and Middle Belait Formations*

In the Labuan anticline (LTB-2; Fig. 2c), there is a sharp contact from rippled mud-dominated heterolithics at the base (Lower Belait Formation) towards thick conglomerates and pebbly sandstones at the top (Middle Belait Formation) (Fig. 10a). The conglomerates form a distinct NW-SE trending ridge across northern Labuan (Fig. 2c). They are sand-matrix-supported to clast-supported, generally unsorted, and consist of pebbles and cobbles of rounded quartz and mud clasts (Fig. 10b), red laterite clasts (Fig. 10c), and coal fragments. The conglomerates are interbedded with cross-bedded centimetre-thick sandstones. The succession is overlain by thick lenticular cross-bedded sandstone bodies that grade into carbonaceous or reddish-coloured siltstone - mudstone alternations with thin coal seams (Fig. 10d). Coalified logs and coal fragments are also common in the thicker sandstone bodies (Fig. 10e).

4.8.2 *Upper Belait Formation*

To the north of the island, the Belait Formation is composed mainly of subhorizontal thick sandstones, forming large channels (Fig. 10f), which are interbedded with mudstones and heterolithics assigned here to the Upper Belait Formation (Fig. 10g). The sandstones are predominantly medium-grained with cross-bedding and possibly hummocky cross-stratification (Fig. 10h). Channels of various sizes are formed by lenticular beds which consist of 3D mega-ripples and can exceed two metres in thickness (Fig. 10f). Small-scale ripples are common in some exposures and are mainly symmetrical wave ripples (Fig. 10i). Lenticular and wavy bedding, and mud drapes on top of foresets were observed. Beds are generally highly bioturbated with abundant, e.g. *Skolithos*, *Cruziana* and *Ophiomorpha* (Fig. 10k). Water escape structures, load structures, syn-sedimentary faults (Fig. 10i), and slumped beds are present and indicate instability of the deposits. In some places thin lag conglomerates, including coal clasts, are associated with the sandstones. Mudstones are usually dark-coloured and are composed of carbonaceous material. They are interbedded with thin siltstones or sandstones and can form heterolithics.

4.9 Depositional environment interpretations of the Neogene formations

4.9.1 Balingian Formation

Carbonaceous mudstones and thick coal seams indicate predominantly quiet waters in swamp forest areas. Sandstone- and mudstone-dominated heterolithics may represent tidally-influenced sequences, or overbank facies and floodplain deposits (Heldreich et al., 2017). Inclined and/or amalgamated heterolithic packages with erosive bases indicate tidal-dominated point-bar deposits or channel fills (Choi et al., 2004; Olariu et al., 2015) or could be similar to local scour-and-fill structures or syn-sedimentary deformation related to minor tectonic events as described by Madon and Rahman (2007) for the Nyalau Formation. Thin bands of interbedded conglomerates and sandstones with mud rip-up clasts are likely related to flooding events. Thick sandstones show planar and trough cross-bedding, and *Ophiomorpha* burrows, indicating fluvial-dominated channels in a deltaic brackish environment (Benton and Harper, 1997). The lenticular bodies are interpreted as amalgamation of laterally stacked channels (Reading, 1996).

4.9.2 Begrih Formation

Massive conglomerates with subrounded and rounded clasts, and (pebbly) sandstones with erosive bases at the boundary with the underlying Balingian Formation indicate a change to a more fluvial-influenced environment, represented by channels cutting across the tide-dominated delta front and swamp deposits. The conglomerates are interpreted as lag deposits at channel bases or channel bar deposits. Interbedded heterolithics with thin coal layers may represent tidal or floodplain deposits. Herringbone cross-stratification in a sandstone bed within the heterolithics indicates bidirectional flow, often associated with a tidally-influenced sandy shoreface environment (Benton and Harper, 1997; Nichols, 2009), which is supported by abundant bioturbation.

4.9.3 Liang Formation in the Mukah-Balingian province

The Liang Formation is dominated by thick siltstone and mudstone heterolithics with thin lignite and coal layers. The sediments indicate floodplain deposits in a deltaic environment. Flaser bedding and abundant bioturbation, including *Skolithos* Ichnofacies (Benton and

Harper, 1997), supports a tidally-dominated environment. Some beds show hummocky cross-stratification and interbedded thin conglomerate layers, interpreted as shoreface storm deposits (Kumar and Sanders, 1976). The heterolithics alternate with conglomerates and pebbly sandstone beds that have erosive bases and coarsening and fining upward sequences, indicating fluvial-dominated channels in a deltaic brackish environment. Water escape structures observed in the heterolithics indicate high sediment supply and rapid aggradation (Lowe, 1975).

4.9.4 Lower and Middle Belait Formation

The mud-dominated heterolithics at the base are interpreted as shallow marine deposits, interpreted as part of a shoreface or inner shelf environment or possible tidal flats. These resemble the Balingian Formation below the Begrih Formation in the Mukah-Balingian province (Figs. 2b, c and 3). The conglomerates form the base of a fluvial channel complex that shows similarities to the Begrih Formation to the south (Figs. 2b, c and 3). Clast-supported conglomerates indicate bedload deposition from stream flows (Reading, 1996) and matrix-supported conglomerates indicate debris flows or coarse channel fills (Nemec and Steel, 1984; Miall, 1996). Lenticular sandstone bodies are interpreted as fluvial channels and together with the conglomerates and pebbly sandstones they form an amalgamated fluvial channel complex of c. 20 to 40 m thickness. Carbonaceous muds and seams on top of the fluvial channel complex represent floodplain or swamp environment. Red-coloured mudstone-siltstone alternations indicate overbank facies (Nichols, 2009). Above the fluvial complex are shallow marine shoreface deposits, as indicated by the tidally wavy and lenticular bedded heterolithics on top, similar to the sediments below the conglomerates.

4.9.5 Upper Belait Formation

Hummocky cross-stratification indicates storm wave deposits in a shallow marine environment (shoreface, shelf) (Kumar and Sanders, 1976). Lenticular and wavy bedding is typical found in tidal environments (Nichols, 2009). *Ophiomorpha* indicates a high energy shoreface environment (Nagy et al., 2016) and *Skolithos* may indicate a sandy shore to shelf environment (Bromley and Asgaard, 1991; Buatois and Mángano, 2011). Instability of beds and load casts indicate rapid deposition with high sediment supply (Nichols, 2009). Thick sandstones are interpreted as subaqueous or tidal channels. Carbonaceous material and coal clasts were probably washed in from nearby coastal floodplains. The thicker mudstone successions are part of a shoreface or inner shelf environment, or represent tidal flats. The deposits are considered equivalent to the Liang Formation in the Mukah-Balingian province (Figs. 2b, c and 3).

5. Bulk rock chemistry

Two Bukit Piring samples (BP-01, BP-02) were geochemically analysed in this study (Supplementary File 1). The results were compared to a few previous analyses reported by Wolfenden (1960), Kirk (1968) and Wong (2011) from Bukit Piring and the Arip Volcanics, to characterise Eocene magmatism in northwestern Borneo.

The analysed rocks are calc-alkaline and high-K calc-alkaline in the SiO_2 - K_2O diagram of Peccerillo and Taylor (1976), have ferroan, calc-alkalic, and peraluminous compositions (Frost et al., 2001) (Fig. 11a, b), and are classified as granite to alkali-granite (BP-01), and quartzolite (BP-02), determined from the R1-R2 diagram of De La Roche et al. (1980) and the SiO_2 vs. Na_2O + K_2O diagram of Middlemost (1994) (Supplementary File 1). However, the high SiO_2 of BP-02 suggests extensive secondary recrystallization, and interpretations based on alkali element contents are unlikely to be valid.

Both samples are similar to the previously reported analyses from Bukit Piring and the Arip Volcanics (Fig. 11a, b), which are calc-alkaline to high-K calc-alkaline (Peccerillo and Taylor, 1976), magnesian to ferroan, calc-alkalic, and metaluminous to peraluminous (Frost et al., 2001), and classified as andesi-basalt, tonalite, and (alkali-) rhyolites (De La Roche et al., 1980).

Trace element contents of rocks from Bukit Piring (BP-01, BP-02) can help to further characterise the rocks and the tectonic setting in which they formed, although caution is required as they may reflect an earlier tectonic setting (Frost et al., 2001). Both samples have undergone significant secondary alteration, especially BP-02. Therefore, two additional samples reported by Wong (2011) were included which both have very similar major and trace element concentrations as sample BP-01. The four samples plot at the boundary of the within-plate and volcanic-arc granite fields in the diagrams of Pearce et al. (1984) (Fig. 11c), which could support a post-collisional setting, according to Pearce (1996). Similarly, they also plot at the boundary with, or in, the A-type fields in the diagrams of Whalen et al. (1987). Based on the classification scheme of Frost et al. (2001), almost all samples of Bukit Piring and the Arip Volcanics from this study and the literature indicate an A-type signature, which reflects the within-plate post-collisional character; only the andesitic volcanic sample has similarities to Cordilleran batholiths. Samples BP-01, BP-02 and the two samples of Wong (2011) of Bukit Piring form very similar curves in the N-MORB normalised spider diagram of Sun and McDonough (1989) (Fig. 11d). They show enrichment of mobile elements (Rb, Ba, U, K), probably related to late-stage hydrothermal alteration, and relative Nb, Sr, P, and Ti troughs and Pb, Nd-Zr-Sm and Y peaks. Sample BP-02 has more pronounced Nd and Sm peaks, as well as an additional La-Ce peak. The very high LREE contents of BP-02, and the 5000ppm As, are unlikely to be of magmatic origin. This latter suggests that this sample has been mineralized as well as silicified, although the high As is not coupled with elevated Cu, Zn, Pb or S. The spider diagram patterns are very irregular and differ from a classic volcanic-arc signature, which shows characteristic Nb and Ti troughs and a Pb peak, and support a within-plate character for the samples.

6. Biostratigraphy

Thin sections of two limestone samples from the Balingian Formation and three samples of the Arip Limestone were analysed for biostratigraphy (Tab. 1; Supplementary Files 5.1 and 5.2).

Limestone clasts interbedded in heterolithics of the Balingian Formation are classified as micritic packstones of algae which contain *Bacinella irregularis*, *Palaeodasycladus* spp., *Pseudocyclammina* spp., *Pseudocyclammina lituus*, *Choffatella* sp., *Textularia* sp. and small miliolids. They indicate a shallow reefal to backreefal environment and an Early Cretaceous (Berriasian to Barremian, 145.0-125.0 Ma) depositional age (Tab. 1).

These limestone clasts must have been reworked from older rocks. No limestones of late Mesozoic age are known from the Tatau area. The Bau Limestone Formation in the Kuching Zone to the southeast is a potential source but is reported to be mainly Late Jurassic to possibly Early Cretaceous (Bayliss, 1966; Beauvais and Fontaine, 1990). A new sample of the Bau Limestone (TB165) was analysed and yielded an assemblage of *Siphovalvulina* sp., *Dukhania* sp., *Pseudocyclammina* sp., *Nezzazatinella* sp., *Pseudocyclammina vasconica*, *Bacinella* sp., and *Salpingoporella dinarica* that indicates an Early Cretaceous age (Aptian, 125.0 - 113.0 Ma) and deposition in a shallow inner ramp to backreef environment, similar to the clasts of the Balingian Formation (Tab. 1).

The Arip Limestones were sampled at three different locations (AL1, AL2, AL3) north of the Arip ridge. All analysed samples are micritic wackestones of planktonic foraminifera or contain recrystallised planktonic foraminifera which yielded assemblages that indicate an inner neritic environment. Some of the samples contain *Subbotina* sp., *Acarinina pentacamerata*, *Chiloguembelina* sp., *Streptochilus cubensis*, *Subbotina linaperta*, *Aragonella nuttalli*, *Acarinina* sp., *Subbotina eocaenica*, *Turborotalia frontosa, Aqcarinina pentacamerata,* and *Guembelitrioides higginsi* indicating a Middle Eocene (Lutetian, P10 - P11, 47.8 - 42.3 Ma) depositional age. Other samples include *Bolivina* sp., *Porticulasphaera mexicana*, *Catapsydrax* sp., *Globigerinatheka* sp., *Globigerinatheka curryi*, *Globigerinatheka luterbacheri*, *Globigerinatheka barri*, *Guembelitrioides higginsi*, *Spirillina* sp. and *echinoid* spp. which indicate a Late Lutetian age (P11 - P12a, 44.9 - 41.2 Ma). One sample (AL2-3) yielded an assemblage of *Subbotina inaequispira*, *Dentoglobigerina venezuelana*, *Nodosaria* sp. and *Globigerapsis kugleri* suggesting a latest Lutetian age range of 43.2 - 41.2 Ma. All samples overlap at 43.2 - 42.3 Ma, which gives c. 42.3 Ma as the youngest depositional age.

7. Light mineral analysis

Light mineral point-counting was performed on 23 samples from the Unit 4 (Bawang Member), Tatau Formation (Rangsi Conglomerate and upper Tatau Formation), Balingian Formation, Begrih Formation, Liang Formation and Belait Formation (Supplementary File 2). The results are also illustrated in pie-chart diagrams compiled in the Supplementary Files 6.1 and 6.2.

7.1 Composition

Sample TB56 of Unit 4 (Bawang Member) has a relatively large matrix content (26%), and consists mainly of quartz ((undulose-) monocrystalline and polycrystalline), and sedimentary and metamorphic lithic fragments, indicating magmatic and metamorphic sources. Subordinate volcanic quartz and volcanic lithics are present. Minor K-feldspar and plagioclase may be related to a relatively high matrix content that could indicate some alteration processes. Chert, organic material, and opaque minerals are also rare in the sample.

The three samples of the Rangsi Conglomerate (TB54, TA-04, TB199b) show very variable proportions of light minerals and matrix contents that range between c. 6% and 41%. All three samples are dominated by monocrystalline quartz and sedimentary lithics. TA-04 and TB199b have additionally larger contents of undulose and polycrystalline quartz as well as chert, and higher contents of metamorphic (TB199b) or volcanic (TA-04) lithics. The samples contain subordinate K-feldspar and plagioclase (only TA-04 has a higher plagioclase amount of c. 7%), organic material, opaque minerals, and cement. Light minerals of the upper Tatau Formation sandstones (TB200a) have a similar high quartz content of over 50% from (undulose-) monocrystalline and polycrystalline quartz, and some chert, as well as abundant metamorphic and sedimentary lithic fragments. The sample has a relatively high proportion of K-feldspar and plagioclase (c. 10%), and includes minor matrix, volcanic lithics, organic material, opaque minerals, and cement.

Five samples were analysed from the Balingian Formation. Most of the samples have relatively large proportions of matrix (c. 12 - 26%), reflecting a poorly sorted character, as well as variable contents of organic material related to abundant coal in the formation. All samples have relatively high abundances of (undulose-) monocrystalline quartz (c. 36 - 46%), and metamorphic lithics (c. 11 - 19%). Polycrystalline quartz, sedimentary and volcanic lithics, chert, feldspar, and opaque minerals are subordinately present, as well as volcanic quartz in sample MB-05.

Five samples of the Begrih Formation were analysed. Light minerals of a pebbly sandstone layer at the base of the Begrih Formation (MB-07) are dominated by monocrystalline quartz, metamorphic and sedimentary lithics, as well as subordinate polycrystalline and undulose quartz and volcanic lithics. The majority of the overlying samples (MB-08, MB-09, MB-10) have a similar assemblage, but with larger contents of matrix, organic fragments, and partly opaque minerals (MB-09, MB-10). Sample MB-11 from the top of the Begrih Formation is dominated by sedimentary and metamorphic lithics (46% and 26%) and contains only small proportions of the assemblage observed in the other samples from this formation. Small amounts of K-feldspar and plagioclase are present in all five samples (c. 2 - 10%).

Five samples of the Liang Formation show highly variable contents of different light minerals and matrix, reflecting poorly sorted siltstone and (pebbly) sandstone beds. Monocrystalline quartz (c. 23 - 60%) is dominant in almost all samples, and an increase of sedimentary, metamorphic and volcanic lithics can be observed from the base to the top of the Liang Formation. Except for sample MB-12 which has a feldspar content of c. 8%, feldspar is insignificant in the Liang samples.

All three samples analysed from the Belait Formation on Labuan are very similar in their light mineral compositions. They consist predominantly of c. 62 - 72% of (undulose-) monocrystalline and polycrystalline quartz, as well as of c. 16 - 32% of metamorphic and sedimentary lithics. Chert, volcanic quartz, K-feldspar, plagioclase, volcanic lithics, matrix, and cement are rare.

7.2 Classification

The majority of samples, including TB200a (upper Tatau), TA-04, TB199b (Rangsi Conglomerate), MB-05 (Balingian), MB-07, -10, -11, TB201 (Begrih), MB-01, -14, -15 (Liang) and LTB-2, -4, -5 (Belait) have 0 to 15% matrix content and are classified as lithic arenites to sublitharenites (LTB-2, -5, MB-14) based on the QFL diagram of Pettijohn et al. (1987) (Fig. 12a). Samples TB56 of Unit 4 (Bawang Member) and TB54 of the Rangsi Conglomerate, as well as samples MB-02, -03, -04 (Balingian), MB-08, -09 (Begrih) and MB-13 (Liang) have between 15 and 75% matrix content and are classified as lithic greywacke, while sample MB-12 of the Liang Formation falls into the arkosic wacke field (Fig. 12a).

The Unit 4 (Bawang Member) sample TB56 indicates a transitional recycled orogenic character in the QFL and QmFLt diagrams (Dickinson et al., 1983) (Fig. 12b). The unconformably overlying Rangsi Conglomerate (TB54, TA-04, TB199b) and upper Tatau sandstone (TB200a) plot close to this sample. TB54 plots a bit further away at the boundary to the quartzose recycled orogen field in the QmFLt diagram.

Almost all samples of the Mukah-Balingian province and Belait Formation (Labuan) plot along the right margin in the classification diagrams (Fig. 12b), indicating compositions from quartz-rich to lithic-rich end members. Notably, all samples of the Balingian Formation, including the uppermost sandstone layer, plot in a relatively small area of the quartzose to transitional recycled orogen fields. Except for sample MB-11, which plots in the undissected arc field (QFL) or the lithic recycled orogen field (QmFLt), all samples of the Begrih Formation also plot close to one another in the transitional recycled orogen field. In contrast, the samples of the Liang Formation are much more widely spread and fall along the quartzose and transitional recycled orogen fields, or at the boundary of the transitional continental block fields (MB-12), which reflects the variability of light mineral compositions of this formation. The three samples of the Belait Formation are relatively similar and overlap with those of the Balingian and Begrih Formations in the quartzose to transitional recycled orogen fields (Fig. 12b).

8. Heavy mineral analysis

Heavy minerals were analysed from the Paleogene Unit 4 (TB56) and the Tatau Formation (TA-04, TB54, TB200a), as well as from the Neogene Mukah-Balingian province (MB-01, MB-03, MB-07, MB-12, TB201) (Fig. 13). The samples contain ultra-stable mineral assemblages dominated by zircon, rutile, and tourmaline. Apatite is rare in sample TB56 and absent in all other samples which indicates chemical weathering. Aluminium phosphate-sulphate minerals (APS) are subordinate in all samples, which are usually formed as alteration products of phosphorite deposits or by weathering of tropical soils (Dill, 2001), and ilmenite and rutile which occasionally contained Al and P, indicating alteration processes (Dill et al., 2007).

Sample TB56 contains predominantly zircon (28%), rutile (56.5%) and tourmaline (9.6%). Subordinate monazite (3.1%), chrome-spinel (1%), APS (0.7%), xenotime (0.7%), and apatite (0.5%) were identified.

Sample TA-04 of the Rangsi Conglomerate has a very similar heavy mineral composition to sample TB56. It includes a higher proportion of zircon at 43%, as well as rutile (43%), tourmaline (6.8%), monazite (2%), APS (1.8%), chrome-spinel (2.8%), and xenotime (0.8%). Compared to this sample, TB54 has very similar zircon (44.9%), rutile (32.8%) and tourmaline (7.6%) contents, but shows some minor variations, with a higher proportion of chrome-spinel (9.7%) as well as garnet which is present at 2.1% and was not detected in sample TA-04. Subordinately, baryte (1.6%) intergrown with albite, monazite (0.8%), and APS (0.6%) were found.

The sandstone TB200a of the upper Tatau Formation differs from the Rangsi Conglomerate by significantly lower zircon (19.7%) and higher tourmaline (30%) contents. Rutile is similar (37.9%). Subordinate APS (3.9%), chrome-spinel (2.5%), xenotime (2.5%), monazite (2%), and baryte (0.5%) were identified, as well as small quantities of hornblende (1%).

Samples of Mukah-Balingian province have generally similar assemblages with small variations. Sample MB-03 of the Balingian Formation contains similar amounts of zircon and tourmaline (c. 17%) and rutile at 58.5%. Minor APS (1.9%), monazite (1.4%), chrome-spinel (2.4%), garnet (0.9%), xenotime (0.3%), and chloritoid (0.3%) were recorded. Sample TB201 at the boundary with the Begrih Formation has high proportions of zircon and rutile at 42% and 47.2% respectively, and subordinate tourmaline at 4.1%, as well as chrome-spinel (3.9%), garnet (2.3%), monazite (0.3%) and APS (0.2%). Sample MB-07 of the Begrih Formation contains predominantly rutile (73.3%) and significantly less zircon (17%) compared to TB201, while tourmaline is also subordinate at 6%. Other minerals identified were chrome-spinel (2.1%), garnet, monazite and xenotime, each at 0.5%, and APS (0.2%). Sample MB-12 of the Liang Formation is dominated by rutile (83.1%) and has only minor proportions of tourmaline (10%) and zircon (4.7%). It contains subordinate APS (0.9%), chrome-spinel (0.6%), monazite (0.3%), and garnet (0.3%). Another sample of the Liang Formation (MB-01) has a significantly higher content of zircon at 38.6%, and contains rutile at 51.8%, and minor tourmaline (3.7%), chrome-spinel (2.2%), APS (1.8%), monazite (1.1%), xenotime (0.5%), and garnet (0.3%).

9. U-Th-Pb zircon analysis

9.1 Eocene magmatism in the Tatau area

9.1.1 Bukit Piring (BP-01 - granite)

Thirty-nine concordant ages were acquired from 56 zircons. The ages analysed range from 39 ± 1 Ma to 48 ± 1 Ma forming a wide age distribution that includes a dominant younger subpeak with a weighted mean age of 42.3 ± 0.5 Ma (MSWD = 1.3; n = 32) (Supplementary File 4), interpreted to represent the main phase of crystallisation, and a small older subpeak at c. 47 Ma which probably represents inherited zircons from an earlier pulse of magmatism.

9.1.2 Bukit Piring (BP-02 - quartzolite)

Thirty-nine concordant ages were analysed from 55 zircons. The majority of zircons are Eocene, ranging from 38 ± 2 to 49 ± 2 Ma. The wide peak gives a weighted mean age of 41.7 ± 0.6 Ma (MSWD = 2.6; n = 34) (Supplementary File 4). Two older inherited ages are Cretaceous (110 ± 3 Ma; 124 ± 2 Ma).

9.1.3 Arip Volcanics (TB55 - rhyolitic volcanic rock)

Seventy-two concordant ages were acquired from 82 zircons. Sixty-seven of these zircons yielded Eocene ages between 39 ± 1 Ma and 50 ± 1 Ma, which give a weighted mean age of 43.3 ± 0.3 Ma (MSWD = 1.6; n = 57) (Supplementary File 4). Five older inherited zircons are Cretaceous, Triassic, Devonian and Mesoproterozoic.

9.2 Unit 4 (Bawang Member)

9.2.1 North of the Arip River (TA-01 - tuffaceous sandstone)

112 concordant ages were acquired from 120 zircons (Fig. 14.1). They include dominant age populations in the Early Cretaceous (107 ± 2 to 145 ± 2 Ma) and Jurassic (148 ± 2 to 191 ± 9 Ma), and small age populations in the Permo-Triassic (205 ± 3 to 260 ± 3 Ma), Paleoproterozoic (1806 ± 21 to 1884 ± 13 Ma) and Paleoproterozoic to Archean (2406 ± 14 to 2498 ± 14 Ma) with scattered ages in the Paleozoic and Neo- to Mesoproterozoic. There are five Eocene ages (39.5 ± 0.8 to 46.0 ± 1.0 Ma), including a younger subpeak which has a weighted mean age of 40.0 ± 0.9 Ma (MSWD = 0.86; n = 3), which is similar to the age of the Arip magmatic rocks and indicate magmatic activity at the time of deposition.

9.2.2 South of the Arip River (TB56 - tuffaceous siltstone)

101 concordant ages were analysed from 102 zircons (Fig. 14.1). They form a main age populations in the Cretaceous to Jurassic (77 ± 2 to 176 ± 2 Ma) and Permo-Triassic (203 ± 3 to 270 ± 4 Ma). Other grains are one Carboniferous and four Proterozoic zircons with a possible minor peak at c. 1.7 Ga.

9.3 Tatau Formation

9.3.1 Rangsi Conglomerate (TB54 - conglomerate)

132 concordant ages of 133 zircons were acquired from this sample (Fig. 14.1). There is a main Cretaceous to Jurassic age population (79 ± 1 to 187 ± 4 Ma), and subordinate peaks in the Permo-Triassic (203 ± 6 to 256 ± 3 Ma), Silurian-Ordovician (428 ± 6 to 479 ± 7 Ma), and Paleoproterozoic at c. 1.7 - 1.9 Ga (1737 ± 10 to 1901 ± 11 Ma) and c. 2.4 Ga (2254 ± 10 to 2391 ± 11 Ma).

9.3.2 Rangsi Conglomerate (TA-04 - conglomerate)

123 concordant ages were obtained from 128 zircons (Fig. 14.1). The dominant age populations are Cretaceous to Jurassic (94 ± 1 to 188 ± 2 Ma), including two subpeaks at c. 120 Ma and c. 145 Ma, and Permian-Triassic (207 ± 5 to 289 ± 4 Ma). Other small age peaks are Silurian to Ordovician (422 ± 6 to 449 ± 6 Ma) and Paleoproterozoic (1766 ± 12 to 1860 ± 15 Ma). The youngest zircons analysed are Eocene (37.3 ± 0.7 to 49.0 ± 2.0 Ma) and include

a dominant younger age population which has a weighted mean age at 39.2 ± 1.7 Ma (MSWD = 6.5; n = 8). The zircons are interpreted to be derived from rhyolitic clasts of the Arip Volcanics which were reworked into the conglomerate.

9.3.3 Rangsi Conglomerate (TB199b - conglomerate)

126 concordant ages were acquired from 128 zircons of this sample (Fig. 14.1). The majority of the zircons have Cretaceous and Jurassic ages between 91 ± 1 Ma and 196 ± 3 Ma, recording two main age populations at c. 130 Ma and c. 145-180 Ma. Small peaks are formed by Permo-Triassic zircons (210 ± 3 to 265 ± 4 Ma) and Paleoproterozoic zircons (1782 ± 20 to 1992 ± 5 Ma) with a main peak at c. 1.8 Ga. A small number of zircons have Neoproterozoic (884 ± 11 to 967 ± 12 Ma) and Paleoproterozoic to Archean (2388 ± 10 to 2489 ± 8 Ma) ages.

9.3.4 Upper Tatau Formation (TB200a - sandstone)

131 concordant ages were obtained from 131 zircons (Fig. 14.1). The main age populations are Permian-Triassic (225 ± 3 to 284 ± 5 Ma) and Paleoproterozoic (1827 ± 23 to 1942 ± 17 Ma) which is different to the Rangsi Conglomerate samples. Other differences include a generally larger number of Precambrian grains with minor peaks at c. 800 Ma and c. 1.0 Ga, and only a minor Cretaceous peak (97 ± 2 to 133 ± 4 Ma).

9.4 Neogene sediments of the Mukah-Balingian province

9.4.1 Balingian Formation (MB-03 - sandstone)

114 concordant ages were acquired from 119 zircons (Fig. 14.2). They form dominant age populations in the Cretaceous to Jurassic (72 ± 1 to 180 ± 3 Ma), including a main peak at c. 120 Ma and two smaller subpeaks at c. 80 Ma and c. 165 Ma, and in the Permo-Triassic (209 ± 2 to 255 ± 3 Ma). Several minor age populations were identified in the Proterozoic at c. 850-900 Ma, 1.1 Ga, 1.9 Ga, 2.3 Ga and 2.5 Ga.

9.4.2 Balingian Formation (TB201 - sandstone)

114 concordant ages were obtained from 115 zircons of this sample (Fig. 14.2). The majority of zircons have Cretaceous to Jurassic ages (76 ± 1 to 190 ± 7 Ma) and form a main younger subpeak at c. 120 Ma and two older subpeaks at c. 145 Ma and 180 Ma. Additionally, there are minor peaks in the Permian-Triassic (214 ± 9 to 263 ± 2 Ma) and Paleoproterozoic at c. 1.8 Ga (1746 ± 14 to 1846 ± 13 Ma).

9.4.3 Begrih Formation (MB-07 - sandstone)

110 concordant ages were acquired from 117 zircons (Fig. 14.2). The main age populations are Cretaceous to Jurassic (66 ± 1 to 180 ± 2 Ma) with a dominant peak at c. 120 Ma, Permo-Triassic (202 ± 3 to 256 ± 3 Ma) and a smaller peak at c. 1.7 - 1.9 Ga. Three zircons have Eocene ages between 40.6 ± 0.9 Ma and 42 ± 1 Ma, interpreted as reworked from Arip magmatic rocks in the Tatau area.

9.4.4 Begrih Formation (MB-11 - pebbly sandstone)

The sample contained much Fe-oxide, indicating interactions with atmospheric waters. Only 65 concordant ages were obtained from 68 zircons of this sample (Fig. 14.2). There are age populations in the Cretaceous to Jurassic (105 ± 3 to 159 ± 2 Ma), with subpeaks at c. 110 Ma, 140 Ma and possibly c. 180 Ma (182 ± 2 to 199 ± 3 Ma), in the Permo-Triassic at c. 240 Ma (232 ± 3 to 257 ± 3 Ma), and small peaks in Silurian, Proterozoic (c. 0.7 - 0.8 Ga, 1.0 Ga, 1.7 - 1.9 Ga) and Paleoproterozoic to Archean (c. 2.5 Ga).

9.4.5 Liang Formation (MB-12 - siltstone)

109 concordant ages were acquired from 119 zircons (Fig. 14.2). The main age populations are Cretaceous to Jurassic (90 ± 2 to 177 ± 4 Ma), with subpeaks at c. 110 Ma, 140 Ma and 175 Ma, and Permo-Triassic (201 ± 2 to 257 ± 4 Ma). Smaller peaks were identified in the Neo- to Mesoproterozoic at c. 0.9 - 1.2 Ga, in the Paleoproterozoic (c. 1.8 Ga), and Paleoproterozoic to Archean (c. 2.5 Ga). One grain yielded an age of 41.8 ± 0.7 Ma, probably recording Eocene magmatism in the nearby Tatau area.

9.4.6 Liang Formation (MB-01 - sandstone)

111 concordant ages were obtained from 119 zircons (Fig. 14.2). The main age populations identified were Cretaceous (80 ± 1 to 132 ± 2 Ma), Permo-Triassic (208 ± 2 to 258 ± 4 Ma), Paleoproterozoic (1.7 - 1.9 Ga) and Paleoproterozoic to Archean (2.5-2.6 Ga). Smaller peaks of Jurassic (147 ± 3 to 177 ± 3 Ma), and Neo- (0.8 - 1.0 Ga) and Mesoproterozoic (c. 1.1 Ga) ages, resemble sample MB-12 of the Liang Formation. Both samples also show similar proportions of Phanerozoic and Precambrian zircons, and closely resemble sample MB-03 of the Balingian Formation.

9.5 Belait Formation on Labuan

9.5.1 Middle Belait Formation (LTB-2 - sandstone)

133 concordant ages from 136 zircons of this sample (Fig. 14.3) yielded approximately two thirds Phanerozoic ages and one thirds Precambrian ages. The main age population is in the Cretaceous to Jurassic (73 ± 3 to 186 ± 3 Ma) with a peak at c. 120 Ma, and smaller age populations were identified in the Permian-Triassic at c. 240 Ma (216 ± 3 to 282 ± 6 Ma), Neo- (757 ± 10 to 997 ± 13 Ma), Meso- (1068 ± 18 to 1248 ± 30 Ma), Paleoproterozoic (1704 ± 29 to 1874 ± 24 Ma) and Paleoproterozoic to Archean (2408 ± 14 to 2509 ± 11 Ma).

9.5.2 Upper Belait Formation (LTB-4 - sandstone)

119 concordant ages from 127 zircons of this sample have a similar ratio of Phanerozoic and Precambrian zircons to sample LTB-2 (Fig. 14.3). Dominant zircon age populations in the Cretaceous to Jurassic (67 ± 1 to 170 ± 2 Ma), have a main peak at c. 120 Ma and subpeaks at c. 90 Ma, 140 Ma and 160 Ma; other peaks are Permian-Triassic (203 ± 3 to 275 ± 3 Ma) and Paleoproterozoic (1712 ± 30 to 1895 ± 10 Ma). Small peaks were identified in the Paleozoic (382 ± 5 to 450 ± 9 Ma), at c. 500 Ma, 800-900 Ma, at c. 1.2 Ga and at c. 2.5 Ga. The youngest ages analysed are Paleogene, including the youngest age of 44 ± 1 Ma.

9.5.3 Upper Belait Formation (LTB-5 - sandstone)

126 concordant ages were obtained from 130 zircons (Fig. 14.3). The sample has a similar age spectrum to LTB-2 and LTB-4 and also includes a wide Cretaceous to Jurassic age

population (81 ± 1 to 180 ± 3 Ma) with main peaks at c. 120 Ma and 160 Ma, and large peaks in the Permian-Triassic (232 ± 3 to 287 ± 5 Ma) and Paleoproterozoic (1702 ± 15 to 1951 ± 12 Ma). There are minor peaks in the Paleozoic at c. 350 Ma and 440 Ma, as well as in the Neo- and Mesoproterozoic (c. 600 Ma, 800 Ma, 1.1 Ga) and Paleoproterozoic to Archean at c. 2.5 Ga.

10. Discussion

10.1 Revised stratigraphy and major unconformities in the Miri Zone

10.1.1 Upper Paleogene to Early Miocene

The Paleogene sediments of the Tatau region in the Miri Zone are poorly exposed and little studied. This has led to a previously confusing and ambiguous stratigraphy. Rocks in the southern Miri Zone were assigned to the Metah Member, Bawang Member, or Tatau Formation by Wolfenden (1960), Liechti et al. (1960), and Heng (1992) and it was not clear when deep marine sedimentation of the Rajang Group ceased and uplift of central Borneo began.

In this study we now conclude that sediments in this area are lithologically and structurally very similar to the Belaga Formation in the Sibu Zone, and are therefore assigned here to the Belaga Formation (Figs. 2a and 3). Locally, differences were observed in the metamorphic grade of the turbidite sequences, which indicate variations in the burial depth of the sediments, and are interpreted to be different faulted blocks of older units in the Belaga Formation (Fig. 2a). These include slates in turbidites north of the Bukit Mersing Line which contain folded quartz veins and are quite different to the Unit 3 south of the Bukit Mersing Line (Galin et al., 2017). The strong cleavage and abundant quartz veining indicates they are upfaulted parts of an older Unit of the Belaga Formation (Fig. 3).

Similarly, intensely cleaved slates were observed locally east of the Bawang River. The rocks are similar to those described from the lowermost part of the Sibu Zone represented by the Lupar Formation of Unit 1 (Galin et al., 2017). Galin et al. (2017) noted that detrital zircon U-Pb analysis from this supposed Bawang Member showed some similarities to zircon age populations of Unit 1 (Lupar Formation) with a Triassic age population and absence of

Permian, Paleozoic, and abundant Precambrian ages. Since these rocks differ from the abundant shale sequences observed in the surrounding area and lack any volcaniclastic beds, they are here also assigned as older Belaga Formation, potentially equivalent to Unit 1 (Lupar Formation), and interpreted as a faulted block exposed in the younger Unit 4 (Bawang Member), based on lineaments on SRTM images. Furthermore, shales with a moderate cleavage were observed in the northern Tatau high which may suggest slightly deeper levels compared to Unit 4 (Bawang Member). These rocks were considered as potential equivalents of Unit 2 of Galin et al. (2017) based on a dominant Cretaceous age population and a few Precambrian zircons. A comparison of detrital zircons of samples TA-01 and TB56 from Unit 4 (Bawang Member) with the two samples reported by Galin et al. (2017) from the Tatau area showed both are very similar (Fig. 15) but differ to Units 1 or 2 of the Sibu Zone by having a more significant Early Cretaceous to Jurassic peak, in contrast to abundant Late Cretaceous zircons and minor Jurassic grains in Units 1 and 2, indicating regional variations of sources between the Sibu and Miri turbidites.

The sediments of Unit 4 (Bawang Member) between the Pelugau River and the Tatau high (Fig. 2a) usually comprise siltstones, sandstones, and shales which are moderately to steeply dipping to the NW to N. They are locally intruded by the Piring stock, and interbedded with the Arip Limestones, Arip Volcanics, and volcaniclastic beds. Zircon U-Pb analysis of the magmatic rocks yielded weighted mean ages between c. 42 and 43 Ma. Biostratigraphy of the limestones yielded a very similar maximum depositional age of c. 42.3 Ma (Lutetian). These ages indicate that the surrounding conformable bedded turbidite sequences were deposited during the late Middle Eocene, and support a classification of these rocks as the youngest part of the Belaga Formation, termed here Unit 4 (Bawang Member), following the unit classification used by Galin et al. (2017). Thus, the interbedded lavas, volcaniclastics and limestones of Unit 4 (Bawang Member) are all positioned in our new stratigraphy at the top of the Belaga Formation below the unconformity (Fig. 3), which is different to the proposal of Hutchison (2005) and Wong (2011) who included the Arip Volcanics and Arip Limestones in the Tatau Formation above the unconformity.

The upper boundary of Unit 4 (Bawang Member) is relatively well constrained based on the youngest zircons obtained from the volcanic rocks of c. 39 - 37 Ma, which defines the maximum depositional age as Late Eocene (Priabonian), and indicates that the Rajang Unconformity cannot be older than 37 Ma. The lower boundary of Unit 4 is poorly constrained. Unit 4 seems to be of similar age to Unit 3 in the Sibu Zone, which may be much thinner or missing in the Miri Zone.

The Rangsi Conglomerate forms the base of the Tatau Formation above the Rajang Unconformity. It contains rounded clasts of Arip Volcanics, and shows a similar zircon age spectrum to Unit 4 (Bawang Member) (Fig. 16), including a dominant Cretaceous to Jurassic peak, a subordinate Triassic peak, minor Paleoproterozoic peaks, and a few Eocene zircons, which indicates reworking of Unit 4 (Bawang Member) and potentially older parts of the Belaga Formation into the Tatau Formation. There are no age constraints on the lower Tatau Formation (Rangsi Conglomerate) but the resumption of sedimentation is constrained to the earliest Early Oligocene by the overlying Early Oligocene upper Tatau Formation, Buan Formation and lower part of the Nyalau and Setap Shale Formations.

The upper part of the Tatau Formation is conformable on the Rangsi Conglomerate but shows a very different provenance and is dominated by Permo-Triassic and Paleoproterozoic zircons, indicating a change in sediment supply for the upper Tatau Formation.

A second major unconformity, termed Nyalau Unconformity, was identified between the upper Tatau/ Nyalau successions and the overlying Balingian Formation at c. 17 Ma, which is accompanied by a change in provenance.

10.1.2 Late Early Miocene – Middle Miocene

The Balingian, Begrih and Liang Formations above the Nyalau Unconformity have similar tidally-dominated depositional environments, zircon age spectra, and heavy mineral assemblages. They do not show major differences in provenance, therefore could be all related to a single succession, which is different to previous interpretations (e.g. Wolfenden, 1960). Minor provenance differences were interpreted for thick sandstone packages of the Balingian (TB201) and Begrih (MB-07) Formations, which have smaller Permo-Triassic peaks and rare Paleozoic and Paleoproterozoic to Archean grains compared to the samples from sandstone-dominated heterolithics of the Balingian (MB-03) and Liang (MB-12) Formations. The overall number of Precambrian grains is also significantly smaller in samples of the thick sandstone packages. Sample MB-01 of the Liang Formation and MB-11 of the Begrih Formation are pebbly sandstones layer which are interbedded with heterolithic beds and show features of both age spectra, i.a. a small Permo-Triassic peak but relative abundant Precambrian ages, including a small peak at c. 2.5 Ga.

Heavy minerals of the Mukah-Balingian province samples are all similar, with stable to ultra-stable assemblages of abundant rutile, zircon and subordinate tourmaline, with minor chrome-spinel, garnet, monazite, APS, xenotime, and chloritoid. The zircon-tourmaline (Zr/Tur) ratio shows lithology-dependent variations, i.e. high Zr/Tur ratios for the thick (pebbly) sandstones that suggest high-energy conditions, and low Zr/Tur ratios for the heterolithic samples that formed, partially, under lower-energy conditions. This correlation of grain size and energy in the depositional environment might also account for the age spectra variations observed, but could also reflect local contributions from different units of the Belaga Formation.

On Labuan, the fluvial conglomerates were previously interpreted to have been deposited on top of the Setap Shale Formation (Fig. 3) and to mark an important change of depositional environment, referred as the Deep Regional Unconformity (Wilson and Wong, 1964; Bol and van Hoorn, 1980; Balaguru and Lukie, 2012). However, although there is a clear change from the underlying marginal marine heterolithics, the conglomerates are also overlain by similar marginal-marine, tidally-influenced deposits, indicating the conglomerates represent only a sequence boundary related to eustatic changes or temporary flood events.

The heterolithics below the conglomerate unit were assigned either to the Setap Shale Formation (Wilson and Wong, 1964) or the Layang-Layangan beds which were considered to be between the deep marine Temburong Formation and the fluvial to marginal marine Belait Formation (Madon, 1994) (Fig. 3). Wan Hasiah et al. (2013) included this unit in the Belait Formation and termed it Lower Belait; however, they still put the Setap Shale underneath it. Here we consider all steeply dipping shale-slate-sandstone alternations that show evidence of deformation and deep marine environment as Temburong Formation, and interpret the Belait Formation to lie directly and unconformably above the turbiditic Temburong Formation (Fig. 3). The contact, however, is not exposed on Labuan. The proposed correlation of the Belait Formation with the Mukah-Balingian formations suggest the marginal-marine heterolithics are part of the Belait Formation (Lower Belait) and are equivalent to the Balingian Formation, followed by the conglomerates (Middle Belait) and tidally-influenced deposits (Upper Belait), similar to the Begrih and Liang Formations. As in the Mukah-Balingian province, the sharp contact of the conglomerates may represent only a small sequence boundary.

The three samples analysed from the Belait Formation indicate a tidally-influenced fluvio-deltaic environment and have similar light mineral assemblages and zircon age populations to the Mukah-Balingian province samples (Fig. 16). Sample LTB-2 of the Middle Belait Formation was collected from a massive conglomerate - sandstone unit interpreted as channelized bodies in a fluvial-dominated environment and shows a small (Permian-) Triassic peak, similar to the equivalent (pebbly) sandstones of the Begrih Formation. The other two samples (LTB-4, LTB-5), from the Upper Belait marginal-marine sequences above the fluvial deposits, yielded a larger number of Permo-Triassic zircons and are similar to the overlying Liang Formation in the Mukah-Balingian province.

10.2 Paleo-drainage reconstructions

The Rajang Group represents the deep marine equivalents of the terrestrial Kuching Supergroup (Galin et al., 2017; Breitfeld et al., 2018). Unit 4 (Bawang Member) has similar zircon age spectra to the Tutoop Sandstone (Breitfeld and Hall, 2018), and thus is correlative with the youngest sediments of the Kuching Supergroup. Furthermore, Unit 4 (Bawang Member) has similarities to the Upper Eocene Crocker Formation (van Hattum et al., 2013). Sediments of Unit 4 (Bawang Member) are interpreted here to be derived mainly from the Schwaner Mountains and West Borneo with little contribution from the Malay Peninsula based on subordinate Precambrian zircons, suggesting proximal capture areas for the river system which is retracting eastwards (Fig. 17a) in comparison to the wider capture area for Unit 3 (Middle Eocene) as shown by Breitfeld and Hall (2018).

Unit 4 (Bawang Member) records a shallowing transition from deep open marine sedimentation of Units 1 to 3 of the Belaga Formation to an inner neritic environment, in which interbedded limestones formed. But the major abrupt change is at the base of the overlying Rangsi Conglomerate, proposed here to represent the base of the fluvio-deltaic Tatau Formation, which marks the Rajang Unconformity (Fig. 3).

The Rajang Unconformity marks a major phase of uplift in central Borneo which is likely related to tectonic processes associated with the onset of subduction of the proto-South China Sea. Hall and Breitfeld (2017) proposed subdcution started at c. 45 Ma which would be contemporaneous to the initial stage of uplift inferred from the change from deep marine to inner neritic deposition of Unit 4 (Bawang Member).

The three samples of the Rangsi Conglomerate (TA-04, TB54, TB199b) yielded similar zircon age populations, including a main peak in the Cretaceous to Jurassic, and smaller peaks in the Permo-Triassic and Paleoproterozoic (c. 1.7-1.9 Ga and c. 2.3-2.4 Ga) (Fig. 16). Samples TB199b and TA-04 have a larger number of Jurassic zircons than TB54, and sample TA-04 has more Triassic zircons. The age spectra are similar to those of samples TA-01 and TB56 of Unit 4 (Bawang Member), including a few Eocene grains (Fig. 16). The (Permian-) Triassic zircons of TA-04 may have been derived from older Belaga Formation units and the zircon spectrum resembles the sample reported by Galin et al. (2017) as Bawang Member equivalent to Unit 1, indicating very local sources. Likewise, Cretaceous and Jurassic zircons in TB199b resemble zircon ages of Unit 2 equivalent in the northern Tatau high (Galin et al., 2017). We interpret these results to indicate that the Rangsi Conglomerate was derived from nearby Unit 4 (Bawang Member) and local fault blocks of older units in the Belaga Formation of the southern Miri Zone (Fig. 17b), which is also supported by similar light and heavy mineral assemblages (Figs. 13 and 18a). An elevated mountain range (*Unit 4* on Fig. 17b) is proposed to have shut down NE-directed drainage from West and SW Borneo, causing reversal of rivers and possibly the formation of a proto-Kapuas River in west Kalimantan (Fig. 17b).

Sample TB200a from the upper Tatau Formation has a very different zircon age distribution from the Rangsi Conglomerate and Unit 4 (Bawang Member) (Fig. 14.1). The dominant age populations are Permo-Triassic and Paleoproterozoic (c. 1.7-1.9 Ga) with minor Cretaceous, Jurassic, Paleozoic, and Neo- to Paleoproterozoic ages. This indicates a significant change in provenance to a source with more Permo-Triassic peak and fewer Cretaceous zircons, as well as abundant Neo- to Mesoproterozoic zircons. The signature is dissimilar to sources in Borneo and suggests river systems changed and sediment was coming from sources in the Malay Peninsula (Fig. 17c), which is dominated by Permo-Triassic and Neo- to Paleoproterozoic zircons (Hall and Sevastjanova, 2012). This would require crossing the Natuna Arch which has often been considered an elevated area in the Oligocene to Miocene (Morley and Morley, 2013; Hall, 2013b), although Miocene fluvial to marginal marine sediments (Pengadah or Natuna Sandstones) have been reported from Natuna island (Haile, 1970; Haile and Bignell, 1971; Franchino and Liechti, 1983; Hakim and Hidayat, 1993). Reorganisation of the drainage system was possibly related to coeval rifting of the South China Sea. The zircon age populations of the upper Tatau Formation are similar to those of the overlying Nyalau Formation (Breitfeld et al., 2017b), indicating the river system was likely active until the late Early Miocene and shed large amounts of sediments into the Sarawak Basin. The upper Tatau/ Nyalau formations sediments are also similar to the Oligocene Crocker fan sediments (van Hattum et al., 2013) which indicates the Crocker sediments are probably the deep-marine equivalents of the Nyalau Formation (Fig. 17c).

Zircon ages of all samples from the Balingian, Begrih and Liang Formations show Cretaceous-Jurassic, Permo-Triassic, Neo- and Mesoproterozoic (c. 800 Ma, 900 Ma and 1.1 Ga, and Paleoproterozoic (c. 1.8 Ga and 2.5 Ga) peaks, as well as several Paleozoic grains (Fig. 16). They are very similar to the samples analysed from the Belait Formation (Fig. 16) which have similar lithologies, indicating a similar provenance. The age populations resemble the Rajang Group analysed by Galin et al. (2017), including Unit 4 (Bawang Member) (Fig. 16) which is also supported by a few analyses with Eocene ages, as well as the Kuching Supergroup samples reported by Breitfeld and Hall (2018) (Fig. 16), indicating reworking of these deposits with main sediment supply again from Borneo. In contrast, the upper Tatau and Nyalau Formations which are unconformably below the Balingian Formation show very different age spectra, including a dominant Permo-Triassic peak, and therefore were likely not exposed at the time of deposition of the Mukah-Balingian and Belait formations.

An indication that sediments were also derived from the Kuching Supergroup is the Early Cretaceous limestone clasts found in the Balingian Formation that were likely derived from the Bau Limestone Formation which underlies the Kuching Supergroup south of Kuching. Furthermore, light minerals of the Mukah-Balingian and Belait formations are low in feldspar and plot across the sublitharenite, lithic arenite, or lithic greywacke fields; this is different from the Rajang Group which has slightly more feldspar-rich assemblages and plots across a smaller area (Fig. 18b). This could indicate breakdown of feldspar and/or lithic fragments in the Mukah-Balingian and Belait samples. However, the Kuching Supergroup light mineral assemblages show a similar distribution to the Mukah-Balingian and Belait formations (Fig. 18b) suggesting they represent a similar source. Furthermore, Unit 4 (Bawang Member) could be another local source because it also has low feldspar contents, as well as comparable heavy mineral assemblages. This indicates that large areas of west and central Borneo were uplifted in the Middle - Late Miocene and provided sediments to the Miri Zone and the Sarawak Basin (Fig. 17d).

The upper Tatau/ Nyalau Formations were deposited in a coastal area with a NW-SE directed coastline. The Nyalau Unconformity (Fig. 3) marks a change of the coastline to NE-SW orientated similar to the present-day (Fig. 17c, d). On Labuan, we identified a similar development based on the change from deep marine environment (Crocker – Temburong Formations) to the marginal marine Belait Formation (Figs. 3 and 17d). It is uncertain whether the Mukah-Balingian and Belait Formations were deposited in one large fan system or formed distinct fans, since similar sediments are missing in the Tatau region. Hageman (1987) interpreted a phase of uplift in the SE Balingian area in the late Middle Miocene, which would support that uplift occurred after deposition and thus could have resulted in erosion of equivalent sediments of the Mukah-Balingian and Belait formations.

10.3 Implications for offshore unconformities

The Sarawak and Sabah offshore regions have been subdivided by several unconformities according to different authors. For example, Levell (1987) identified five regional unconformities in the Middle Miocene and younger sequences offshore West Sabah, and Hageman (1987) also recognised several cycles separated by unconformities for the Oligocene to Pliocene sequences in the Sarawak Basin offshore. However, some of these horizons may represent sequence or tectonic boundaries rather than actual unconformities.

The three most important and often discussed unconformities in the offshore Sarawak and Sabah regions are the Deep Regional Unconformity (DRU), the Middle Miocene Unconformity (MMU) and the Top Crocker Unconformity (TCU). The unconformities have not aided understanding of regional tectonics, partly because of a confusing time-labelled nomenclature or uncertain position, and different authors have assigned them different ages.

The DRU, for example, has previously been proposed to be at c. 15 Ma based on seismic interpretations and on-land Sabah stratigraphy (Levell, 1987; Hazebroek and Tan, 1993; van Hattum et al., 2013), although Lunt and Madon (2017b) put the DRU at 12.5 Ma. Levell, (1987) and Hazebroek and Tan (1993) also identified an older unnamed unconformity below the DRU at c. 22-23 Ma. Van Hattum et al. (2013) identified the Top Crocker Unconformity (TCU) on land (also discussed by Lunt and Madon, 2017b) and estimated a similar age. However, the top of the Crocker Formation and its deep-marine equivalent of the Temburong Formation were determined as late Early Miocene by Wilson & Wong (1964) and Hutchison (2005), which is closer to the DRU age of Levell (1987). Furthermore, Clark (2017) argued that the DRU previously identified on seismic lines was more likely to be the TCU, and he considered the DRU to be a tectonic contact between much younger, late Middle Miocene, sand-dominated mini-basins and underlying mobile shale which can be seen in seismic data.

On land, the DRU has been located at the base of thick conglomerates on Labuan (Balaguru and Lukie, 2012) which are described as part of the Belait Formation (Madon, 1994). In this section of the Belait Formation there are several conglomerate beds within a sandstone unit. Based on our field observations we do not interpret the base of the conglomerates as the DRU but consider the conglomerates represent rather brief eustatic changes or storm deposits, which is supported by the fact that they are overlain and underlain by similar fluvio-deltaic deposits. There are also several small conglomerate beds above and below the Begrih Formation in the Mukah-Balingian province, indicating there is no single main event that formed massive conglomerates in the Begrih and Middle Belait Formations. Thus, we conclude that the conglomerates do not mark the DRU and the whole facies association of heterolithics, conglomerates, and sandstones on Labuan is assigned here to the Belait Formation. This is supported by Wan Hasiah et al. (2013) who also re-interpreted the previous DRU contact on Labuan as an intraformational erosive surface. The contact with the underlying Temburong Formation on Labuan is not exposed but would be the TCU, which marks the change from deep marine to deltaic- shallow marine deposition.

Interestingly, Hageman (1987) and Lunt and Madon (2017a, b) identified a change in direction of sediment supply from the SW to the SE between Sarawak Cycles II and III. This correlates very well with our Nyalau Unconformity which marks the change from sediments derived from the Malay Peninsula in the west to Borneo-derived sediments from the Kuching - Rajang range to the SE. Lunt and Madon (2017a, b) further suggested that there was uplift of Borneo at this time, which is also supported by our results, and confirm the Nyalau Unconformity as an important unconformity in the area. Based on age data of the Temburong Formation reported by Wilson and Wong (1964) the TCU is likely younger than c. 22.5 Ma estimated by van Hattum et al. (2006, 2013) and we interpret the TCU to be of similar age to the Nyalau Unconformity, thus representing an equivalent and enabling a correlation of these two important unconformities in Sarawak and Sabah, possibly related to the end of spreading in the South China Sea.

Cycle III is usually a thin unit in the Sarawak Basin and the top to Cycle IV is marked by carbonate growth in the Dangerous Grounds area (Wilson et al., 2013) which was interpreted as the main event in the Middle Miocene at c. 15-16 Ma, termed MMU (e.g. Doust, 1981; Lunt and Madon, 2017a). This age is similar to the previously reported age of the DRU and therefore some authors consider the MMU to be the same as the DRU (e.g.

Balaguru and Lukie, 2012). Adding to the confusion, some authors interpret the MMU to be between c. 20 - 15 Ma (e.g. Cullen et al., 2010; Steuer et al., 2014; Kessler and Jong, 2015), and others to be c. 11-10 Ma (e.g. Nagura et al., 2000; Racey, 2011). These unconformities must represent different events.

On land, we see the main event at c. 17 Ma is marked by the Nyalau Unconformity, and not at c. 15.5 Ma which can only be correlated with the massive conglomerates found at the base of the Begrih Formation and in the Middle Belait Formation. The top of the Liang Formation in the Mukah-Balingian province and Upper Belait Formation on Labuan is approximately c. 11 Ma which possibly could be correlated to an offshore unconformity of similar age.

11. Conclusions

The southern Miri Zone in western Borneo contains thick Paleogene to Neogene sedimentary successions that extend offshore into the Sarawak Basin and form hydrocarbon reservoirs. These rocks include Eocene sediments that have previously been subdivided into the Metah Member, Tatau Formation and Bawang Member. New field observations suggest that this subdivision is not appropriate. Different parts of the turbidite sequences in the southern Miri Zone include either cleaved slates or uncleaved shales. The latter, exposed between the Pelugau River and the Tatau high, represent the youngest unit, termed Unit 4 (Bawang Member), which is of upper Middle - Late Eocene age. In contrast, cleaved rocks found east of the Bawang River and in the northern Tatau high are interpreted to be faulted blocks of turbidite sequence exhumed from greater depth and are likely equivalent to Units 1 and 2 of the Sibu Zone.

The boundary between deep marine sediments of the Belaga Formation and the overlying fluvial-deltaic dominated Tatau Formation is marked by the Rangsi Conglomerate, at the base of which is the Rajang Unconformity. The conglomerates have been reworked from Unit 4 (Bawang Member) and older parts of the Belaga Formation, indicating a major phase of uplift in central Borneo at c. 37-34 Ma.

The upper Tatau Formation on top of the Rangsi Conglomerate has a very different detrital zircon age spectrum to that of underlying rocks. Instead, it is similar to the overlying Nyalau Formation and indicates sediment that originated ultimately from the Malay Peninsula.

Sedimentation stopped at c. 17 Ma (Nyalau Unconformity) which represents the second phase of uplift, corresponding to a change of coastline orientation from NW-SE to NE-SW, similar to the present-day, and after that sedimentation resumed with supply from Borneo, mainly from the elevated Kuching-Rajang range (Fig. 17d).

Neogene sediments of the Mukah-Balingian province (Balingian, Begrih and Liang Formations) all have zircon age populations that resemble Unit 4 (Bawang Member) and older parts of the Belaga Formation, as well as the Kuching Supergroup, indicating widespread uplift of Borneo in the Middle Miocene.

The Belait Formation on Labuan includes very similar sediments to the Mukah-Balingian Formations with similar provenance and is considered an equivalent to them. In both areas, massive conglomerate beds are between marginal-marine heterolithic sediments, suggesting the contact represents a sequence boundary only, and questioning the previous interpretation of the conglomerates as marking the Deep Regional Unconformity on Labuan.

The results of this work suggest that the uppermost Cretaceous to Eocene strata of western Borneo (Rajang fan) have been reworked into the Lower Oligocene Rangsi Conglomerate above the Rajang Unconformity, as well as into the Lower to Middle Miocene Mukah-Balingian/ Belait Formations above the Nyalau Unconformity, while Lower Oligocene to Lower Miocene strata (Tatau – Nyalau – Crocker fan) have been reworked from the Malay Peninsula. In summary, this shows that upper Paleogene to Neogene sedimentation in western Borneo was dominated by large-scale reworking related to changing large river systems and was not derived from arc-related magmatism.

Acknowledgements

This study was funded by the SE Asia Research Group which is supported by a consortium of oil companies. We thank Thomson Galin and Liew Shan Hian from the Minerals and Geoscience Department Malaysia, Sarawak for great logistical support during field trips. Many thanks also to our driver Zulfairy Abdullah around Sibu. Yasir Said is kindly acknowledged for sampling of the Arip Limestones. TB and RH are grateful to Narender Pendkar and Tg. Mohd Syazwan Tg. Hassan for an insightful field excursion to the island of Labuan. We thank Martin Rittner for help with the LA-ICP-MS analysis at UCL/Birkbeck College (UK). The manuscript was greatly improved by the thorough comments and suggestions of two anonymous reviewers.

References

Adams, C.G., Butterlin, J., Samanta, B.K., 1986. Larger foraminifera and events at the Eocene/Oligocene boundary in the Indo-West Pacific region. Developments in Palaeontology and Stratigraphy 9, Elsevier, 237-252.

Andersen, T., 2002. Correction of common lead in U–Pb analyses that do not report 204Pb. Chemical Geology 192, 59-79.

Bakar, Z.A.A., Madon, M., Muhamad, A.J., 2007. Deep-marine sedimentary facies in the Belaga Formation (Cretaceous-Eocene), Sarawak: Observations from new outcrops in the Sibu and Tatau areas. Geological Society of Malaysia, Bulletin 53, 35-45.

Balaguru, A., Lukie, T., 2012. Tectono-stratigraphy and development of the Miocene delta systems on an active margin of Northwest Borneo, Malaysia. Warta Geologi 38, 127-129.

Bayliss, D.D., 1966. Foraminifera from the Bau Limestone Formation, Sarawak, Malaysia. Geological Survey Borneo Region, Annual Report for 1965, 173-175.

Beauvais, L., Fontaine, H., 1990. Corals from the Bau Limestone Formation, Jurassic of Sarawak, Malaysia. Ten years of CCOP research on the Pre-Tertiary of east Asia, 209-239.

Benton, M.J., Harper, D.A., 1997. Basic Palaeontology. Prentice Hall, Upper Saddle River, N.J, 342 pp.

Bladon, G.M., Pieters, P.E., Supriatna, S., 1989. Catalogue of Isotopic Ages Commissioned by the Indonesia-Australia Geological Mapping Project for Igneous and Metamorphic Rocks in Kalimantan: Preliminary Geological Report. Indonesia-Australia Geological Mapping Project, Geological Research and Development Centre, Indonesia.

Bol, A.J., van Hoorn, B., 1980. Structural styles in western Sabah offshore. Geological Society of Malaysia, Bulletin 12, 1-16.

BouDagher-Fadel, M.K., 2008. Evolution and Geological Significance of Larger Benthic Foraminifera. Developments in Palaeontology and Stratigraphy, 21. Elsevier, 544 pp.

BouDagher-Fadel, M.K., 2018a. Evolution and Geological Significance of Larger Benthic Foraminifera. UCL Press, London, UK.

BouDagher-Fadel, M.K., 2018b. Biostratigraphic and Geological Significance of Planktonic Foraminifera (Updated 2nd Edition). UCL Press, London, UK, 298 pp.

BouDagher-Fadel, M.K., Banner, F.T., 1999. Revision of the stratigraphic significance of the Oligocene-Miocene “Letter-Stages”. Revue de Micropaléontologie 42, 93-97.

Breitfeld, H.T., Hall, R., Galin, T., Forster, M.A., BouDagher-Fadel, M.K., 2017a. A Triassic to Cretaceous Sundaland-Pacific subduction margin in West Sarawak, Borneo. Tectonophysics 694, 35-56.

Breitfeld, H.T., Hennig, J., BouDagher-Fadel, M.K., Hall, R., 2017b. The Rajang Unconformity: Major provenance change between the Eocene and Miocene sequences in NW Borneo. Fall Meeting, AGU, New Orleans, LA, 11-15 Dec, Abstract EP21A-1829.

Breitfeld, H.T., Hall, R., 2018. The eastern Sundaland margin in the latest Cretaceous to Late Eocene: Sediment provenance and depositional setting of the Kuching and Sibu Zones of Borneo. Gondwana Research 63, 34-64.

Breitfeld, H.T., Hall, R., Galin, T., BouDagher-Fadel, M.K., 2018. Unravelling the stratigraphy and sedimentation history of the uppermost Cretaceous to Eocene sediments of the Kuching Zone in West Sarawak (Malaysia), Borneo. Journal of Asian Earth Sciences 160, 200-223.

Bromley, R.G., Asgaard, U., 1991. Ichnofacies: a mixture of taphofacies and biofacies. Lethaia 24, 153-163.

Buatois, L.A., Mángano, M.G., 2011. Ichnology; Organism-Substrate Interactions in Space and Time. Cambridge University Press, Cambridge, UK, 366 pp.

Choi, K.S., Dalrymple, R.W., Chun, S.S., Kim, S.-P., 2004. Sedimentology of Modern, Inclined Heterolithic Stratification (IHS) in the Macrotidal Han River Delta, Korea. Journal of Sedimentary Research 74, 677–689.

Clark, J., 2017. Neogene Tectonics of Northern Borneo: A Simple Model to Explain Complex Structures within Miocene-recent Deltaic-Deepwater Sediments, Proceedings of the 2017 Asia Petroleum Geoscience Conference & Exhibition (APGCE), 88-91.

Cohen, K.M., Finney, S.C., Gibbard, P.L., Fan, J.X., 2013, updated 2017. The ICS International Chronostratigraphic Chart. Episodes 36, 199-204.

Cullen, A., Reemst, P., Henstra, G., Gozzard, S., Ray, A., 2010, Rifting of the South China Sea: new perspectives. Petroleum Geoscience 16, 273-282.

Davies, L., Hall, R., Armstrong, R., 2014. Cretaceous crust in SW Borneo: petrological, geochemical and geochronological constraints from the Schwaner Mountains. Indonesian Petroleum Association, 38th Annual Convention and Exhibition, Proceedings, IPA14-G-025.

De Boer, N.P., Milroy, W.V., Crews, W.E., 1952. Geology of the Balingian-Bintulu-Rajang area (unpublished report). Sarawak Oilfields Limited.

De La Roche, H., Leterrier, J.T., Grandclaude, P., Marchal, M., 1980. A classification of volcanic and plutonic rocks using R1R2-diagrams and major-element analyses - Its relationships with current nomenclature. Chemical Geology 29, 183-210.

De Silva, S., 1986. Stratigraphy of the South Mukah-Balingian Region, Sarawak. Warta Geologi, Geological Society of Malaysia Newsletter 12, 215-219.

Dickinson, W.R., 1970. Interpreting detrital modes of graywacke and arkose. Journal of Sedimentary Petrology 40, 695-707.

Dickinson, W.R., Beard, L.S., Brakenridge, G.R., Erjavic, J.L., Ferguson, R.C., Inman, K.F., Knepp, R.A., Lindeberg, F.A., Ryberg, P.T., 1983. Provenance of North American Phanerozoic sandstone in relation to tectonic setting. Geological Society of America, Bulletin 94, 222-235.

Dill, H.G., 2001. The geology of aluminium phosphates and sulphates of the alunite group minerals. Earth Science Reviews 53, 35-93.

Dill, H.G., Melcher, F., Fuessl, M., Weber, B., 2007. The origin of rutile-ilmenite aggregates (“nigrine”) in alluvial-fluvial placers of the Hagendorf pegmatite province, NE Bavaria, Germany. Mineralogy and Petrology 89, 133-158.

Doust, H. 1981. Geology and exploration history of offshore Central Sarawak. In: Halbouty, M.T. (Ed.), Energy Resources of the Pacific Region, AAPG Studies in Geology No. 12, 117-132.

Franchino, A., Liechti, P., 1983. Geological notes on the stratigraphy of the island of Natuna-Indonesia. Memorie di Scienze Geologiche Universita di Padova 36, 171-193.

Frost, B.R., Barnes, C.G., Collins, W.J., Arculus, R.J., Ellis, D.J., Frost, C.D., 2001. A Geochemical Classification for Granitic Rocks. Journal of Petrology 42, 2033-2048.

Galin, T., Breitfeld, H.T., Hall, R., Sevastjanova, I., 2017. Provenance of the Cretaceous-Eocene Rajang Group submarine fan, Sarawak, Malaysia from light and heavy mineral assemblages and U-Pb zircon geochronology. Gondwana Research 51, 209-233.

Gazzi, P., Zuffa, G.G., Gandolfi, G., Paganelli, L., 1973. Provenienza e dispersione litoranea delle sabbie delle spiagge adriatiche fra le foci dell’Isonzo e del Foglia: inquadramento regionale. Societá Geologica Italiana, Memoria 12, 1-37.

Gradstein, F. M., Ogg, J. G., Schmitz, M. D., Ogg, G. M., (eds.), 2012. The Geologic Time Scale 2012. Elsevier, 1144 pp.

Griffin, W.L., Powell, W.J., Pearson, N.J., O'Reilly, S.Y., 2008. GLITTER: data reduction software for laser ablation ICP-MS. In: Sylvester, P.J. (Ed.), Laser Ablation-ICP-MS in the Earth Sciences: Current Practices and Outstanding Issues. Mineralogical Association of Canada, Short Course Series, 308-311.

Hageman, H., 1987. Paleobathymetrical changes in NW Sarawak during Oligocene to Pliocene. Geological Society of Malaysia, Bulletin 21, 91-102.

Haile, N.S., 1962. The geology and mineral resources of the Suai-Baram area, north Sarawak. Geological Survey Department British Territories in Borneo, Memoir 13, 176 pp.

Haile, N.S., 1970. Notes on the geology of the Tambelan, Anambas, and Bunguran Islands, Sunda Shelf, Indonesia, including radiometric age determinations. UNESCO-ECAFE, CCOP Technical Bulletin 3, 55-90.

Haile, N.S., 1973. The recognition of former subduction zones in Southeast Asia. In: Tarling, D.H., Runcorn, S.K. (Eds.), Implications of continental drift to the Earth Sciences 2, Academic Press, London, 885-891.

Haile, N.S., 1974. Borneo. In: Spencer, A.M. (Ed.), Mesozoic-Cenozoic Orogenic Belts. Geological Society of London Special Publication 4, 333-347.

Haile, N.S., Bignell, J.D., 1971. Late Cretaceous age based on K/Ar dates of granitic rock from the Tambelan and Bunguran Islands, Sunda Shelf, Indonesia. Geologie en Mijnbouw 50, 687-690.

Hakim, Hidayat, 1993. Map of Natuna Besar and Pulau Laut, Geological Research and Development Centre, Bandung.

Hakimi, M.H., Abdullah, W.H., Sia, S.-G., Makeen, Y.M., 2013. Organic geochemical and petrographic characteristics of Tertiary coals in the northwest Sarawak, Malaysia: implications for palaeoenvironmental conditions and hydrocarbon generation potential. Marine and Petroleum Geology 48, 31-46.

Hall, R., 2012. Late Jurassic–Cenozoic reconstructions of the Indonesian region and the Indian Ocean. Tectonophysics 570, 1-41.

Hall, R., 2013a. Contraction and extension in northern Borneo driven by subduction rollback. Journal of Asian Earth Sciences 76, 399-411.

Hall, R., 2013b. The palaeogeography of Sundaland and Wallacea since the Late Jurassic. Journal of Limnology 72, 1-17.

Hall, R., Sevastjanova, I., 2012. Australian crust in Indonesia. Australian Journal of Earth Sciences 59, 827-844.

Hall, R., Breitfeld, H.T., 2017. Nature and demise of the Proto-South China Sea. Geological Society of Malaysia, Bulletin 63, 61-76.

Hassan, M.H.A., Johnson, H.D., Allison, P.A., Abdullah, W.H., 2013. Sedimentology and stratigraphic development of the upper Nyalau Formation (Early Miocene), Sarawak, Malaysia: a mixed wave-and tide-influenced coastal system. Journal of Asian Earth Sciences 76, 301-311.

Hazebroek, H.P., Tan, D.N.K., 1993. Tertiary Tectonic Evolution of the NW Sabah Continental Margin. Geological Society of Malaysia, Bulletin 33, 195-210.

Heldreich, G., Redfern, J., Legler, B., Gerdes, K. and Williams, B.P.J., 2017. Challenges in characterizing subsurface paralic reservoir geometries: a detailed case study of the Mungaroo Formation, North West Shelf, Australia. In: Hampson, G.J., Reynolds, A.D., Kostic, B., Wells, M.R. (Eds.), Sedimentology of Paralic Reservoirs: Recent Advances. Geological Society, London, Special Publications 444, 59-108.

Heng, Y.E., 1992. Geological Map of Sarawak, 1:500,000. Geological Survey of Malaysia.

Hennig, J., Breitfeld, H.T., Hall, R., Nugraha, A.M.S., 2017a. The Mesozoic tectono-magmatic evolution at the Paleo-Pacific subduction zone in West Borneo. Gondwana Research 48, 292-310.

Hennig, J., Breitfeld, H.T., Gough, A., Hall, R., Long, T.V., Kim, V.M. and Quang, S.D., 2017b. Correlating the Da Lat Zone on land with the Cuu Long Basin offshore. , Abstract EP21A-1830 presented at 2017 Fall Meeting, AGU, New Orleans, LA, 11-15 Dec.

Hennig, J., Breitfeld, H.T., 2018. Sources of Cenozoic Sediments around the Southern South China Sea. Proceedings of the 2018 South East Asia Petroleum Exploration Society (SEAPEX) Conference, Asia-Pacific E&P Conference, London, 27-28 Jun, p. 17.

Hennig, J., Breitfeld, H.T., Gough, A., Hall, R., Long, T.V., Kim, V.M. and Quang, S.D., 2018. U-Pb Zircon Ages and Provenance of Upper Cenozoic Sediments from the Da Lat Zone, SE Vietnam: Implications For an Intra-Miocene Unconformity and Paleo-Drainage of the Proto–Mekong River. Journal of Sedimentary Research 88, 495-515.

Hutchison, C.S., 1996. The 'Rajang Accretionary Prism' and 'Lupar Line' problem of Borneo. In: Hall, R., Blundell, D.J. (Eds.), Tectonic Evolution of SE Asia. Geological Society of London Special Publication 106, 247-261.

Hutchison, C.S., 2005. Geology of North-West Borneo. Elsevier, Amsterdam, 421 pp.

Janoušek, V., Farrow, C.M., Erban, V., 2006. Interpretation of whole-rock geochemical data in igneous geochemistry: Introducing Geochemical Data Toolkit (GCDkit). Journal of Petrology 47, 1255-1259.

Kessler, F.L., Jong, J., 2015. Tertiary Uplift and the Miocene Evolution of the NW Borneo Shelf Margin. Berita Sedimentologi 33, 21-46.

Khan, A.A., Abdullah, W.H., Hassan, M.H., Iskandar, K., 2017. Tectonics and sedimentation of SW Sarawak basin, Malaysia, NW Borneo. Journal of the Geological Society of India 89, 197-208.

Kho, C.H., 1968. Bintulu area, Central Sarawak, East Malaysia. Geological Survey Borneo Region, Malaysia, 83 pp.

Kirk, H.J.C., 1957. The Geology and Mineral Resources of the Upper Rajang and adjacent areas. British Territories Borneo Region Geological Survey, Memoir 8, 181 pp.

Kirk, H.J.C., 1968. The igneous rocks of Sarawak and Sabah. Geological Survey of Malaysia, Borneo Region, Bulletin 5, 210 pp.

Kumar, N., Sanders, J.E., 1976. Characteristics of shoreface storm deposits; modern and ancient examples. Journal of Sedimentary Research 46, 145-162.

Levell, B.K., 1987. The Nature and Significance of Regional Unconformities in the Hydrocarbon–Bearing Neogene Sequence Offshore West Sabah. Geological Society of Malaysia Bulletin 21, 55-90.

Liechti, P., Roe, F.W., Haile, N.S., 1960. The Geology of Sarawak, Brunei and the western part of North Borneo 3, 360 pp.

Lowe, D.R., 1975. Water escape structures in coarse-grained sediments. Sedimentology 22, 157-204.

Lunt, P., Madon, M., 2017a. A review of the Sarawak Cycles: History and modern

application. Geological Society of Malaysia, Bulletin 63, 77-101.
Lunt, P., Madon, M., 2017b. Onshore to offshore correlation of northern Borneo; a regional perspective. Geological Society of Malaysia, Bulletin 64, 101-122.

Madon, M.B.H., 1994. The stratigraphy of northern Labuan, NW Sabah Basin, East Malaysia. Geological Society of Malaysia, Bulletin 36, 19-30.
Madon, M.B.H., 1999. Basin types, tectono-stratigraphic provinces and structural styles. In: Leong, K.M. (Ed.), The Petroleum Geology and Resources of Malaysia, PETRONAS, Kuala Lumpur, 77-112.
Madon, M.B.H., Rahman, A.H.A., 2007. Penecontemporaneous deformation in the Nyalau Formation (Oligo-Miocene), Central Sarawak. Geological Society of Malaysia, Bulletin 53, 67-73.
Mat-Zin, I.C., 2000. Stratigraphic Position of Rangsi Conglomerate in Sarawak. Platform 1, 25-31.
McGowran, B., 2005. Biostratigraphy: Microfossils and Geological Time. Cambridge University Press, 459 pp.
Miall, A.D., 1996. The Geology of Fluvial Deposits. Sedimentary Facies, Basin Analysis, and Petroleum Geology. Berlin, Heidelberg, Springer-Verlag, 582 pp.
Middlemost, E.A., 1994. Naming materials in the magma/igneous rock system. Earth Science Reviews 37, 215-224.
Morley, R.J., Morley, H.P., 2013. Mid Cenozoic freshwater wetlands of the Sunda region. Journal of Limnology 72, 18-35.
Murtaza, M., Rahman, A.H.A., Sum, C.W., Konjing, Z., 2018. Facies associations, depositional environments and stratigraphic framework of the Early Miocene-Pleistocene successions of the Mukah-Balingian Area, Sarawak, Malaysia. Journal of Asian Earth Sciences 152, 23-38.
Nagura, H., Honda, H., Katori, S., 2000. Tertiary inversion tectonics and petroleum systems in West Natuna Sea Basins, Indonesia. Journal of the Japanese Association for Petroleum Technology 65, 91-102 (in Japanese with English abstract).
Nagy, J., Tovar, F.J.R., Reolid, M., 2016. Environmental significance of *Ophiomorpha* in a transgressive–regressive sequence of the Spitsbergen Paleocene, Polar Research 35, 24192.
Nemec, W., Steel, R.J., 1984. Alluvial and coastal conglomerates: their significant features and some comments on gravelly mass-flow deposits. In: Koster, E.H., Steel, R.J. (Eds.), Sedimentology of Gravels and Conglomerates. Canadian Society of Petroleum Geology, Memoir 10, Calgary, 1-31.
Nichols, G.J., 2009. Sedimentology and stratigraphy. Wiley-Blackwell, 419 pp.
Nugraheni, R.D., Chow, W.S., Rahman, A.H.A., Nazor, S.N.M., Abdullah, M.F., 2014. Tertiary coal-bearing heterolithic packages as low permeability reservoir rocks in the Balingian Sub-basin, Sarawak, Malaysia. Geological Society of Malaysia, Bulletin 60, 85-93.
Olariu, C., Steel, R.J., Olariu, M.I., Choi, K., 2015. Facies and architecture of unusual fluvial–tidal channels with inclined heterolithic strata: Campanian Neslen Formation, Utah, USA. In: Ashworth, P.J., Best, J.L., Parsons, D.R. (Eds.), Fluvial-Tidal Sedimentology. Development in Sedimentology 68, Elsevier, 353-394.
Pearce, J., 1996. Sources and settings of granitic rocks. Episodes 19, 120-125.
Pearce, J.A., Harris, N.B.W., Tindle, A.G., 1984. Trace element discrimination diagrams for

the tectonic interpretation of granitic rocks. Journal of Petrology 25, 956-983.

Pearce, N.J.G., Perkins, W.T., Westgate, J.A., Gorton, M.P., Jackson, S.E., Neal, C.R., Chenery, S.P., 1997. A compilation of new and published major and trace element data for NIST SRM 610 and NIST SRM 612 glass reference materials. Geostandards Newsletter 21, 115-144.

Peccerillo, A., Taylor, S.R., 1976. Geochemistry of Eocene calc-alkaline volcanic rocks from the Kastamonu area, northern Turkey. Contributions to Mineralogy and Petrology 58, 63-81.

Peng, L.C., Leman, M.S., Nasib, B.M., Karim, R., 2004. Stratigraphic lexicon of Malaysia. Geological Society of Malaysia.

Pettijohn, F.J., Potter, P.E., Siever, R., 1987. Sand and Sandstone. Springer Science & Business Media, New York, 553 pp.

Pieters, P.E., Trail, D.S., Supriatna, S., 1987. Correlation of Early Tertiary rocks across Kalimantan. Proceedings Indonesian Petroleum Association 16th Annual Convention, 291-306.

Racey, A., 2011. Petroleum Geology. In: Ridd, M.F., Barber, A.J., Crow, M.A. (Eds.), Geology of Thailand, Geological Society of London Special Publication, 251-392.

Ramkumar, M., Santosh, M., Nagarajan, R., Li, S.S., Mathew, M., Menier, D., Siddiqui, N., Rai, J., Sharma, A., Farroqui, S., 2018. Late Middle Miocene volcanism in Northwest Borneo, Southeast Asia: Implications for tectonics, paleoclimate and stratigraphic marker. Palaeogeography, Palaeoclimatology, Palaeoecology 490, 141-162.

R Core Team, 2014. R: A language and environment for statistical computing. R Foundation for Statistical Computing, Vienna, Austria. URL https://www.R-project.org/.

Reading, H.G., 1996. Sedimentary Environments: Processes, Facies and Stratigraphy. Blackwell, Oxford, UK, 704 pp.

Sandal, S.T. (Ed.), 1996. The Geology and Hydrocarbon Resources of Negara Brunei Darussalam. Syabas, Bandar Seri Begawan, Brunei Darussalam, 243 pp.

Sia, S.-G., Abdullah, W.H., Konjing, Z., Koraini, A.M., 2014. The age, palaeoclimate, palaeovegetation, coal seam architecture/mire types, paleodepositional environments and thermal maturity of syn-collision paralic coal from Mukah, Sarawak, Malaysia. Journal of Asian Earth Sciences 81, 1-19.

Sircombe, K.N., 2004. AgeDisplay: an EXCEL workbook to evaluate and display univariate geochronological data using binned frequency histograms and probability density distributions. Computers & Geosciences 30, 21-31.

Sláma, J., Košler, J., Condon, D.J., 2008. Plešovice zircon - A new natural reference material for U–Pb and Hf isotopic microanalysis. Chemical Geology 249, 1-35.

Steuer, S., Franke, D., Meresse, F., Savva, D., Pubellier, M., Auxietre, J.L., 2014. Oligocene–Miocene carbonates and their role for constraining the rifting and collision history of the Dangerous Grounds, South China Sea. Marine and Petroleum Geology 58, 644-657.

Sun, S.S., McDonough, W., 1989. Chemical and isotopic systematics of oceanic basalts: implications for mantle composition and processes. Geological Society of London Special Publications 42, 313-345.

Tan, D.N.K., 1979. Lupar Valley, west Sarawak, Malaysia. Geological Survey of Malaysia, Report 13, 159 pp.

Tongkul, F., 1997. Sedimentation and tectonics of Paleogene sediments in central Sarawak. Geological Society of Malaysia, Bulletin 40, 135-155.

van Hattum, M.W.A., Hall, R., Pickard, A.L. & Nichols, G.J. 2006. Southeast Asian sediments not from Asia: Provenance and geochronology of north Borneo sandstones. Geology, 34, 589-592.

van Hattum, M.W.A., Hall, R., Pickard, A.L., Nichols, G.J., 2013. Provenance and geochronology of Cenozoic sandstones of northern Borneo. Journal of Asian Earth Sciences 76, 266-282.

Wan Hasiah, A.W., Lee, C.P., Gou, P., Shuib, M.K., Ng, T.F., Albaghdady, A.A., Mislan, M.F., Mustapha, K.A., 2013. Coal-bearing strata of Labuan: Mode of occurrences, organic petrographic characteristics and stratigraphic associations. Journal of Asian Earth Sciences 76, 334-345.

Whalen, J.B., Currie, K.L., Chappell, B.W., 1987. A-type granites: geochemical characteristics, discrimination and petrogenesis. Contributions to Mineralogy and Petrology 95, 407-419.

Wilson, M.E.J., 2008. Global and regional influences on equatorial shallow-marine carbonates during the Cenozoic. Palaeogeography, Palaeoclimatology, Palaeoecology 265, 262-274.

Wilson, R.A.M., Wong, N.P.Y., 1964. The geology and mineral resources of the Labuan and Padas Valley area, Sabah, Malaysia 17, 150 pp.

Wilson, M.E.J., Wah, E.C.E., Dorobek, S., Lunt, P., 2013. Onshore to offshore trends in carbonate sequence development, diagenesis and reservoir quality across a land-attached shelf in SE Asia. Marine and Petroleum Geology 45, 349-376.

Witts, D., Hall, R., Nichols, G.J., Morley, R.J., 2012. A new depositional and provenance model for the Tanjung Formation, Barito Basin, SE Kalimantan, Indonesia. Journal of Asian Earth Sciences 56, 77-104.

Wolfenden, E.B., 1960. The Geology and Mineral Resources of the Lower Rajang Valley and adjoining areas, Sarawak. British Territories Borneo Region Geological Survey Department, Memoir 11, 167 pp.

Wong, Y.L., 2011. Stratigraphy of the Ransi Member of the Middle Eocene to Oligocene Tatau Formation in the Tatau-Bintulu area, Sarawak, East Malaysia. MSc Thesis, University of Malaya, Kuala Lumpur, 256 pp.

Figure captions

Fig. 1: Northwestern Borneo overview map showing the four zones of Sarawak defined by Haile (1974), the units of the Sibu Zone as defined by Galin et al., (2017), and the West Borneo region (Mesozoic Sundaland in Borneo) (Hennig et al., 2017a). The red boxes highlight the study areas. Inset: regional map of Southeast Asia using NASA ASTER Global DEM V002 (search.earthdata.nasa.gov/search) and GEBCO bathymetry data (www.gebco.net/data_and_products/gridded_bathymetry_data/).

Fig. 2: Geological maps with sample locations of a) the Tatau region and b) the Mukah-Balingian province modified from Wolfenden (1960), Liechti et al. (1960) and Heng (1992), and of c) Labuan island modified from Wilson and Wong (1964), Madon (1994) and Balaguru and Lukie (2012). Bt. – Bukit (hill).

Fig. 3: Revised stratigraphy proposed in this study for the Upper Cretaceous to Neogene sediments of the Miri Zone (adapted from Hutchison, 2005; Galin et al., 2017). The black and white column on the left summarises the previous stratigraphy for comparison. Lay – Layang-Layangan Formation; TCU – Top Crocker Unconformity.

Fig. 4: Field photographs of the Belaga Formation in the Miri Zone. a, b) Steeply dipping slates which include folded quartz lenses (upper Balingian River). c) Whitish-grey volcaniclastic layer interbedded with weathered sandstones (east of Bawang River). d, e) Steeply dipping alternations of sandstones and slates which show a pervasive cleavage (east of Bawang River). f) Sandstones and mudstones to shales interbedded with thin greyish volcaniclastic layers (north of Arip Ridge). g) White volcaniclastic layer interbedded with sandstones and shales south of the Tatau high (TA-01). h, i) Sandstone and shale to slate alternations in the northern Tatau high showing mud drapes on ripple foresets.

Fig. 5: Field and thin section photographs of the subvolcanic rocks and limestones interbedded with Unit 4 (Bawang Member). a) Photomicrograph of a micro-granitic rock of Bukit Piring (BP-01). b) Exposure of the Arip Limestones along the ‘stone road’ mine north of the Arip ridge (AL1, AL2).

Fig. 6: Field photographs of the Tatau Formation. a-d) Massive beds of the Rangsi Conglomerate south of the Tatau high. The layers have a sand- or mud-dominated matrix (b, d). Pebbles are angular to rounded quartz pebbles and subordinate rhyolite clasts (c). Locally, a clastic dyke was observed between beds (d). e, f) Moderately dipping beds of the Rangsi Conglomerate north of the Tatau high. The conglomerates show erosive bases (e) and sandstones are interbedded with thin mudstone layers showing current ripple cross-lamination (f). g, h) Sandstone beds and mudstones of the upper Tatau Formation overlying the Rangsi Conglomerate north of the Tatau high.

Fig. 7: Field photographs of the Balingian Formation. a) Conglomerate layer with limestone clast (arrow) interbedded with the heterolithics. b) Heterolithics interbedded with thick layers of carbonaceous mudstones and coal seams. c) Heterolithics with inclined bedding. d) Contact between mudstone-dominated heterolithics capped by a coal seam and pebbly sandstones on top. e) Large exposure of pebbly sandstones at the top of the Balingian Formation. f) The sandstones are interbedded with thin mudstone layers and show planar cross-bedding with mud and coaly/ carbonaceous material deposited on the foresets. Abundant *Skolithos* burrows were observed in the sandstones. g) Small vertical mud-filled fault indicating syn-sedimentary displacement. h) Stacked lenticular sandstones capped by mudstones.

Fig. 8: Field photographs of the Begrih Formation. a) Mudstones and heterolithics at the base overlain by thick deposits of conglomerates and pebbly sandstones with erosive bases. b) Convolute bedding in the heterolithics with carbonaceous mudstones. c) Inverse-graded sandstones to conglomerates with an erosive base of coarse-grained sandstones. d) Pebbly sandstones with planar cross-bedding. e) Sandstones with mudstone and lignite layers showing wavy lamination. f) Stacked packages of heterolithics with erosive bases. g-l) Succession of conglomerates with scours (h) at the base overlain by pebbly sandstone and heterolithics which are interbedded with thin conglomerate layers (i). Sandstone and carbonaceous mudstone heterolithics at the top contain abundant *Ophiomorpha* burrows (k) and show herringbone cross-stratification at centimetre-scale (l).

Fig. 9: Field photographs of the Liang Formation. a, b) Subhorizontally laminated mudstone - siltstone heterolithics showing flaser and current ripple cross-lamination (a) and convolute bedding and thin coal bands in places (b). c) Planar-bedded sandstones interbedded with mudstones. d) Moderately-dipping alternations of conglomerates/ pebbly sandstones and heterolithics. e) Conglomerate showing coarsening upward sequence. f-k) Heterolithics with hummocky cross-stratification (f), thin coal layers, and *Ophiomorpha* and *Skolithos* burrows (g, h), flute casts (i) and flame structures (k).

Fig. 10: Field photographs of the Lower and Middle Belait Formation (a-d) and Upper Belait Formation (e, f, h-k). a) Sharp contact between heterolithics (Lower Belait) and massive conglomerates (Middle Belait) (central Labuan anticline). Some conglomerate beds are clast-supported (b), including rounded laterite clasts (c). d) Carbonaceous siltstone - mudstone alternations with thin coal seams (central Labuan anticline). e) Sandstones contain elongate coal fragments. f, g) Successions of thick sandstone beds with channel structures interbedded with mudstones and heterolithics (N Labuan; SE Labuan). h) Sandstones showing hummocky cross-stratification or trough cross-bedding with asymptotic foresets. i) Wavy lamination in the heterolithics cut by synsedimentary fault. k) Highly bioturbated sandstone bed with abundant burrows (h-k: NE Labuan).

Fig. 11: Geochemical discrimination diagrams for samples of Bukit Piring and the Arip Volcanics from Wolfenden (1960), Wong (2011) and this study. a) The samples are calc-alkaline to high-K calc-alkaline in the SiO_2 vs. K_2O diagram of Peccerillo and Taylor (1976). b) Discrimination diagrams of Frost et al. (2001), c) Geotectonic discrimination diagram of Pearce et al. (1984), and d) Spider diagram normalised to the NMORB composition of Sun and McDonough (1989), supporting an A-type signature.

Fig. 12: Summary of light minerals of Unit 4 (Bawang Member), Tatau Formation, Mukah-Balingian formations and Belait Formation plotted in the ternary diagrams of a) Pettijohn et al. (1987) and b) Dickinson et al. (1983).

Fig. 13: Summary of heavy minerals of the Unit 4 (Bawang Member), Tatau Formation, and Mukah-Balingian formations. The samples show comparable ultra-stable assemblages dominated by zircon, rutile and tourmaline.

Fig. 14.1: Histograms and probability density plots for samples of Unit 4 (Bawang Member), Rangsi Conglomerate, and upper Tatau Formation.

Fig. 14.2: Histograms and probability density plots for samples of the Mukah-Balingian formations.

Fig. 14.3: Histograms and probability density plots for samples of the Belait Formation on Labuan.

Fig. 15: Comparison of the zircon histograms of the deeper parts of the turbidite sequence in the Miri Zone (Galin et al., 2017) and Unit 4 (Bawang Member) from this study interpreted as the uppermost part of the succession. Both histograms show very similar age spectra with only a few Precambrian zircons, indicating the Miri Zone turbidites are mainly sourced by the Schwaner Mountains and West Borneo.

Fig. 16: Summary of combined histograms and probability density plots of the Kuching Supergroup (Breitfeld and Hall, 2018), Rajang Group (Galin et al., 2017; this study) and Unit 4 (Bawang Member), as well as of their reworked products of the Rangsi Conglomerate, Mukah-Balingian formations and Belait Formation. n = number of concordant analyses; X = number of samples.

Fig. 17: Paleogeography maps and reconstruction of major fluvial systems at a) 42-37 Ma, b) 33-30 Ma, c) 30-25 Ma, and d) 15-10 Ma based on the biostratigraphy (Arip Limestones), U-Pb age dating (Bukit Piring, Arip Volcanics) and provenance results of this study, and earlier work by Wilson (2008), Witts et al. (2012), Hall (2013b), Morley and Morley (2013), Hennig et al. (2017b), Breitfeld and Hall (2018), Hennig and Breitfeld (2018) and Hennig et al., (2018). Abbreviations: K - Karimunjawa Arch; S - Schwaner Mountains; W - West Borneo; B - Barito Basin; MB - Mukah-Balingian; Pr. - Proto; R. - River.

Fig. 18: Light minerals summary diagrams showing a) the latest Cretaceous to Eocene Rajang Group of the Sibu Zone and Miri Zone (Unit 4 Bawang Member and older parts) and their reworked equivalents of the Rangsi Conglomerate, and b) the Neogene Mukah-Balingian and Belait Formations which both contain very little feldspar, similar to sediments of the Kuching Supergroup (Breitfeld et al., 2018).

Tab. 1: Summary of biostratigraphy from the Arip Limestones, limestone clasts in the Balingian Formation, and the Bau Limestone Formation.

Supplementary File 1: Results of XRF whole-rock analysis of samples collected in this study from Bukit Piring. Also shown are the R1-R2 and SiO_2 vs. Na_2O + K_2O nomenclature diagrams of De La Roche et al. (1980) and Middlemost (1994).

Supplementary File 2: Summary of light mineral modes of Unit 4 (Bawang Member), Tatau Formation, Mukah-Balingian formations and Belait Formation.

Supplementary File 3: Summary of heavy mineral modes of Unit 4 (Bawang Member), Tatau Formation, and Mukah-Balingian formations.

Supplementary File 4: Data tables of LA-ICP-MS U-Pb zircon analyses. Samples of Bukit Piring (BP-01, BP-02) and the Arip Volcanics (TB55) are plotted in Tera-Wasserburg Concordia diagrams (black - concordant analyses, red - discordant analyses), and histograms with probability density plots. The grey ages were excluded from the main age population and disregarded for the weighted mean age calculation.

Supplementary File 5.1: Selected photomicrographs of planktonic foraminifera. Scale bar = 0.25 mm. 1 - *Acarinina pentacamerata* (Subbotina), AL3-3. 2 - *Dentoglobigerina venezuelana* (Hedberg), AL2-3. 3 - *Turborotalia frontosa* (Subbotina), AL1-2. 4 - *Globigerinatheka* sp., AL2-2. 5 - *Globigerinatheka lutherbacheri* Bolli, AL3-2. 6 - *Chiloguembelina* sp., AL3-4. 7 - *Aragonella nuttalli* Toumarkine, AL1-1. 8 - *Subbotina eocaenica* (Terquem), AL1-2. 9 - *Guembelitrioides higginsi* (Bolli), AL2-1.

Supplementary File 5.2: Selected photomicrographs of benthic foraminifera. Scale bar: Figs. 1, 4, 6 = 1mm; Figs 2, 3, 5 = 0.5mm. 1, 5 - *Pseudocyclammina lituus* Yokoyama, BAL-1. 2 - *Dukhania conica* Henson, TB165. 3 - *Siphovalvulina* sp., TB165. 4, 5 - *Pseudocyclammina vasconica* Maync, MB-03c. 6 - *Palaeodasycladus* sp., MB-03c.

Supplementary Files 6.1 and 6.2: Pie-chart diagrams of light mineral compositions of all samples analysed from Unit 4 (Bawang Member) and Tatau Formation (6.1), and the Balingian, Begrih, Liang and Belait Formations (6.2).

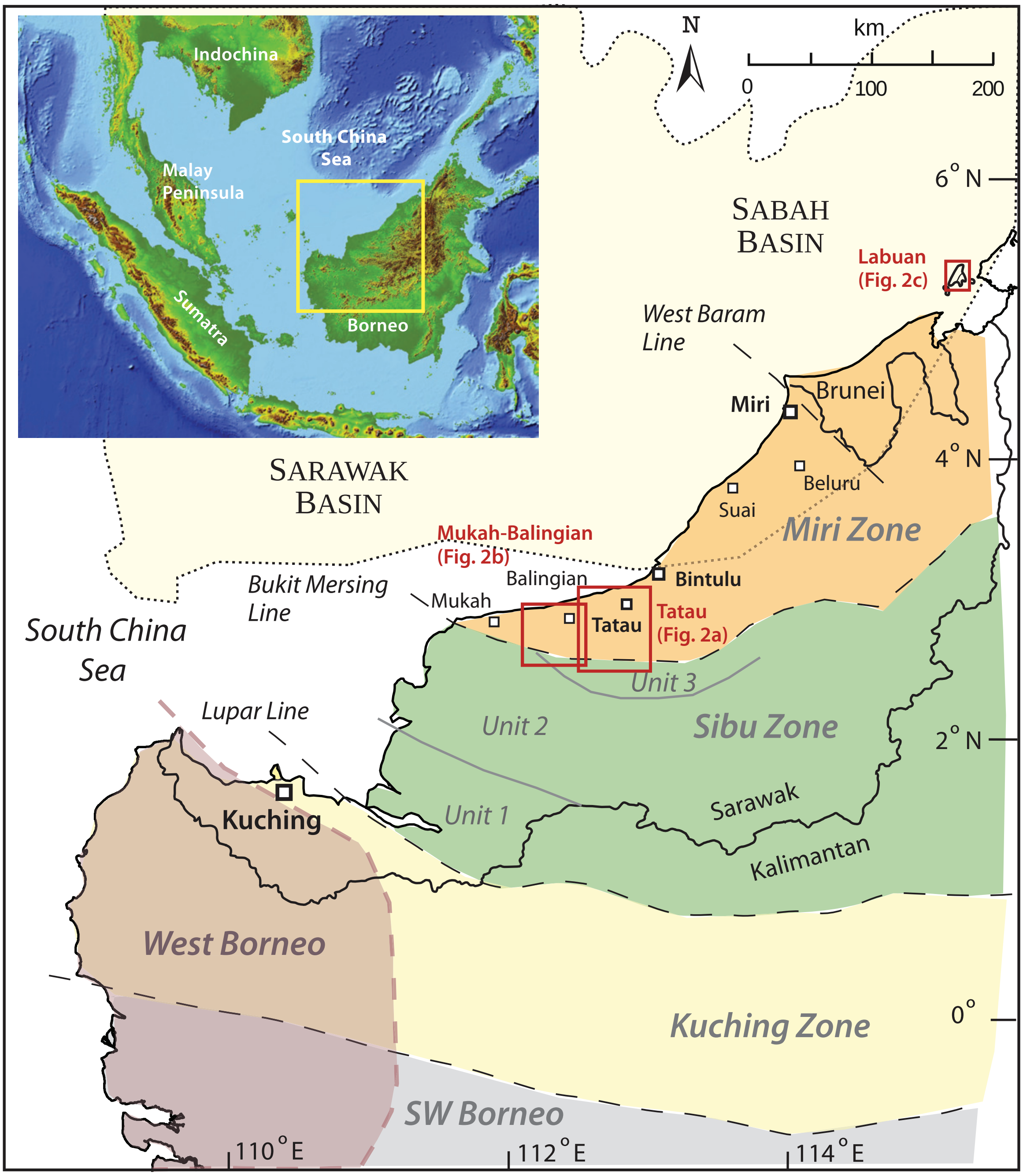

Indochina
South China Sea
Malay Peninsula
Sumatra
Borneo
N
km
0
100
200
6° N
4° N
2° N
0°
SABAH BASIN
SARAWAK BASIN
Labuan (Fig. 2c)
West Baram Line
Miri
Brunei
Beluru
Suai
Miri Zone
Mukah-Balingian (Fig. 2b)
Bintulu
Balingian
Bukit Mersing Line
Mukah
Tatau
Tatau (Fig. 2a)
South China Sea
Unit 3
Lupar Line
Unit 2
Sibu Zone
Kuching
Unit 1
Sarawak
Kalimantan
West Borneo
Kuching Zone
SW Borneo
110°E
112°E
114°E

Fig. 1

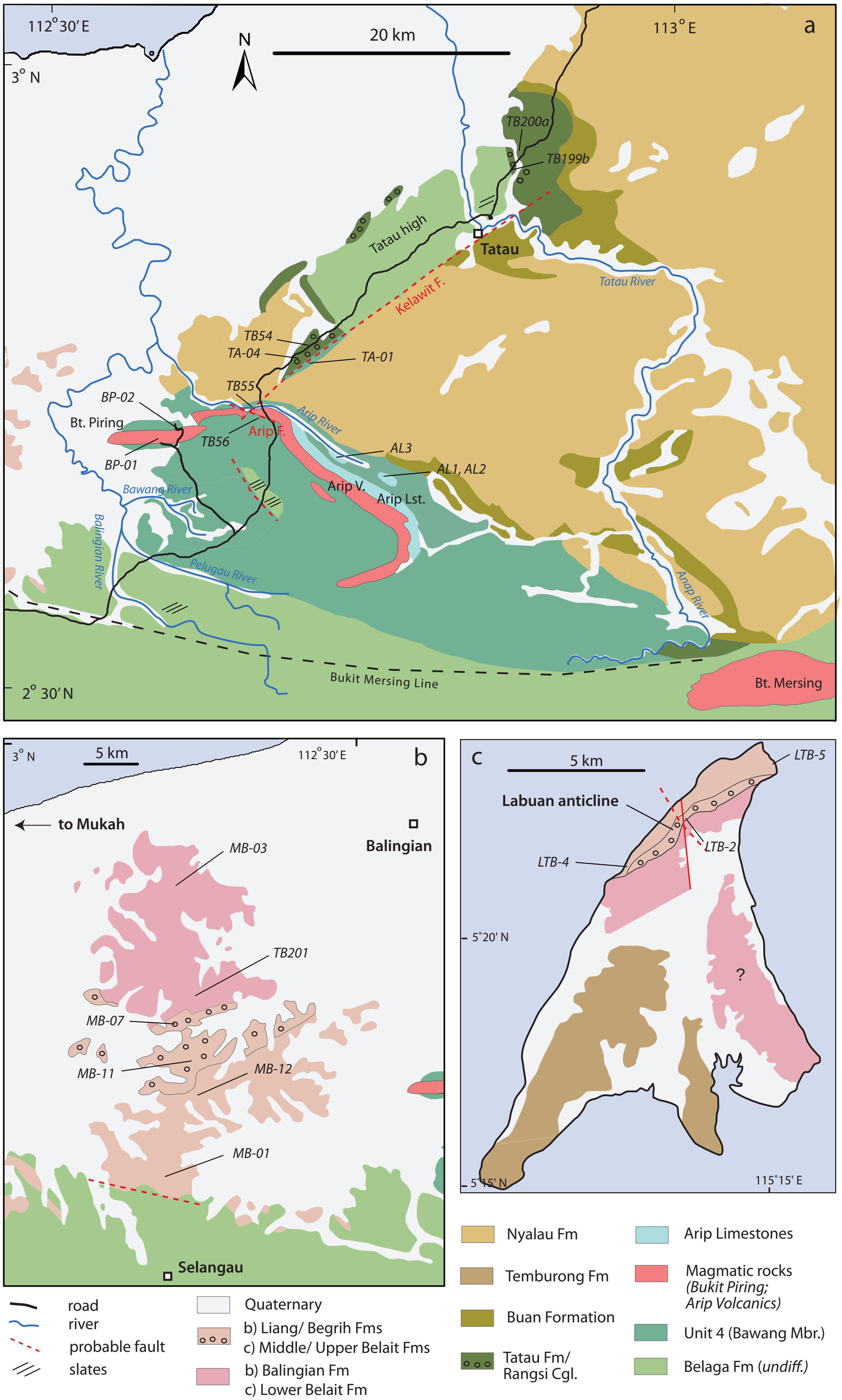

a
112°30′E
113°E
3° N
2° 30′N
N
20 km
Tatau high
TB200a
TB199b
Tatau
Tatau River
Kelawit F.
TB54
TA-04
TA-01
TB55
BP-02
Bt. Piring
TB56
BP-01
Arip F.
Arip River
AL3
AL1, AL2
Arip V.
Arip Lst.
Bawang River
Balingian River
Pelugau River
Anap River
Bukit Mersing Line
Bt. Mersing
b
3° N
5 km
112°30′E
to Mukah
Balingian
MB-03
TB201
MB-07
MB-11
MB-12
MB-01
Selangau
c
5 km
LTB-5
Labuan anticline
LTB-4
LTB-2
5°20′ N
?
5°15′ N
115°15′ E
Nyalau Fm
Temburong Fm
Buan Formation
Tatau Fm/
Rangsi Cgl.
Arip Limestones
Magmatic rocks
(Bukit Piring;
Arip Volcanics)
Unit 4 (Bawang Mbr.)
Belaga Fm (undiff.)
road
river
probable fault
slates
Quaternary
b) Liang/ Begrih Fms
c) Middle/ Upper Belait Fms
b) Balingian Fm
c) Lower Belait Fm

Fig. 2

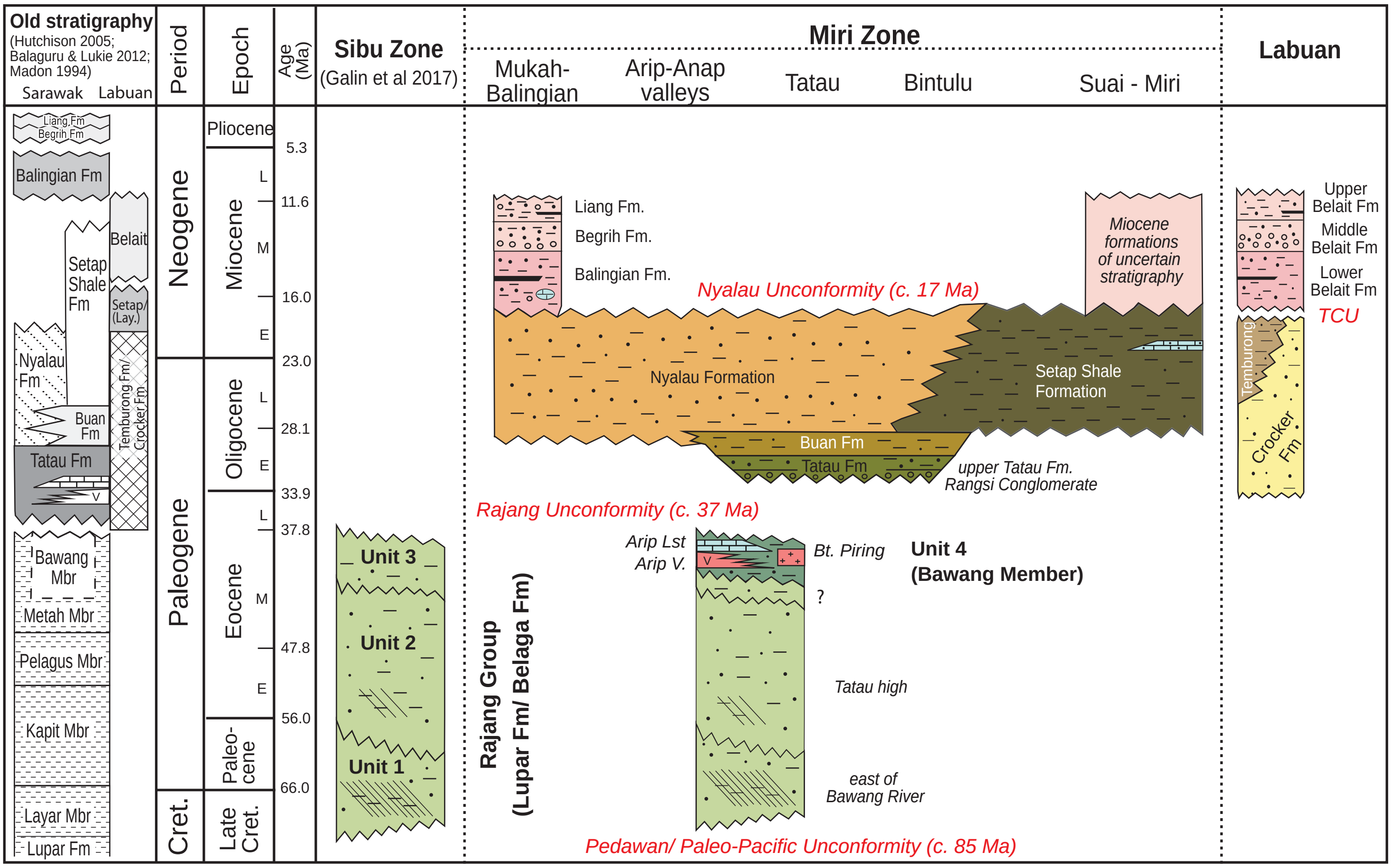
Old stratigraphy
(Hutchison 2005; Balaguru & Lukie 2012; Madon 1994)
Sarawak
Labuan
Period
Epoch
Age (Ma)
Sibu Zone
(Galin et al 2017)
Miri Zone
Mukah-Balingian
Arip-Anap valleys
Tatau
Bintulu
Suai - Miri
Labuan
Liang Fm
Begrih Fm
Balingian Fm
Belait
Setap Shale Fm
Setap/ (Lay.)
Nyalau Fm
Buan Fm
Temburong Fm/ Crocker Fm
Tatau Fm
Bawang Mbr
Metah Mbr
Pelagus Mbr
Kapit Mbr
Layar Mbr
Lupar Fm
Neogene
Paleogene
Cret.
Pliocene
Miocene
Oligocene
Eocene
Paleo-cene
Late Cret.
L
M
E
5.3
11.6
16.0
23.0
28.1
33.9
37.8
47.8
56.0
66.0
Unit 3
Unit 2
Unit 1
Liang Fm.
Begrih Fm.
Balingian Fm.
Nyalau Unconformity (c. 17 Ma)
Miocene formations of uncertain stratigraphy
Nyalau Formation
Setap Shale Formation
Buan Fm
Tatau Fm
upper Tatau Fm.
Rangsi Conglomerate
Rajang Unconformity (c. 37 Ma)
Arip Lst
Arip V.
Bt. Piring
Unit 4
(Bawang Member)
?
Tatau high
east of Bawang River
Rajang Group
(Lupar Fm/ Belaga Fm)
Pedawan/ Paleo-Pacific Unconformity (c. 85 Ma)
Upper Belait Fm
Middle Belait Fm
Lower Belait Fm
TCU
Temburong
Crocker Fm

Fig. 3

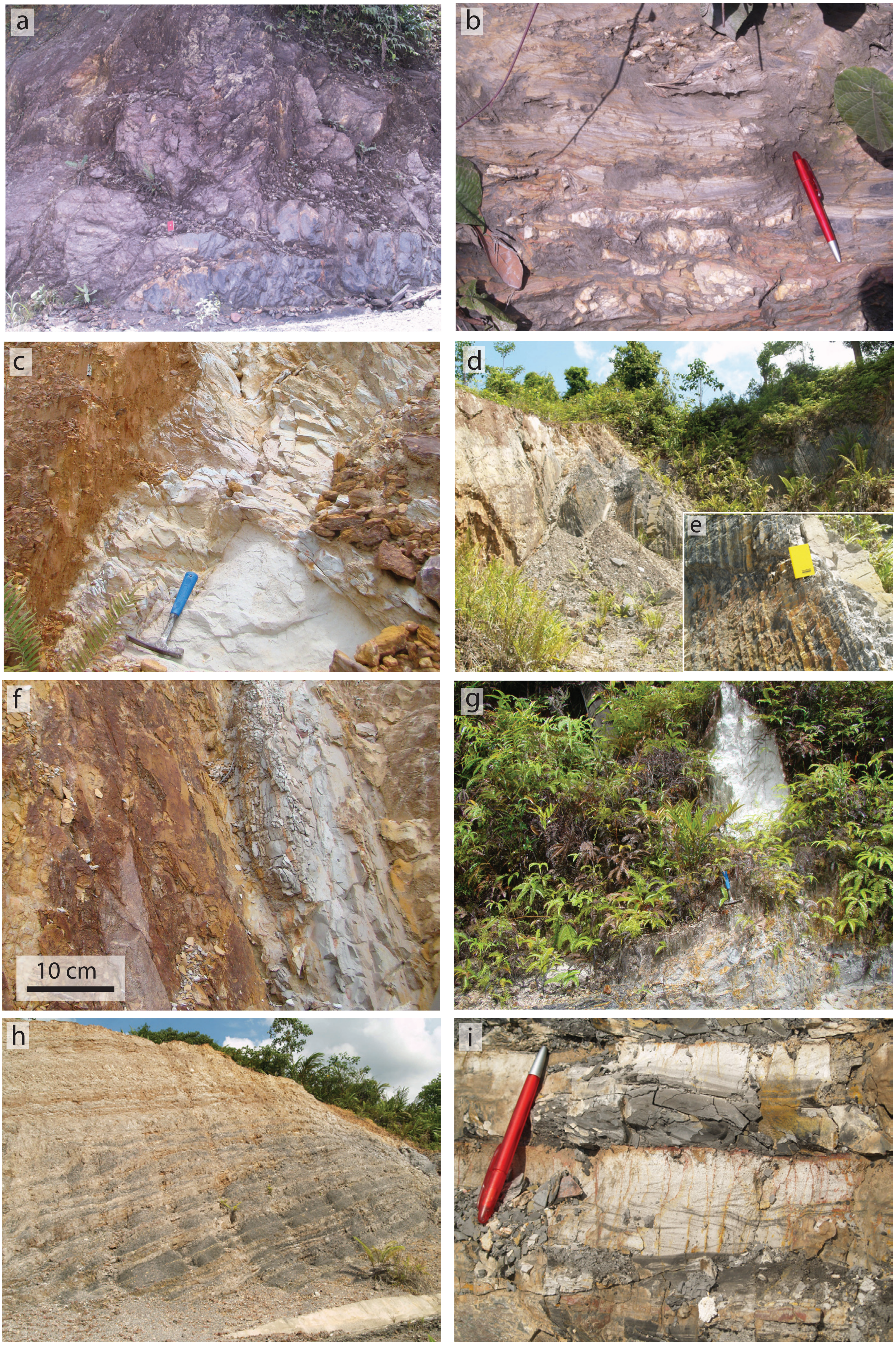

Fig. 4

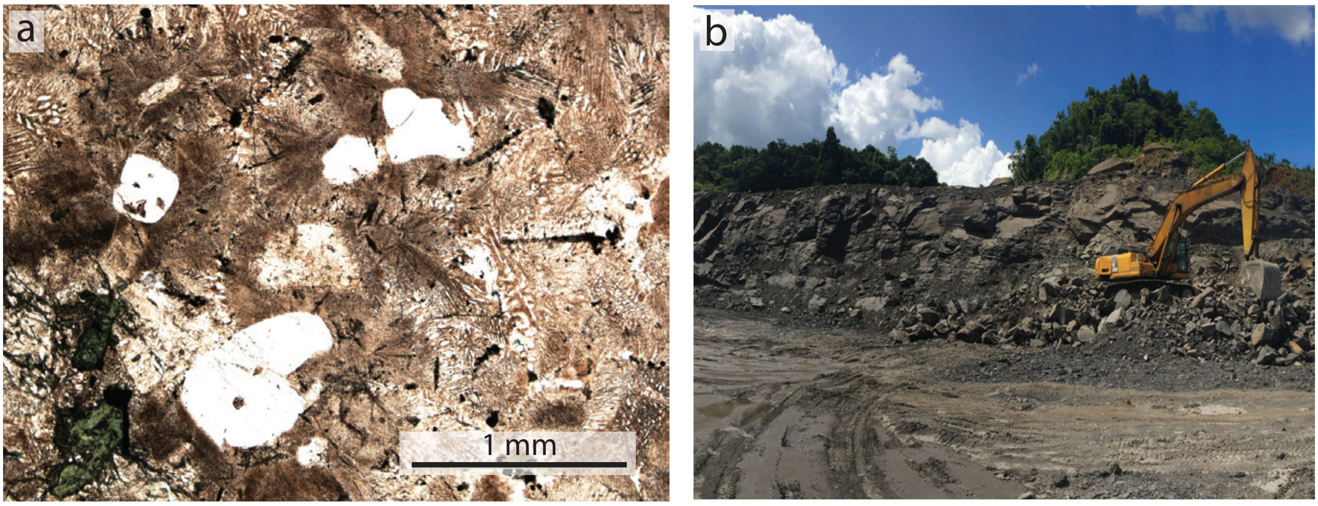

Fig. 5

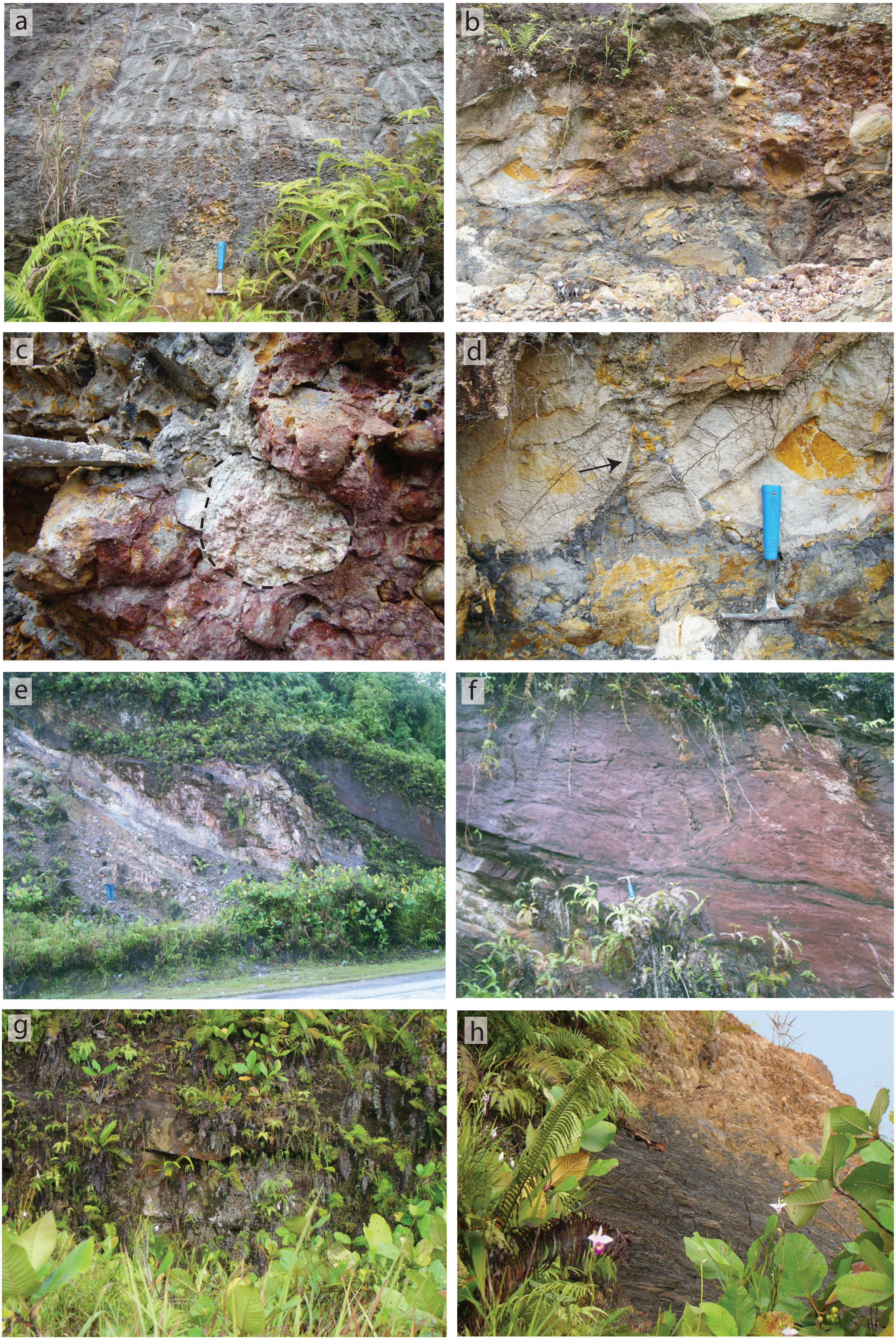

Fig. 6

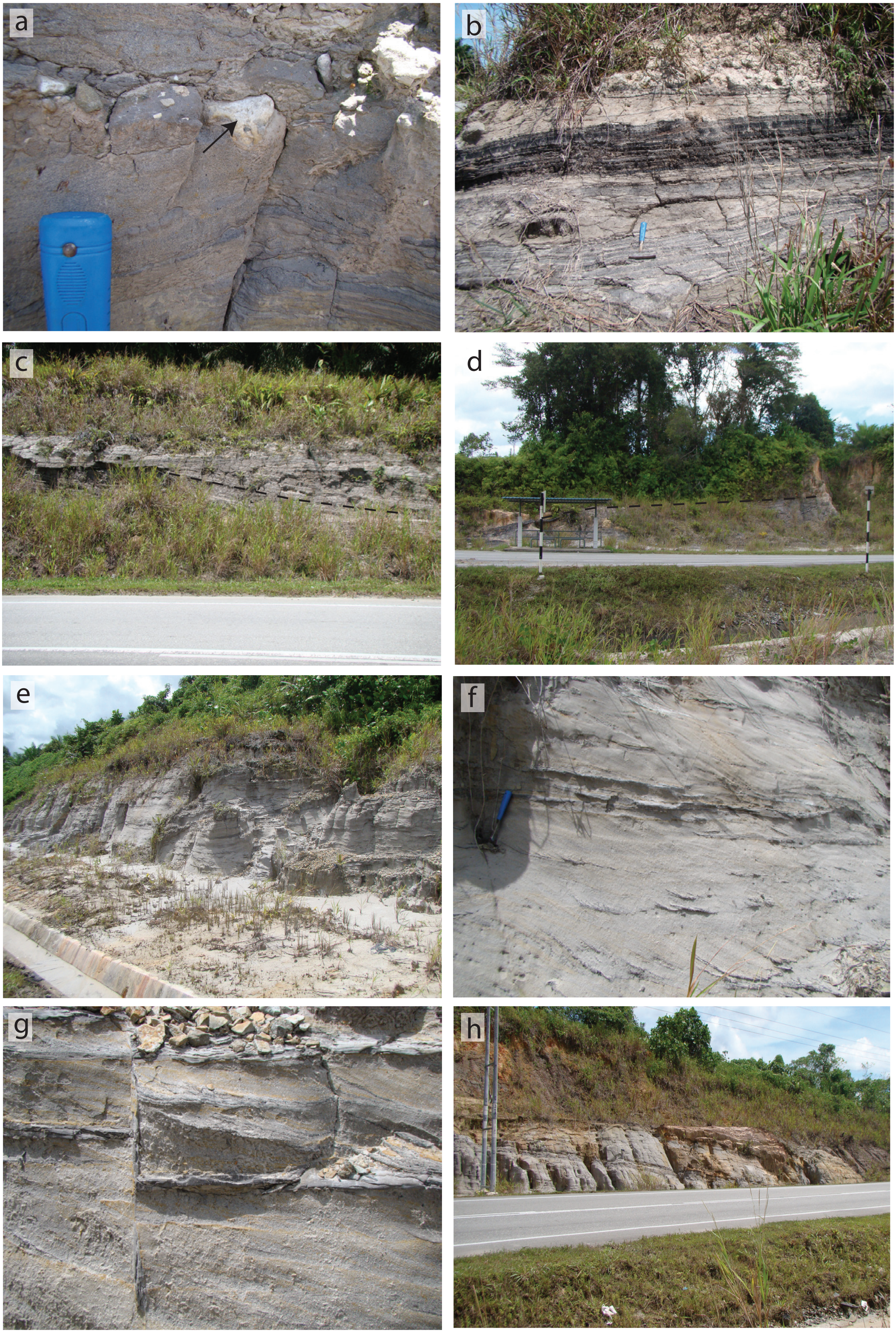

Fig. 7

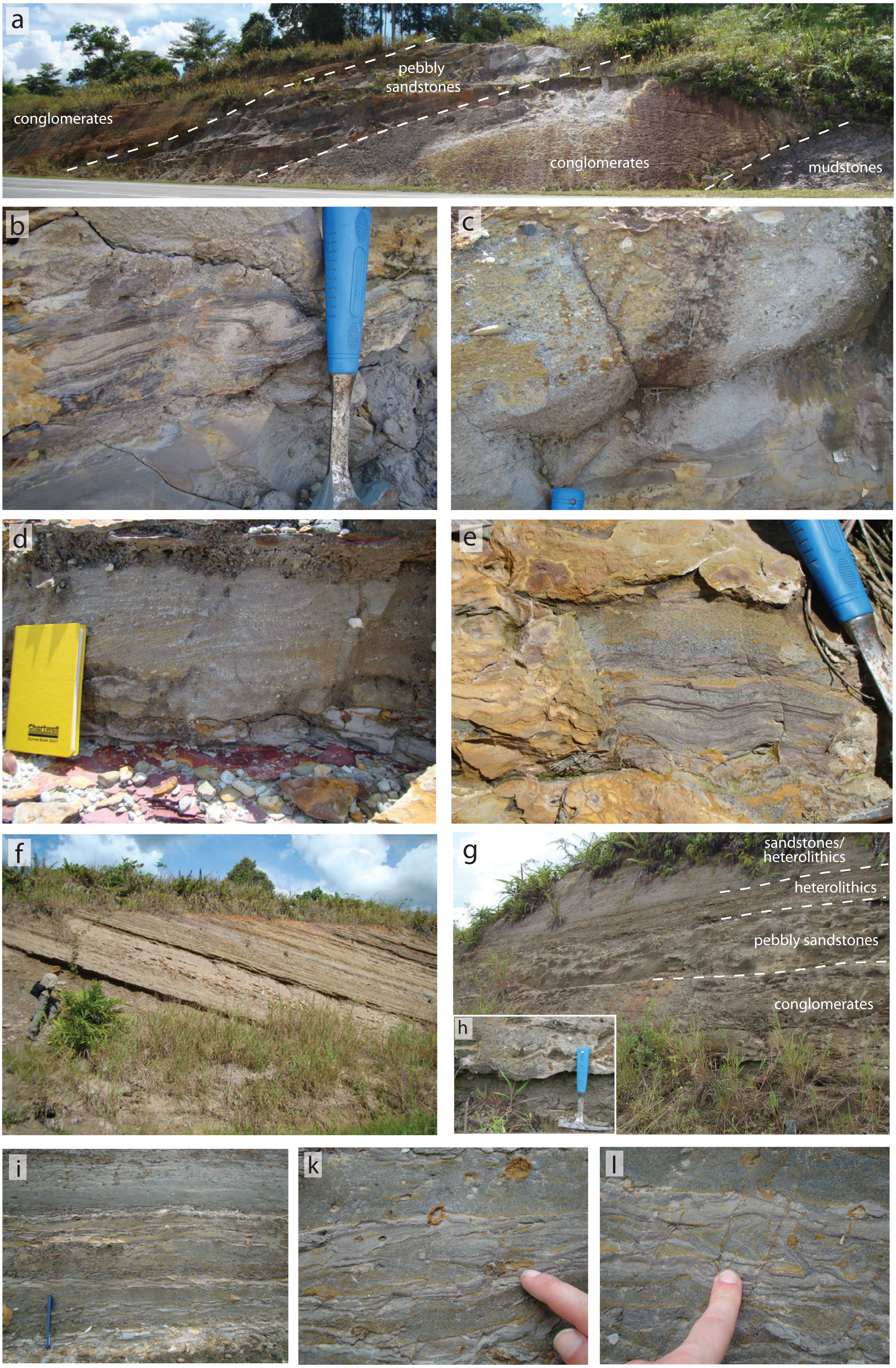
a
pebbly
sandstones
conglomerates
conglomerates
mudstones
b
c
d
e
f
g
sandstones/
heterolithics
heterolithics
pebbly sandstones
conglomerates
h
i
k
l

Fig. 8

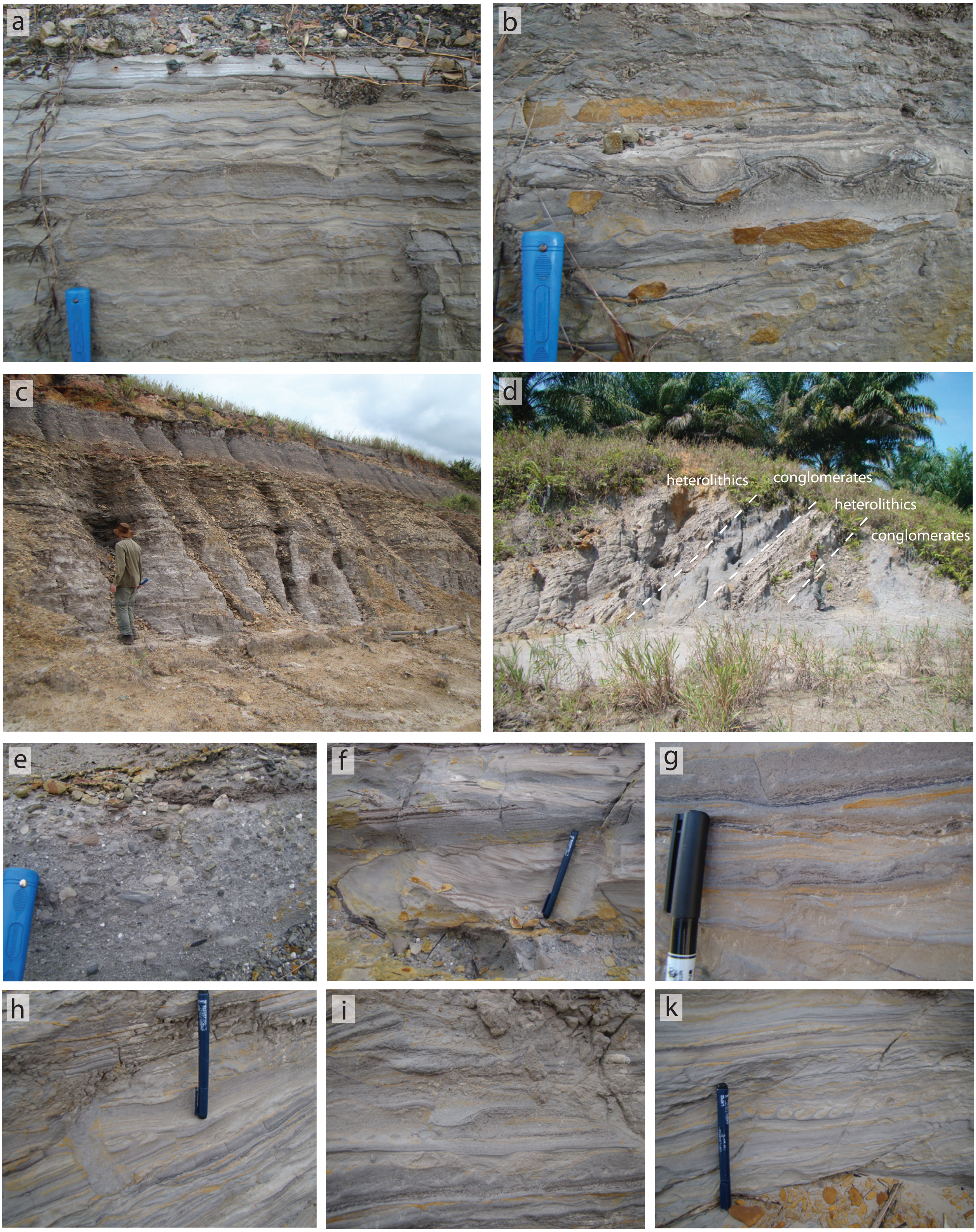
a
b
c
d
heterolithics
conglomerates
heterolithics
conglomerates
e
f
g
h
i
k

Fig. 9

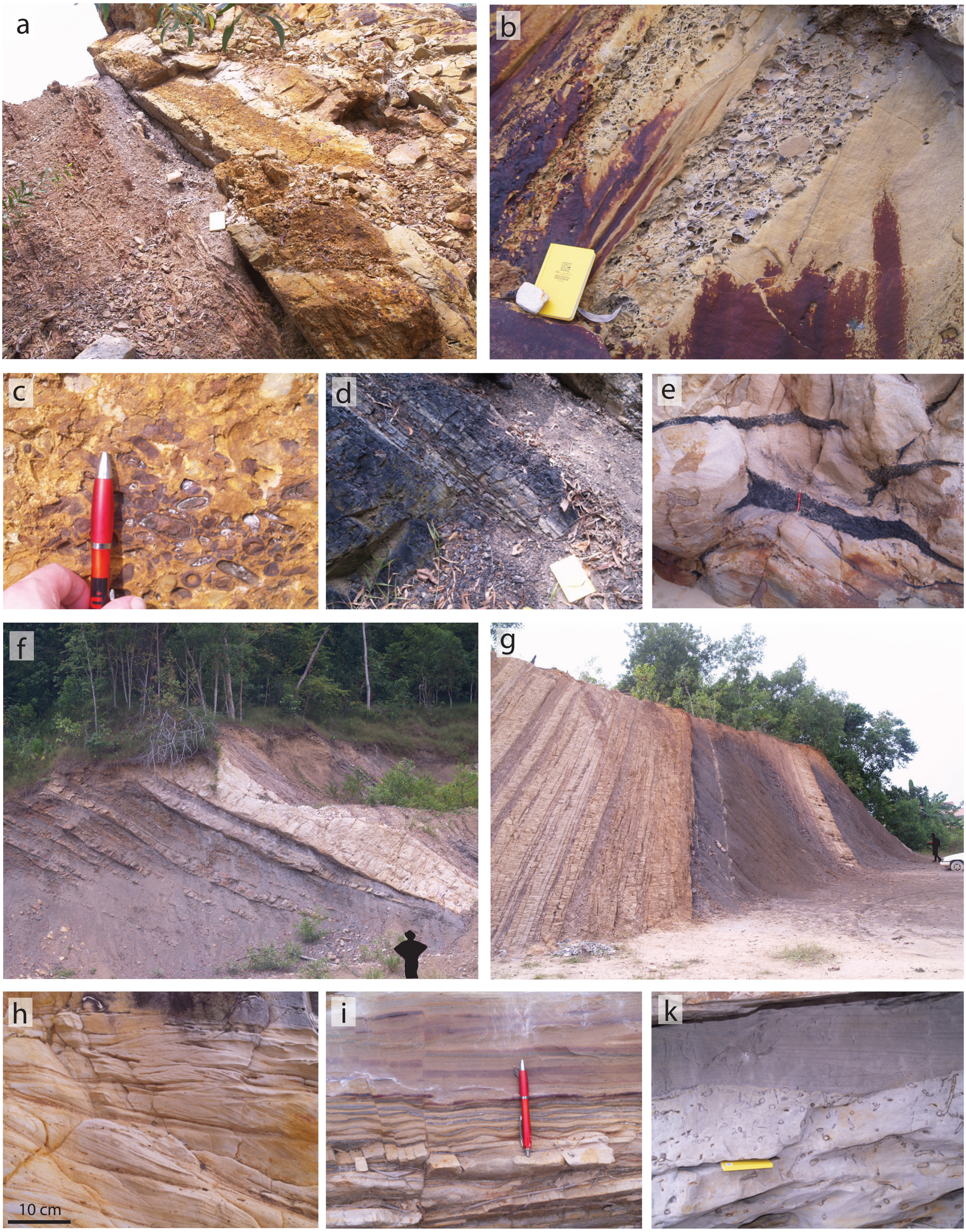

Fig. 10

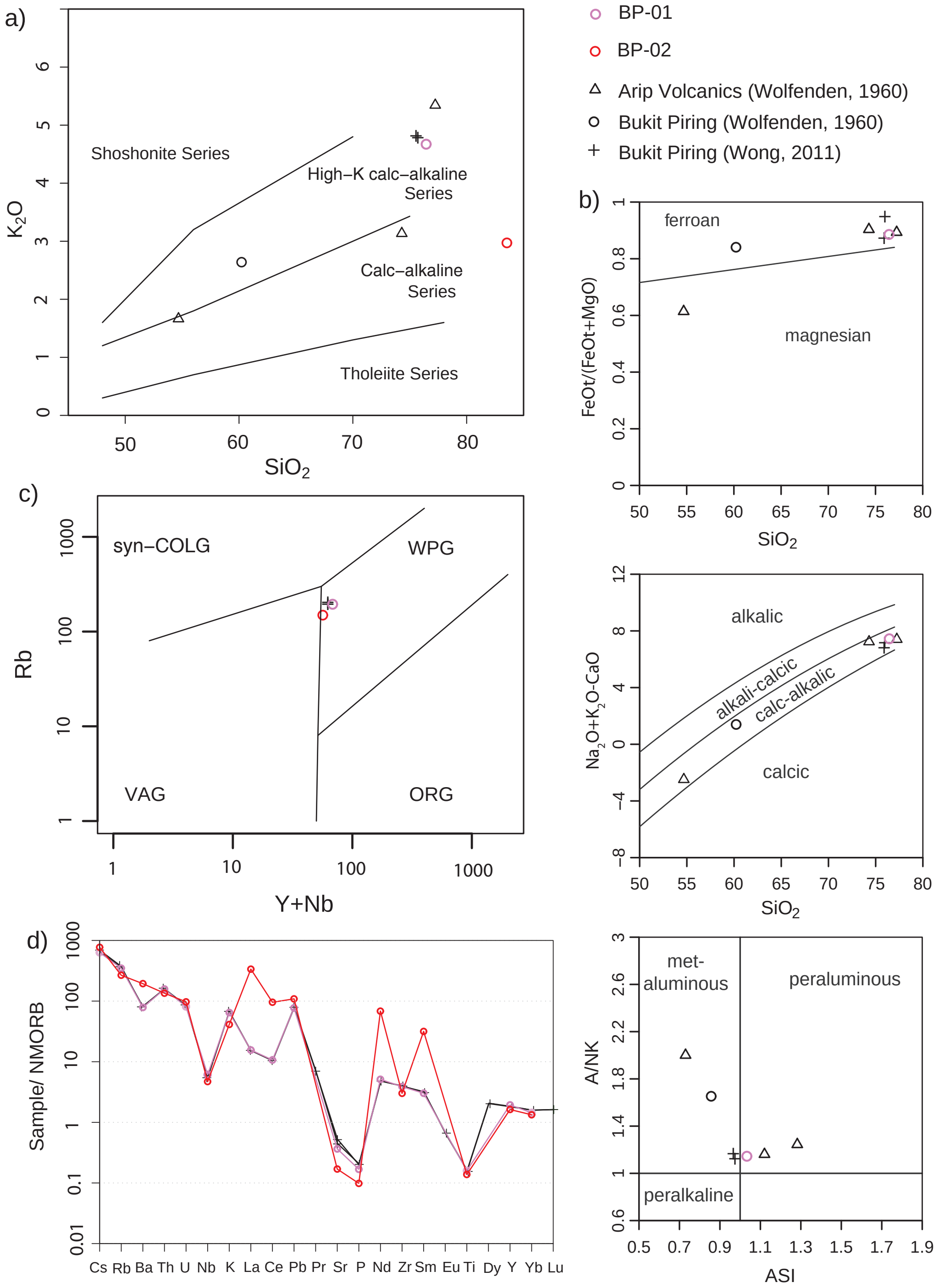
a)
Shoshonite Series
High–K calc–alkaline Series
Calc–alkaline Series
Tholeiite Series
K2O
SiO2
BP-01
BP-02
Arip Volcanics (Wolfenden, 1960)
Bukit Piring (Wolfenden, 1960)
Bukit Piring (Wong, 2011)
b)
ferroan
magnesian
FeOt/(FeOt+MgO)
SiO2
c)
syn–COLG
WPG
VAG
ORG
Rb
Y+Nb
alkalic
alkali-calcic
calc-alkalic
calcic
Na2O+K2O-CaO
SiO2
d)
Sample/ NMORB
Cs Rb Ba Th U Nb K La Ce Pb Pr Sr P Nd Zr Sm Eu Ti Dy Y Yb Lu
met-aluminous
peraluminous
peralkaline
A/NK
ASI

Fig. 11

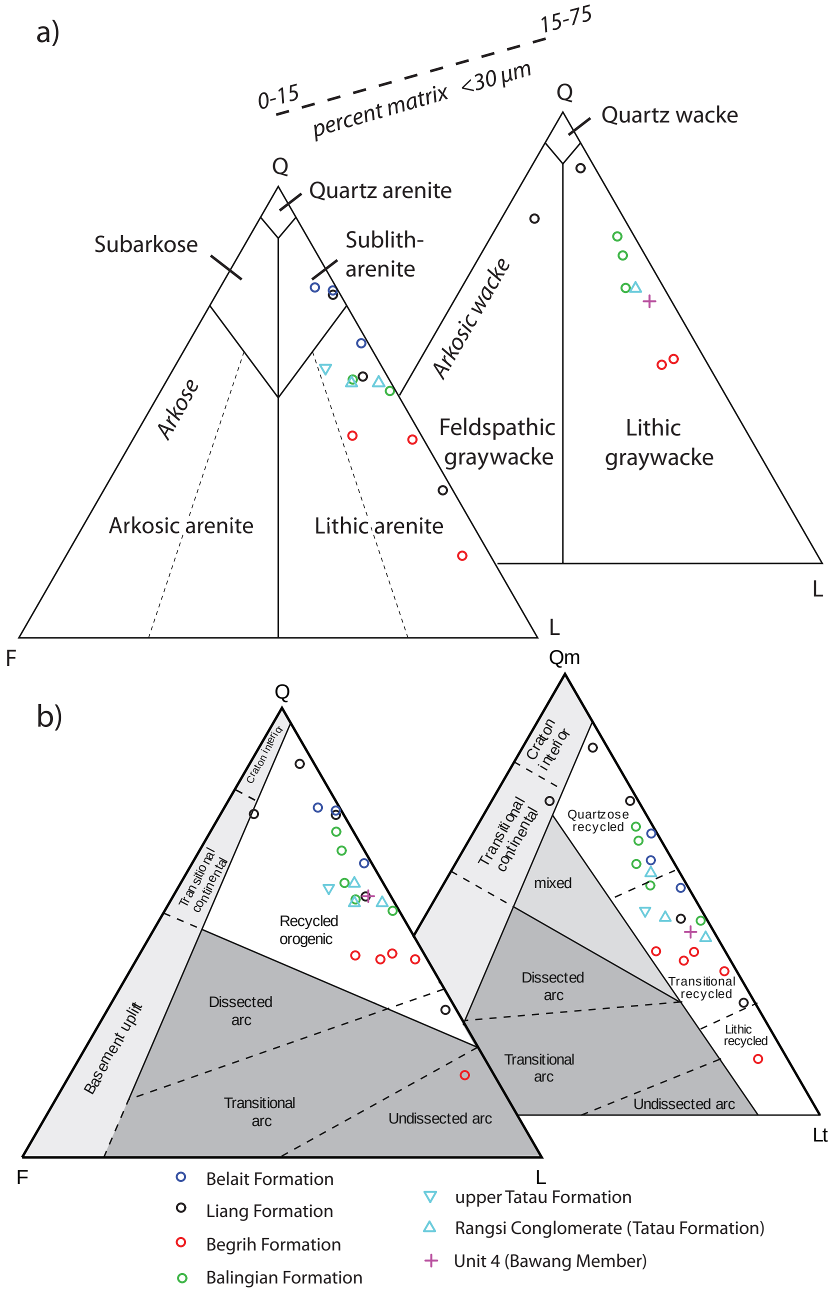
a)
0-15
percent matrix <30 µm
15-75
Q
Quartz arenite
Subarkose
Sublith-
arenite
Arkose
Arkosic arenite
Lithic arenite
F
L
Q
Quartz wacke
Arkosic wacke
Feldspathic
graywacke
Lithic
graywacke
L
b)
Q
Craton interior
Transitional
continental
Basement uplift
Recycled
orogenic
Dissected
arc
Transitional
arc
Undissected arc
F
L
Qm
Craton
interior
Transitional
continental
Quartzose
recycled
mixed
Dissected
arc
Transitional
recycled
Lithic
recycled
Transitional
arc
Undissected arc
Lt
Belait Formation
Liang Formation
Begrih Formation
Balingian Formation
upper Tatau Formation
Rangsi Conglomerate (Tatau Formation)
Unit 4 (Bawang Member)

Fig. 12

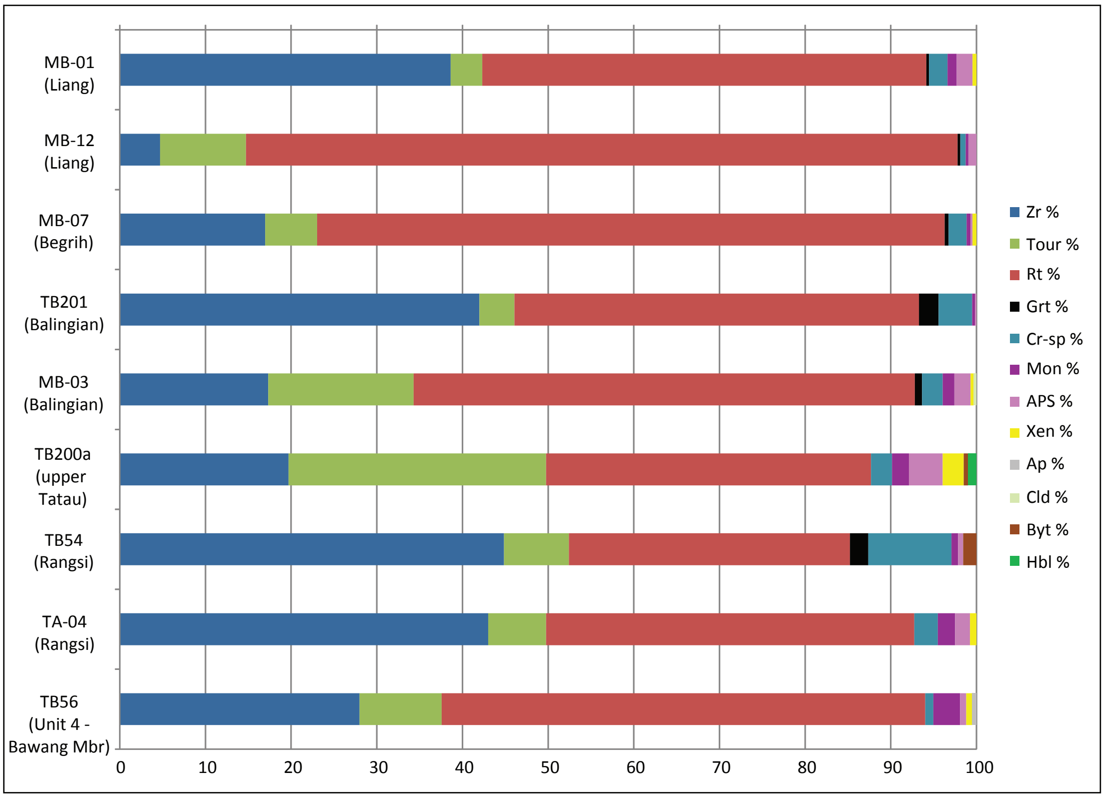
MB-01
(Liang)
MB-12
(Liang)
MB-07
(Begrih)
TB201
(Balingian)
MB-03
(Balingian)
TB200a
(upper
Tatau)
TB54
(Rangsi)
TA-04
(Rangsi)
TB56
(Unit 4 -
Bawang Mbr)
0
10
20
30
40
50
60
70
80
90
100
Zr %
Tour %
Rt %
Grt %
Cr-sp %
Mon %
APS %
Xen %
Ap %
Cld %
Byt %
Hbl %

Fig. 13

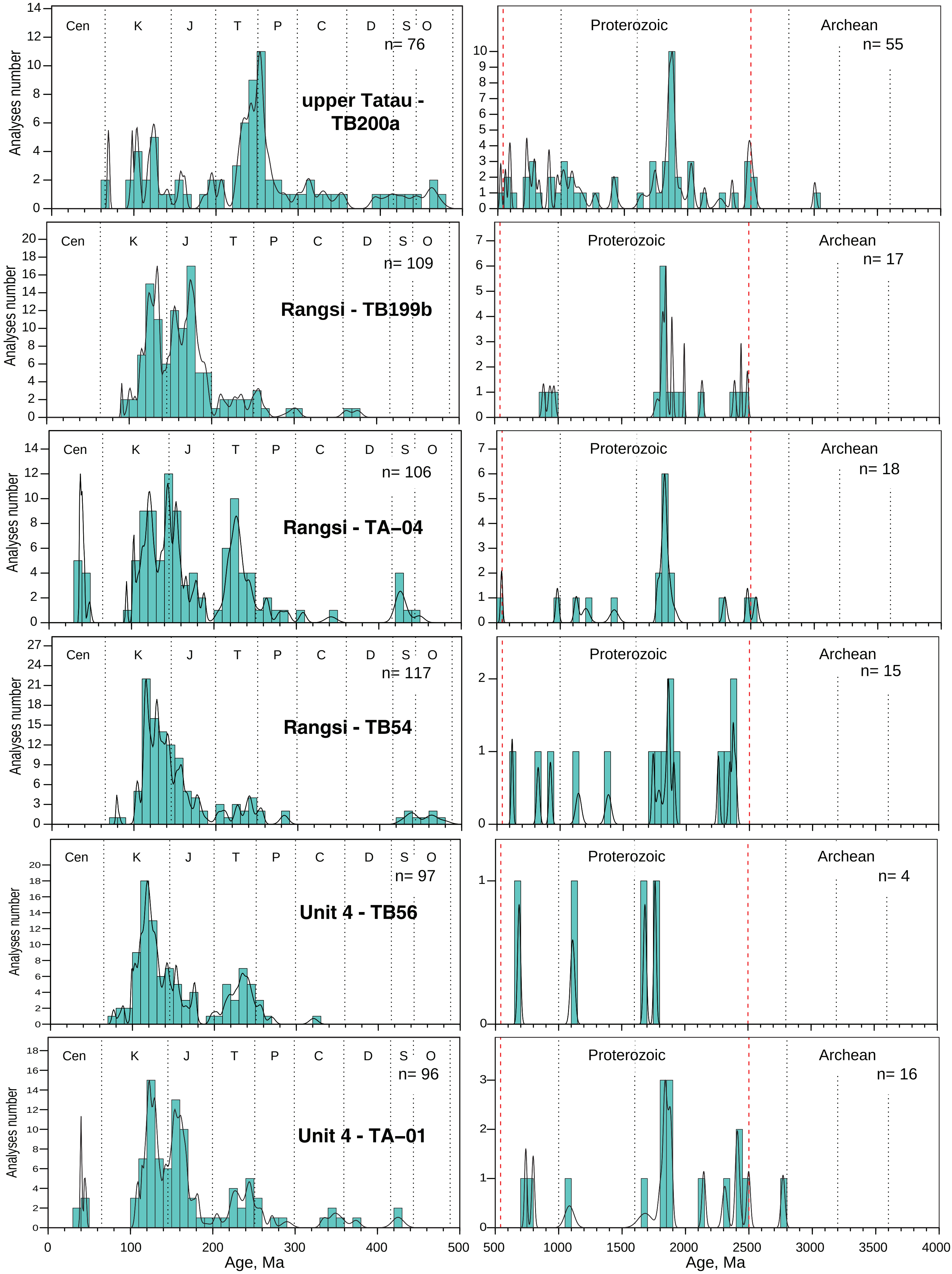

upper Tatau - TB200a
n= 76
n= 55
Rangsi - TB199b
n= 109
n= 17
Rangsi - TA–04
n= 106
n= 18
Rangsi - TB54
n= 117
n= 15
Unit 4 - TB56
n= 97
n= 4
Unit 4 - TA–01
n= 96
n= 16
Cen
K
J
T
P
C
D
S
O
Proterozoic
Archean
Analyses number
Age, Ma

Fig. 14.1

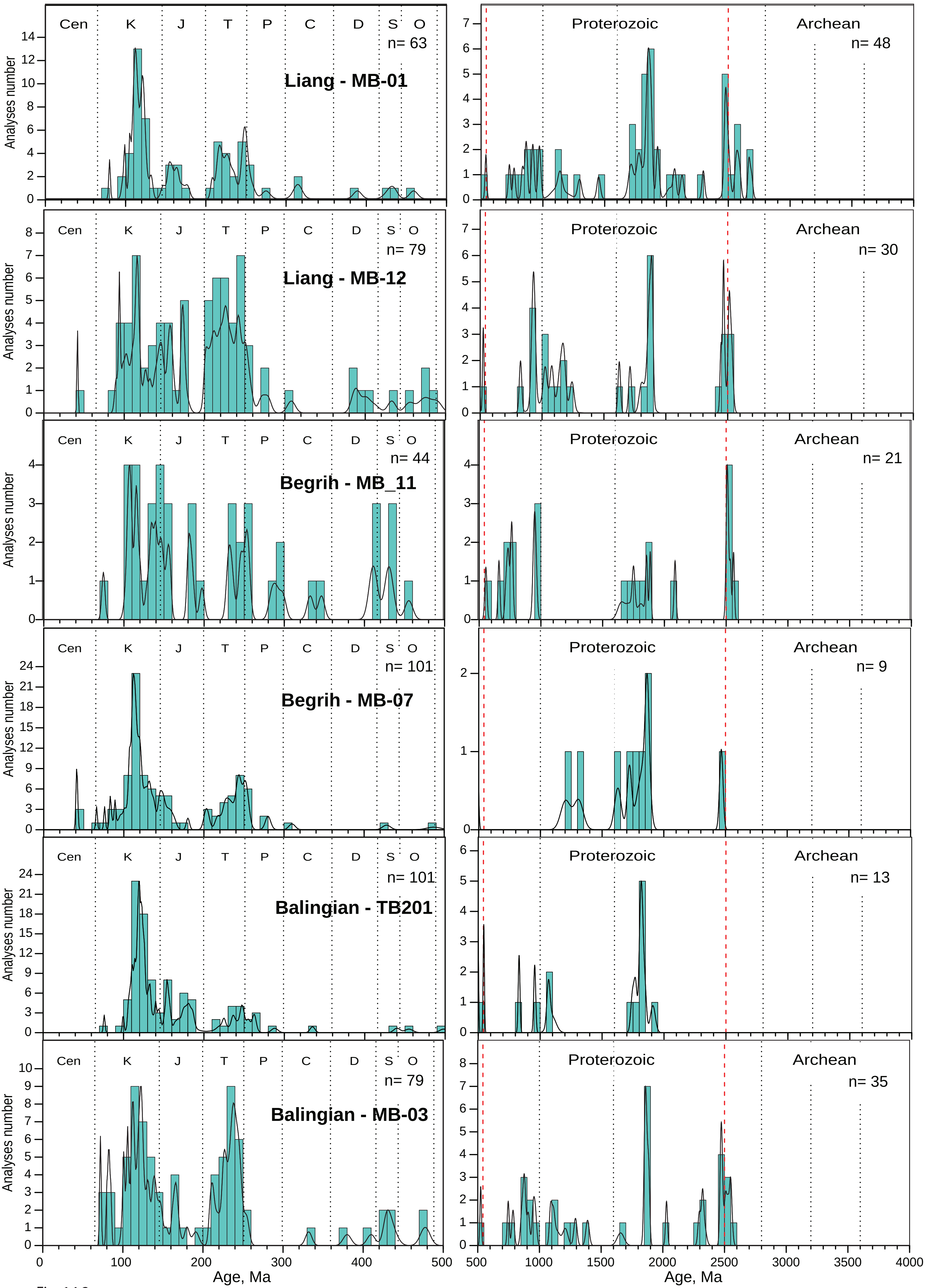
Liang - MB-01
n= 63
n= 48
Liang - MB-12
n= 79
n= 30
Begrih - MB_11
n= 44
n= 21
Begrih - MB-07
n= 101
n= 9
Balingian - TB201
n= 101
n= 13
Balingian - MB-03
n= 79
n= 35
Cen K J T P C D S O
Proterozoic
Archean
Analyses number
Age, Ma

Fig. 14.2

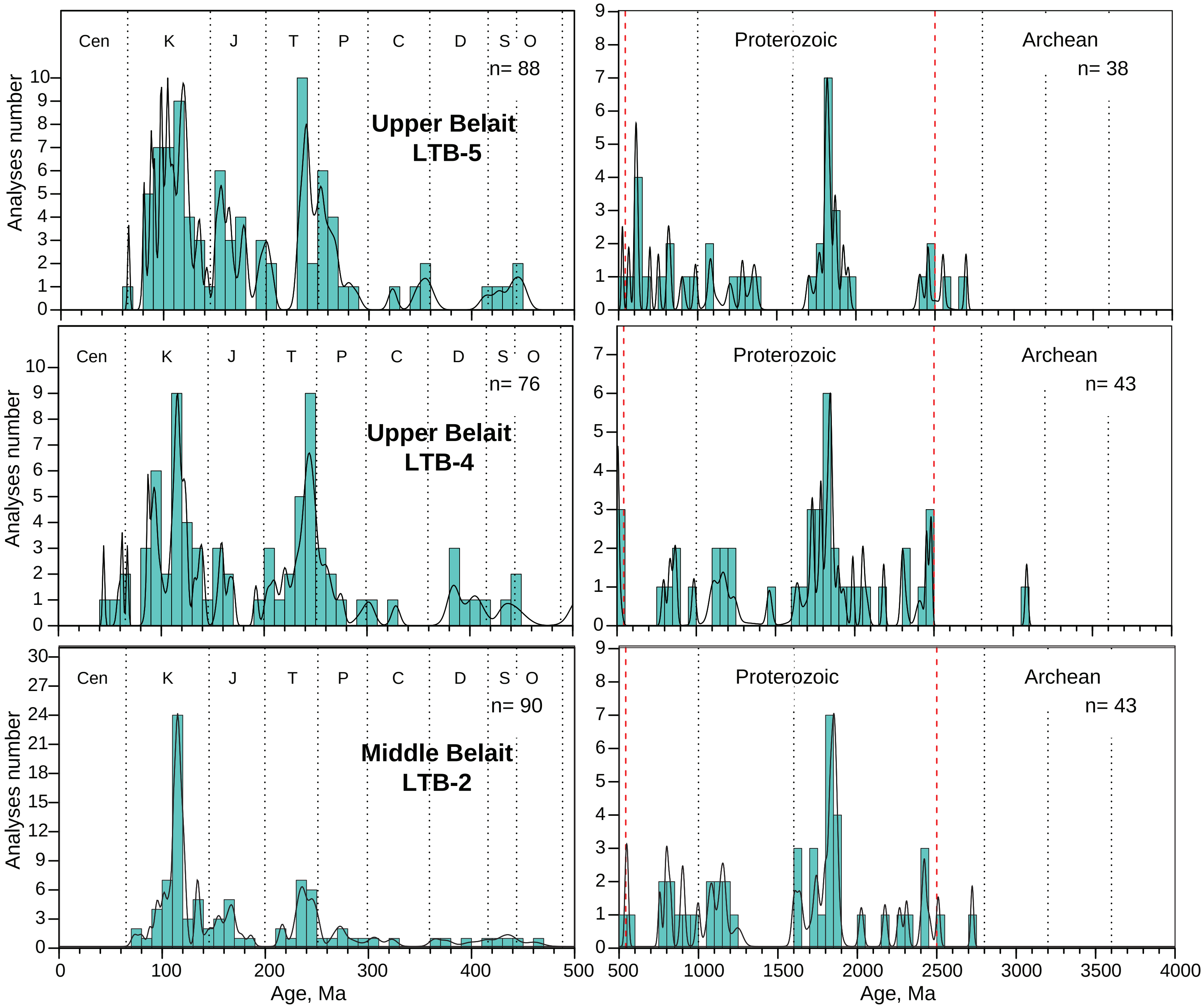
Cen K J T P C D S O
n= 88
Upper Belait
LTB-5
Proterozoic
Archean
n= 38
n= 76
Upper Belait
LTB-4
n= 43
n= 90
Middle Belait
LTB-2
Analyses number
Age, Ma

Fig. 14.3

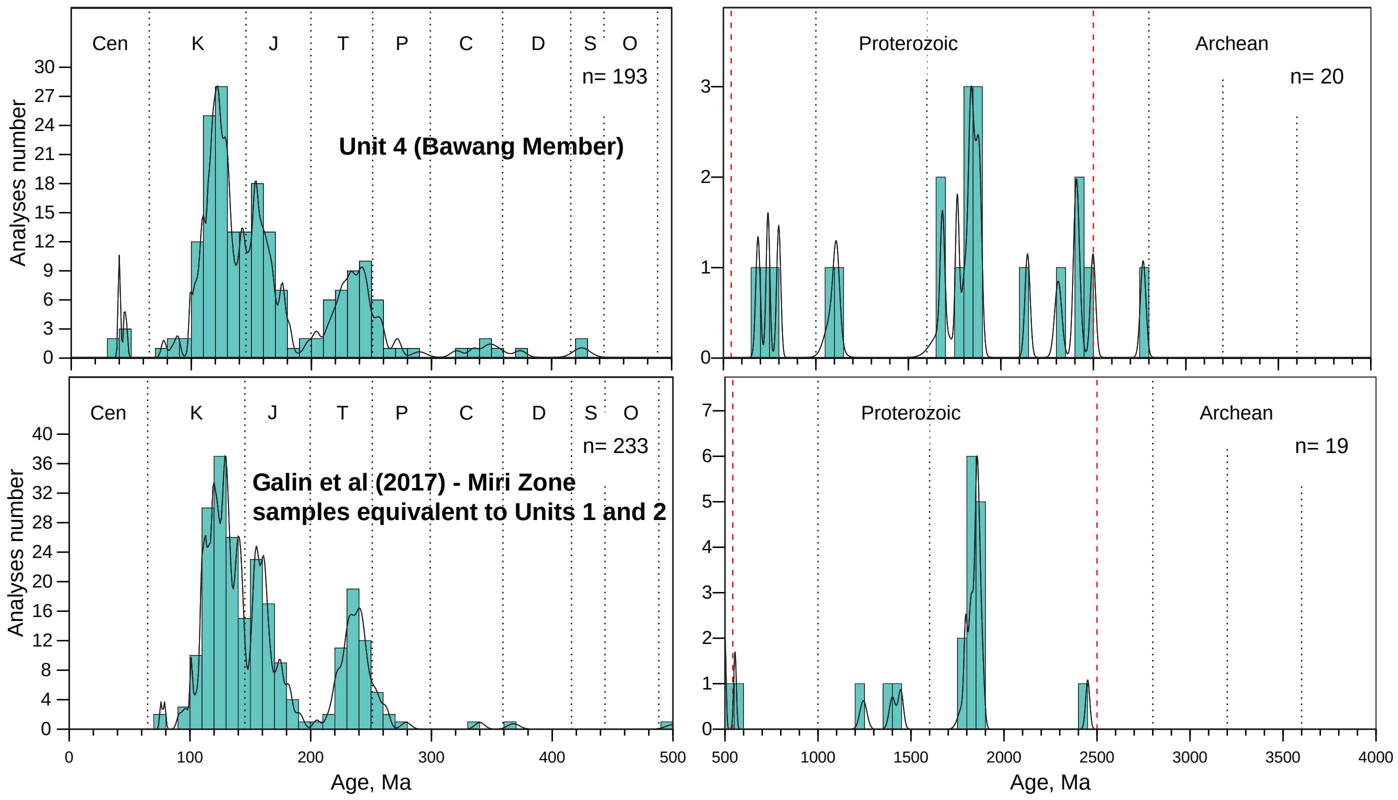
Cen
K
J
T
P
C
D
S
O
n= 193
Unit 4 (Bawang Member)
Analyses number
Proterozoic
Archean
n= 20
n= 233
Galin et al (2017) - Miri Zone
samples equivalent to Units 1 and 2
n= 19
Age, Ma
Age, Ma

Fig. 15

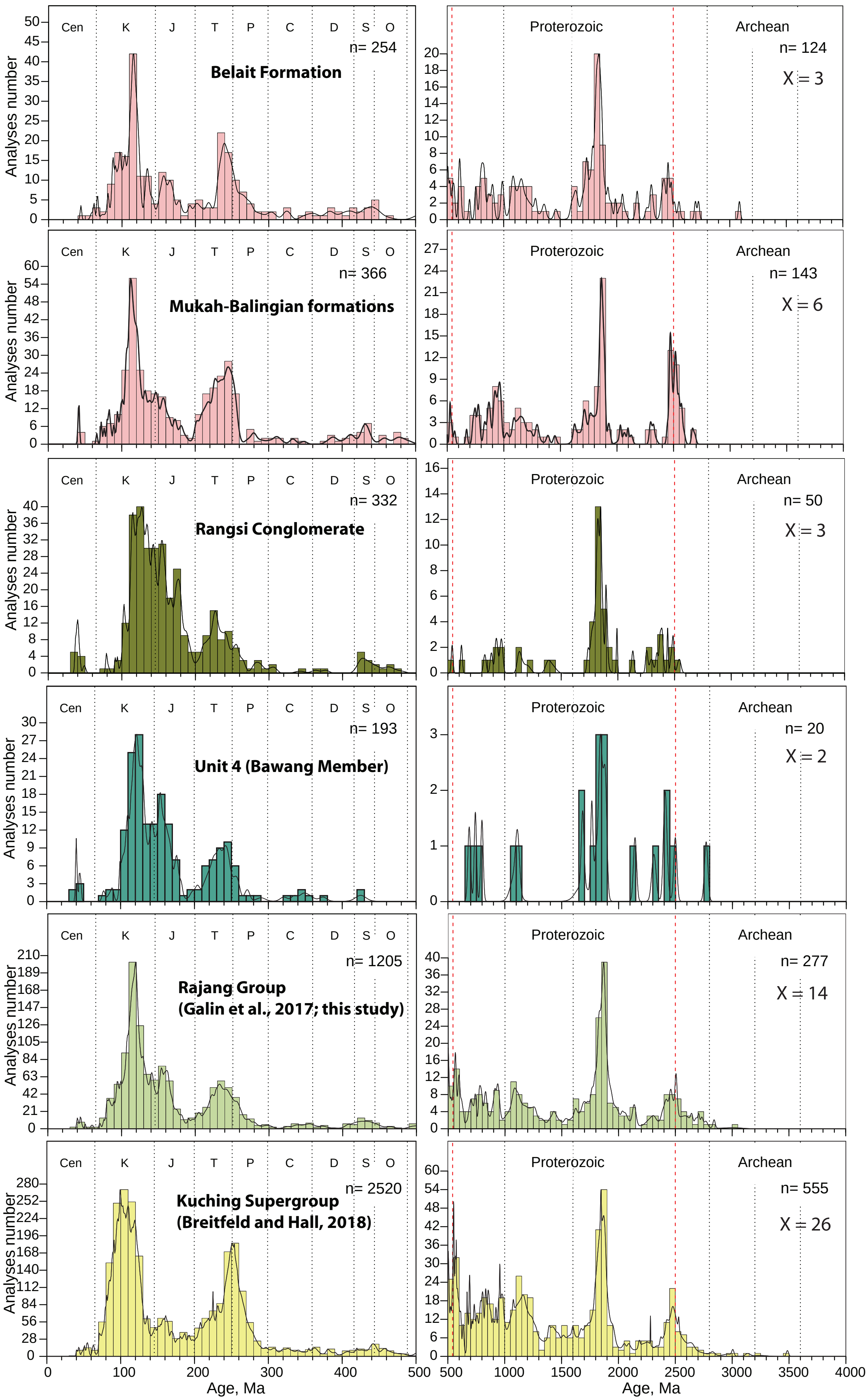
Belait Formation
n= 254
n= 124
X = 3
Mukah-Balingian formations
n= 366
n= 143
X = 6
Rangsi Conglomerate
n= 332
n= 50
X = 3
Unit 4 (Bawang Member)
n= 193
n= 20
X = 2
Rajang Group
(Galin et al., 2017; this study)
n= 1205
n= 277
X = 14
Kuching Supergroup
(Breitfeld and Hall, 2018)
n= 2520
n= 555
X = 26
Cen K J T P C D S O
Proterozoic
Archean
Analyses number
Age, Ma

Fig. 16

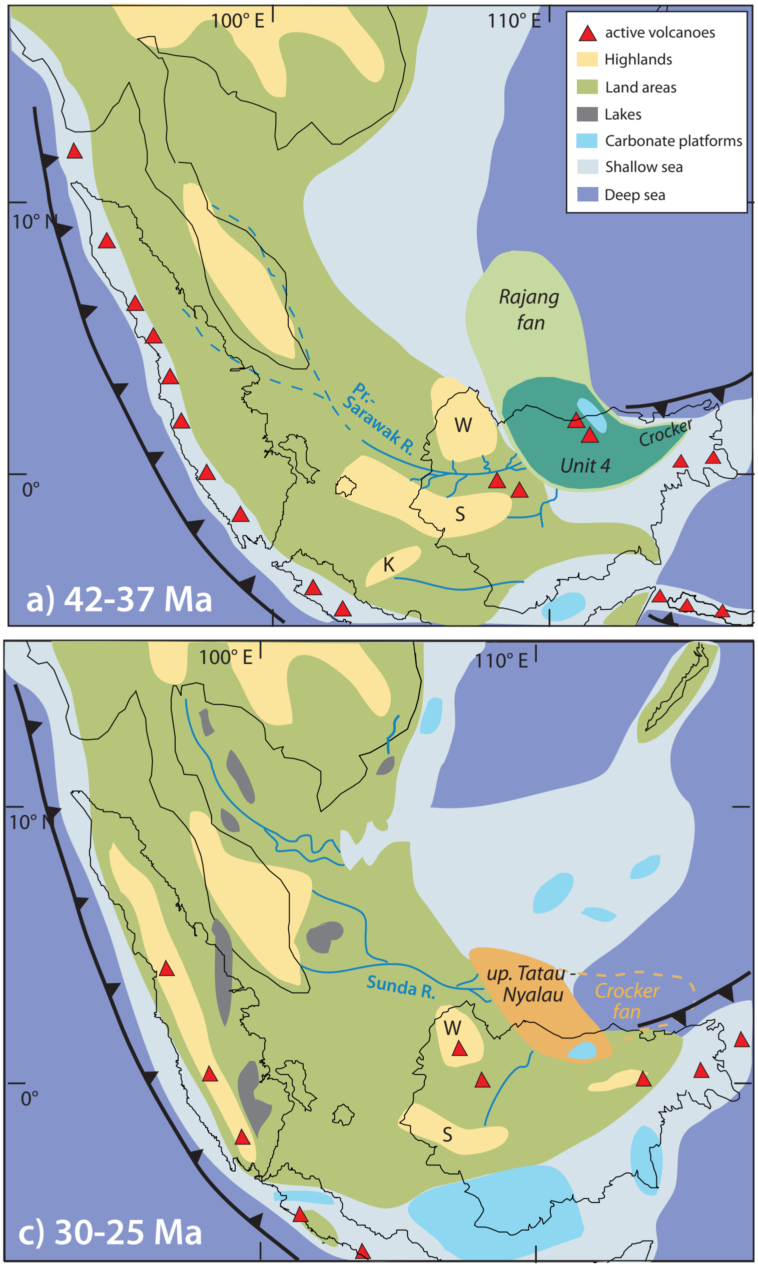
active volcanoes
Highlands
Land areas
Lakes
Carbonate platforms
Shallow sea
Deep sea
100° E
110° E
10° N
0°
Rajang fan
Pr.-Sarawak R.
W
S
K
Unit 4
Crocker
a) 42-37 Ma
?
Pr.-Kapuas R.
Rangsi Cgl.
? Crocker
b) 33-30 Ma
Sunda R.
up. Tatau - Nyalau
Crocker fan
c) 30-25 Ma
Kapuas R.
MB/ Belait
Kuching-Rajang range
B
d) 15-10 Ma

Fig. 17

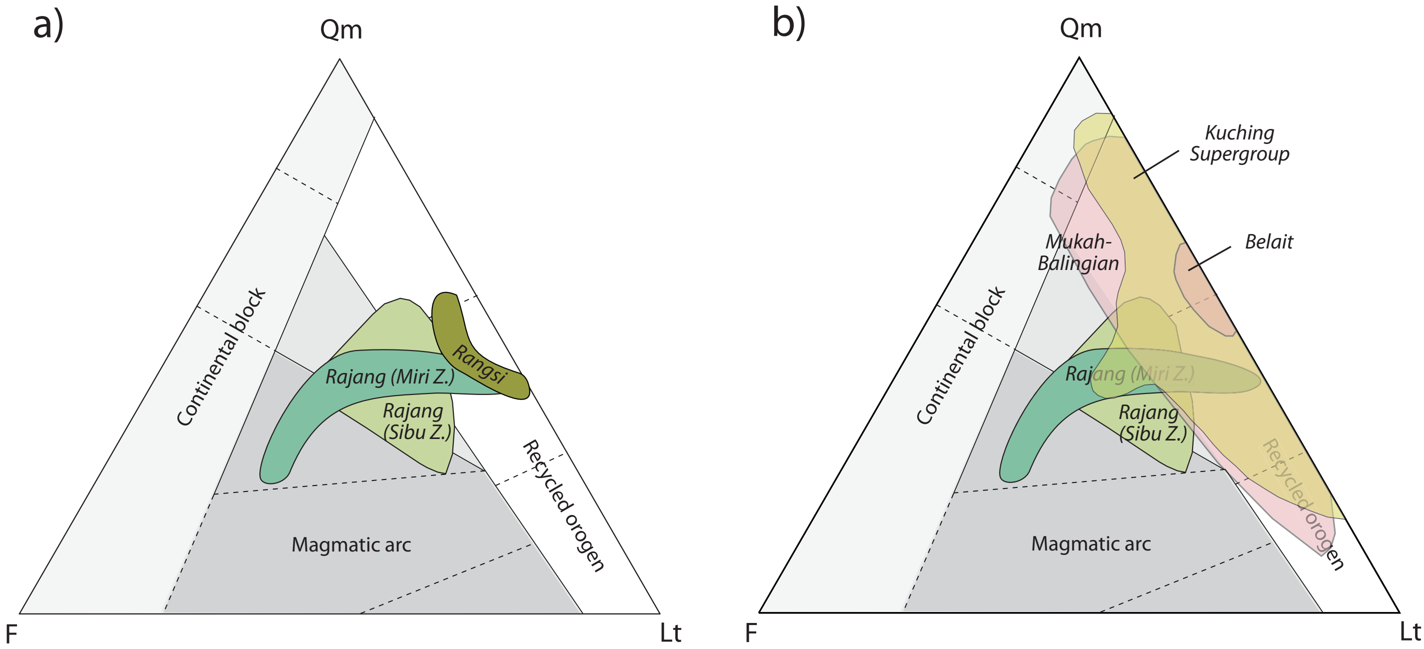
a)
Qm
F
Lt
Continental block
Magmatic arc
Recycled orogen
Rajang (Miri Z.)
Rajang (Sibu Z.)
Rangsi
b)
Qm
F
Lt
Kuching Supergroup
Belait
Mukah-Balingian
Continental block
Rajang (Miri Z.)
Rajang (Sibu Z.)
Magmatic arc
Recycled orogen

Fig. 18

Lithology/ Formation	Samples	Microfacies	components	Depositional environment	Stages/ age ranges
Arip Limestones	AL1-1	Micritic wackestone of planktonic foraminifera	Subbotina sp., Acarinina pentacamerata, Chiloguembelina sp., Streptochilus cubensis, Subbotina linaperta, Aragonella nuttalli, Acarinina sp., Subbotina eocaenica	Inner neritic	Lutetian, P10-P11, 47.8-42.3Ma
	AL1-2	Micritic wackestone of planktonic foraminifera	Aragonella nuttalli, Acarinina sp., Subbotina eocaenica, Turborotalia frontosa	Inner neritic	Lutetian, P10-P11, 47.8-42.3Ma
	AL1-3	Recrystallised planktonic foraminifera	Badly rare recrystallised foraminifera		Indet.
	AL2-1	Micritic wackestone of planktonic foraminifera	Aqcarinina pentacamerata, Guembelitrioides higginsi	Inner neritic	Lutetian, P10-P11, 47.8-42.3Ma
	AL2-2	Micritic wackestone of planktonic foraminifera	Bolivina sp., Porticulasphaera mexicana, Catapsydrax sp., Globigerinatheka sp., Spirillina sp., Globigerinatheka barri, echinoid spp.	Inner neritic	Late Lutetian - Early Bartonian, P11-P12, 44.9-40.2Ma
	AL2-3	Micritic wackestone of planktonic foraminifera	Subbotina inaequispira, Dentoglobigerina venezuelana, Nodosaria sp., Globigerapsis kugleri	Inner neritic	P11b-P12a, 43.2-41.2Ma
	AL3-1	Recrystallised planktonic foraminifera	Badly rare recrystallised foraminifera		
	AL3-3	Micritic wackestone of planktonic foraminifera	Acarinina pentacamerata, Globigerinatheka sp.	Inner neritic	
	AL3-4	Recrystallised planktonic foraminifera	Chiloguembelina sp., Acarinina sp.	Inner neritic	early to Middle Eocene
	AL3-2	Micritic wackestone of planktonic foraminifera	Globigerinatheka luterbacheri, Guembelitrioides higginsi	Inner neritic	Late Lutetian, P11-P12a, 44.9-41.2Ma
	AL3-5	Recrystallised planktonic foraminifera	Globigerinatheka sp., Globigerinatheka curryi		Late Lutetian, P11-P12a, 44.9-41.2Ma
Limestone clasts in Balingian Formation	MB-03b	Packstone of algae	Palaeodasyclad spp., Pseudocyclammina sp., small miliolids, Textularia spp.	Shallow backreefal environment	Jurassic-Cretaceous
	MB-03c	Packstone of algae	Palaeodasyclad spp., Pseudocyclammina sp., Choffatella, small miliolids	Shallow backreefal environment	Cretaceous (not younger than Santonian)
	Bal1	Micritic packstone of algae	Bacinella spp., Pseudocyclammina lituus	Reefal to backreef environment	Early Cretaceous, Berriasian to Barremian, 145.0-125.0Ma
	Bal2	Micritic packstone of algae	Bacinella spp., miliolid, textularid, gastropod	Reefal to backreef environment	Early Cretaceous, Berriasian to Barremian, 145.0-125.0Ma
Bau Limestone Formation	TB165	Wackestone of benthic foraminifera	Siphovalvulina sp., Dukhania sp., Pseudocyclammina sp., Nezzazatinella sp., Pseudocyclammina vasconica, Bacinella sp., Salpingoporella dinarica sp.	Shallow part of the inner ramp/Backreef	Aptian, 125.0Ma-113.0Ma

Table 1